GEOLOGICA ULTRAIECTINA

Mededelingen van het
Instituut voor Aardwetenschappen der
Rijksuniversiteit te Utrecht

No. 34

LATE MIOCENE MAGNETOSTRATIGRAPHY IN THE MEDITERRANEAN

C.G. LANGEREIS

GEOLOGICA ULTRAIECTINA

Mededelingen van het
Instituut voor Aardwetenschappen der
Rijksuniversiteit te Utrecht

No. 34

LATE MIOCENE MAGNETOSTRATIGRAPHY IN THE MEDITERRANEAN

LATE MIOCENE MAGNETOSTRATIGRAPHY IN THE MEDITERRANEAN

Laat Miocene magnetostratigrafie in het Middellandse Zeegebied

(met een samenvatting in het Nederlands)

PROEFSCHRIFT

TER VERKRIJGING VAN DE GRAAD VAN DOCTOR IN
DE WISKUNDE EN NATUURWETENSCHAPPEN AAN
DE RIJKSUNIVERSITEIT TE UTRECHT, OP GEZAG VAN
DE RECTOR MAGNIFICUS PROF.DR. O.J. DE JONG,
VOLGENS BESLUIT VAN HET COLLEGE VAN DECANEN
IN HET OPENBAAR TE VERDEDIGEN OP MAANDAG
17 DECEMBER 1984 DES NAMIDDAGS TE 4.15 UUR

DOOR

CORNELIS GERARD LANGEREIS

GEBOREN OP 19 DECEMBER 1951 TE APELDOORN

1984

Promotor: Prof.Dr. J.D.A. Zijderveld

Co-promotor: Dr. W.J. Zachariasse

Quid est ergo tempus ?
Si nemo ex me quaerat, scio; si quaerenti explicare velim, nescio.

Wat is tijd ?
Als niemand mij ernaar vraagt, weet ik het; als ik het wil uitleggen,
kan ik het niet.

Augustinus, Confessiones, liber XI, caput 14.

Allen die aan de totstandkoming van dit proefschrift een bijdrage, in welke vorm dan ook, hebben geleverd wil ik hartelijk bedanken.

In het bijzonder prof.dr. J.D.A. Zijderveld wiens kritische instelling vaak lastig maar vooral ook onmisbaar bleek. Zijn kleurrijke persoonlijkheid zal mij altijd bijblijven.

Piet-Jan Verplak heeft een groot gedeelte van de 4942 kerntjes en 9254 specimen, die hij zelf enthousiast heeft helpen verzamelen, verwerkt; zoniet psychisch dan toch fysisch.

De samenwerking met leden van de taakgroep Stratigrafie en Micropaleontologie heeft in belangrijke mate bijgedragen tot de resultaten van dit proefschrift. Met name dient genoemd te worden Dr. J.E. Meulenkamp wiens grote kennis van het Neogeen in het Middellandse Zeegebied meer suggesties voor secties opleverde dan door een enkele promovendus bemonsterd kon worden.
Dr. W.J. Zachariasse ben ik zeer erkentelijk voor zijn onontbeerlijke steun op het gebied van de biostratigrafie.

De Nederlandse organisatie voor zuiver wetenschappelijke onderzoek (Z.W.O.) leverde een financiele bijdrage in het kader van het IGCP-project nr. 1, 'Accuracy in time'.

CONTENTS

SAMENVATTING

Omkeringen van de polariteit van het geomagnetische veld in het geologisch verleden worden wereldwijd geregistreerd in de natuurlijke remanente magnetisatie (NRM) van stollingsgesteenten en sedimentaire reeksen. De nauwkeurige en getrouwe reconstructie van deze registratie vormt het fundament van de magnetostratigrafie. De magnetostratigrafie van Laat Miocene sedimenten op verschillende lokaliteiten in het Middellandse Zeegebied is het belangrijkste onderwerp van deze dissertatie. De opeenvolging van de perioden met afwisselend normale en omgekeerde polariteit in het geologisch verleden vormt de magnetische tijdschaal.

In het eerste hoofdstuk worden verschillende methoden besproken om deze magnetische tijdschaal samen te stellen. De eerste methode bestaat uit het bepalen van zowel de radiometrische ouderdom als de polariteit van de NRM van stollingsgesteenten. Magnetische tijdschalen gebaseerd op deze methode zijn slechts betrouwbaar voor gesteenten met ouderdommen minder dan 5 miljoen jaar. Voor hogere ouderdommen neemt de absolute fout in radiometrische dateringen teveel toe. De tweede methode is gebaseerd op mariene magnetische anomalieen patronen. Ervan uitgaande dat spreiding aan weerszijden van Mid-oceanische ruggen met een relatief constante snelheid verloopt, kan een magnetische tijdschaal geconstrueerd worden door middel van interpolatie en extrapolatie. Aan de hand van radiometrische dateringen en biostratigrafie kan de tijdschaal gecalibreerd worden. De derde methode is gebaseerd op de magnetostratigrafie, biostratigrafie en chronostratigrafie van sedimentaire opeenvolgingen, bijvoorbeeld diepzee kernen.

In principe is het mogelijk het polariteitspatroon van mariene sedimenten in secties op het land te correleren met de magnetische tijdschaal. De voetangels en klemmen van deze laatste methode worden

besproken. In het algemeen vormt echter de magnetostratigrafie een belangrijk gereedschap voor de stratigrafie, niet alleen voor correlatie doeleinden, maar ook voor relatieve en zelfs absolute dateringen.

Mariene klei secties van Laat Miocene ouderdom zijn bemonsterd in Kreta, Sicilie en Noord Italie. Hoofdstuk twee beschrijft de geologie, lithologie en biostratigrafie van deze secties, alsmede de methode gevolgd bij het bemonsteren. De meeste secties zijn van Tortonien en Messinien ouderdom. Een belangrijke biostratigrafische datum, het eerste voorkomen van de *G. conomiozea* groep, kenmerkt de grens tussen Tortonien en Messinien in het Middellandse Zeegebied en is als voornaamste biostratigrafisch kenmerk gebruikt.

De laboratorium analyse van de verzamelde monsters wordt besproken in hoofdstuk drie. De karakteristieke remanente magnetisatie (ChRM) vertegenwoordigt het meest waarschijnlijk de originele depositionele remanente magnetisatie (DRM). Om deze ChRM te bepalen is het noodzakelijk visceuze en andere secondaire magnetisaties te verwijderen door middel van thermische of wisselveld demagnetisatie. Een nauwkeurige analyse van de demagnetisatie diagrammen en van de afname curves geeft informatie omtrent de dragers van de remanente magnetisaties. De resultaten maken het waarschijnlijk dat fijnkorrelige, vermoedelijk single-domain magnetiet of titanomagnetiet de belangrijkste drager is van de ChRM. Een geringe en gedeeltelijke oxidatie van de magnetiet wordt vermoed, met als resultaat een maghemiet fase van de ChRM die dezelfde richting heeft als de originele magnetiet. Verdere informatie wordt verkregen door de isothermale remanente magnetisatie (IRM) acquisitie curves en bevestigt de conclusies op basis van de demagnetisaties. In het algemeen leveren de resultaten van de secties op Kreta en in Noord Italie magnetische polariteits zoneringen op, terwijl daarentegen de resultaten van de secties op Sicilie te wensen over laten: remagnetisatie ten gevolge van verwering van de oorspronkelijke magnetische mineralen heeft een recente magnetisatie met normale polariteit veroorzaakt.

De magnetostratigrafie van de secties wordt besproken in hoofdstuk vier. Alle secties van west Kreta kunnen gecorreleerd worden op basis van hun overlappende polariteitsstratigrafie en hun biostrati-

grafie. De correlatie levert een samengestelde magnetische polariteitskolom bestaande uit een opeenvolging van zes polariteits zones. De relatieve lengtes van deze zones correleren uitstekend met de zones van een sectie op centraal Kreta en in mindere mate met die van een sectie op oost Kreta. De polariteitsstratigrafie van Kreta is gecorreleerd met de magnetische tijdschaal door de correlatie coefficienten te bepalen van het gevonden polariteits patroon en iedere mogelijke opeenvolging van zes polariteitszones van deze tijdschaal tussen 0 en 15 miljoen jaar. Van de drie aldus gevonden mogelijke correlaties blijft er slechts een over als de meest waarschijnlijke, op basis van biostratigrafische en chronostratigrafische randvoorwaarden. Deze correlatie houdt in een ouderdom van 5.6 miljoen jaar voor het eerste verschijnen van de *G. conomiozea* groep en dus voor de Tortonien-Messinien grens in het Middellandse Zeegebied.
Dezelfde correlatiemethode toegepast op de resultaten van de Blind River in nieuw Zeeland (Loutit en Kennett, 1979) levert een ouderdom op van 6.1 miljoen jaar voor het eerste verschijnen van de *G. conomiozea* aldaar. Tussen het eerste verschijnen van *G. conomiozea* in Nieuw Zeeland en het verschijnen van de *G. conomiozea* groep in het Middellandse Zeegebied lijkt dus een diachronie van ongeveer 0.4. miljoen jaar te bestaan. Tevens worden de ouderdommen van nog twee biostratigrafische datums in het Middellandse Zeegebied afgeleid; tenslotte kan geconcludeerd worden dat het begin van de 'Messinian main evaporitic phase' jonger is dan 5.3 miljoen jaar.

Een andere bron van informatie omtrent de dragers van de NRM wordt verschaft door gesteentemagnetische parameters. Deze worden besproken in hoofdstuk vijf. Als een standaardprocedure is de magnetische susceptibiliteit (X) en de remanente verzadigingsmagnetisatie (SIRM) gemeten. De verhouding X/SIRM is grotendeels onafhankelijk van de concentratie van de magnetische mineralen (Hartstra, 1982) en duidt in de meeste secties op fijnkorrelige (single-domain) magnetiet als de belangrijkste drager van de ChRM. Voor een aantal secties is tevens de remanente coercitiefkracht bepaald. De gevonden waarden bevestigen de conclusies gebaseerd op de X/SIRM ratio; bovendien werd op deze manier extra informatie verkregen omtrent het voorkomen van mineralen met een hoge coerciviteit tengevolge van oxidatie.

In het laatste hoofdstuk (zes) zijn de richtingen van de karakteristieke remanente magnetisatie geanalyseerd. In het algemeen blijkt dat de inclinaties lager zijn dan de inclinatie van het axiale geocentrische dipoolveld voor de huidige ligging van Kreta. Ten gevolge van de vorm en de eigenschappen van de klei mineralen, zullen de daaraan gekoppelde (verdeling van) magnetische mineralen geneigd zijn zich horizontaal uit te richten bij gravitationele compactie, en dus lagere inclinaties veroorzaken.
Declinaties wijzen in het algemeen op rotaties van de bemonsterde locaties tegen de klok in. De gemiddelde declinatie van één van de gevonden polariteitszones vertoont een westelijke afwijking ten opzichte van de declinaties van de andere polariteitszones. Dit wordt vermoedelijk veroorzaakt door een afwijkende (regionale ?) richting van het aardmagneetveld gedurende deze periode.

Een analyse van de magnetische susceptibiliteits anisotropie wijst op een duidelijk sedimentair magnetisch maaksel. Kleine, maar persistente lineaties zijn vermoedelijk het gevolg van recente extensionele tektoniek in het Aegeisch gebied, en niet het gevolg van depositionele factoren.

SUMMARY

Reversals of the geomagnetic field in the geological past are recorded globally in the natural remanent magnetization (NRM) of igneous and sedimentary rock sequences. The accurate and reliable reconstruction of this record is the basis of magnetostratigraphy. The magnetostratigraphy of Late Miocene sediments at several locations in the Mediterranean area is the main subject of this study.

In the first chapter several methods for determining the polarity reversal time scale are discussed. The first method involves combining radiometric dating and the magnetic polarity of igneous rocks. Polarity reversal time scales based on this method are reliable only for rocks with ages less than 5 million years (Ma) because of the progressive absolute errors in radiometric dating. The second method is based on sea-floor magnetic anomaly patterns. If one assumes a relatively constant spreading rate for the sea-floor, a polarity time scale can be constructed by interpolation and extrapolation. The time scale can be calibrated by radiometric dating and through biostratigraphic evidence. The third method is based on the magnetostratigraphy, biostratigraphy and chronostratigraphy of sedimentary sequences, e.g. deep-sea piston cores.

In principle, it is possible to correlate the polarity pattern of marine sediments in land-based sections to the polarity time scale. The pitfalls associated with this latter method are discussed. In general, however, magnetostratigraphy is an important tool not only for correlation purposes, but also for relative or even absolute dating.

Marine clay sections of Late Miocene age were sampled in Crete, Sicily and northern Italy. Chapter two describes the geology, lithology and biostratigraphy of these sections, as well as the sampling method. Most sections are of Tortonian and Messinian age. An impor-

tant biostratigraphic datum, the first occurrence datum (FOD) of the *G. conomiozea* group, denotes the Tortonian-Messinian boundary in the Mediterranean area and has been used throughout as the major biostratigraphic correlation tool.

The laboratory treatment of the samples is discussed in chapter three. In order to determine the characteristic remanent magnetization (ChRM), which most probably represents the original depositional remanent magnetization (DRM), it is necessary to remove viscous and other secondary remanences by means of alternating field and thermal demagnetization. A careful analysis of the demagnetization diagrams and decay curves yields information concerning the carriers of the remanent magnetizations. The results indicate that fine-grained, probably single-domain magnetite or titanomagnetite is the main carrier of the ChRM. There is evidence that a slight and partial oxidation of the magnetite occurred, resulting in a maghemite phase of the ChRM which has the same remanence direction as the original magnetite. Additional information is provided by isothermal remanent magnetization (IRM) acquisition curves and corroborates the conclusions derived from the demagnetizations. In general, the results from the Cretan and northern Italian sections yield reliable magnetic polarity sequences, whereas the results of the Sicilian sections are less satisfactory: remagnetization due to weathering of the original magnetic minerals has caused a recent overprint of normal polarity.

The magnetostratigraphy of the sections is discussed in chapter four. All western Cretan sections can be correlated on the basis of their overlapping magnetostratigraphy and their biostratigraphy. The correlation yields a composite magnetic polarity stratigraphy consisting of six successive and reliably determined polarity zones. The relative lengths of these zones correlate excellently with those of a single central Cretan section and to a lesser extent with those of an eastern Cretan section. Several other eastern Cretan sections cannot be correlated with the other sections since they have no overlap. We correlated the Cretan polarity stratigraphy with the magnetic polarity time scale by determining the correlation coefficients of this sequence and every sequence of six polarity zones of this time scale between 0 and 15 Ma. Three possible correlations are found, but only one can be regarded as the most probable, on the

basis of the conditions imposed by the biostratigraphy and chronostratigraphy. This correlation provides an age of 5.6 Ma for the FOD of the *G. conomiozea* group and hence for the Tortonian-Messinian boundary in the Mediterranean area. Following the same correlation method, the FOD of *G. conomiozea* in New Zealand can be dated at approximately 6.1 Ma; hence there seems to be a diachrony of 0.4 Ma between the respective FOD's of this datum.
Furthermore, the approximate ages of two more biostratigraphic datums in the Mediterranean are derived and a lower age limit of 5.3 Ma can be inferred for the beginning of the Messinian evaporitic phase.

Another source of information concerning the magnetic minerals of the NRM is supplied by rock-magnetic parameters. As a standard procedure the magnetic susceptibility X and the saturation isothermal remanent magnetization (SIRM) were determined, and these are discussed in chapter five. The ratio X/SIRM is largely independent of the concentration of the magnetic minerals and gives an indication concerning the grain sizes of the magnetic minerals. In most sections this ratio is virtually constant and indicates the presence of fine-grained (single-domain) magnetite as the main carrier of the ChRM. For a number of sections the remanent coercive force (Hcr) was determined. The values of this parameter support the conclusions based on the X/SIRM ratio; in addition, extra information concerning the presence of high coercivity minerals due to oxidation was gained.

The last chapter (six) contains an analysis of the ChRM directions of several of the Cretan sections. In general, inclinations are lower than inclinations of the axial dipole geocentric field at the present latitude of Crete. Due to the shape and the properties of the clay minerals, the magnetic minerals carrying the remanence will tend to align horizontally upon gravitational compaction, thus causing these low inclinations. In these sections declinations generally but not always indicate counter-clockwise rotations of the locations sampled. These rotations are due to local tectonics rather than to a rotation of Crete itself. The mean declination of a particular polarity zone tends to show a westerly offset with respect to the mean declinations of the other polarity zones. This is probably

due to a deviating (regional ?) direction of the geomagnetic field during this period.

An analysis of the magnetic susceptibility anisotropy in a number of sections reveals a predominantly depositional magnetic fabric. Small but persistent lineations are thought to be due to a recent extensional tectonic regime in the Aegean area, and not to depositional factors.

chapter one

INTRODUCTION

Reversals of the polarity of the geomagnetic field in the geological past are recorded globally in the natural remanent magnetization (NRM) of igneous and sedimentary rock sequences.

The discovery of polarity reversals of the geomagnetic field is attributed to Brunhes (1906), who studied the NRM of lavas at two different locations and found normal polarity NRM's at one and reversed polarity NRM's at the other. Some twenty years later, Matuyama (1929) found that recent lavas showed normal polarity, whereas older lavas showed reversed polarity and he attempted to date the most recent reversal. Theories concerning self-reversal mechanisms (e.g. Neèl, 1955) delayed the general acceptance of the field-reversal theory until the sixties. The development of the K/Ar dating technique enabled Cox et al. (1963a,b) to propose a geomagnetic polarity reversal time scale based on direct paleomagnetic measurements and K/Ar dates of volcanic rocks. A more precise polarity time scale for the last 4.5 Ma was given by Cox (1969). Major polarity zones were referred to as "polarity epochs" (the Brunhes, Matuyama, Gauss and Gilbert epochs), in which shorter "polarity events" occurred, e.g. the normal Jaramillo and Olduvai events in the Matuyama reversed epoch. A review of the early development of the radiometrically determined polarity time scale is given by Watkins (1972). Because of the continual addition of new data and a revision of the decay constants used in K/Ar dating, this time scale has been extended, refined and revised many times (e.g. Mankinen and Dalrymple, 1979). Because the error in K/Ar dating is approximately 1-2%, polarity zones older than 5 Ma cannot be dated reliably, since the error may become larger than the duration of individual polarity (sub)zones.

The hypothesis of sea-floor spreading (Hess, 1960) and the existence of polarity reversals were combined by Vine and Matthews

(1963) into one single theory, and they suggested that sea-floor magnetic anomalies might be related to geomagnetic polarity reversals. The observed sea-floor magnetic anomaly patterns could then be used to extend the polarity time scale into the Mesozoic by extrapolation. On the assumption of a constant spreading rate, Heirtzler et al. (1968) used a long magnetic profile in the South Atlantic to construct such a time scale. The positive and more prominent anomalies were numbered from young to old. Numerous additions and revisions have been made since then and more advanced techniques have made many refinements possible. The results of the Deep Sea Drilling Project (DSDP) which combined biostratigraphic and radiometric data of deep-sea sediments, have confirmed the general validity and accuracy of such time scales. Ness et al. (1980) presented a comprehensive and critical review of marine magnetic anomaly time scales. They also constructed a synthesis of previously published time scales, using two calibration points in addition to the present and based on direct paleomagnetic and radiometric age determinations, recalculated for the new K/Ar decay constants (Mankinen and Dalrymple, 1979). One calibration point is the Gauss-Gilbert boundary at 3.40 Ma, the other is the lower boundary of anomaly 5 at 10.30 Ma. They used two more calibration points which were based on biostratigraphic evidence and which were essentially indirect. More recently, Lowrie and Alvarez (1981) employed eleven calibration points, nine of which were determined by directly correlating the combined biostratigraphic and magnetostratigraphic data of Umbrian sections with the polarity time scale based on sea-floor anomalies. Indirectly, the absolute ages of biostratigraphic datum-levels (e.g. such as compiled by Hardenbol and Berggren, 1978) are then assigned to these calibration points and the magnetic anomaly time scale is adjusted.

Whereas lava successions provide an essentially intermittent record of the polarity reversal pattern of the geomagnetic field, deep-sea (piston) cores may reveal a continuous record. Combined biostratigraphic and magnetostratigraphic data can also be obtained from such cores. Since the top of deep-sea cores always contains the most recent sediments and hence represents the most recent polarity zone (Brunhes), it is possible to determine the polarity zones by simply counting downwards providing there are no hiatuses or gaps.

If one assumes a fairly constant sedimentation rate, then continuously deposited sediments in those cores can be used to date short (recent) "events" more precisely than is the case with volcanic outcrops (Opdyke, 1969). The continuous sedimentation and absence of hiatuses can be checked by means of biostratigraphy and radiometric dating, e.g. 14C-dating, K/Ar dating of volcanic ash layers or fission track dating (see also Opdyke, 1972). If piston cores are long and have a low sedimentation rate it may be possible to extend the radiometrically determined polarity reversal sequence and to assign extrapolated ages to the reversal boundaries. Foster and Opdyke (1970) used cores RC 12-65 and RC 12-66 from the central Pacific and arbitrarily divided polarity zones and subzones into magnetic "epochs" and numbered them in order of increasing age (up to epoch 11 in core RC 12-65).
Biostratigraphic correlations can then be used to extend the reversal sequence even further by correlating cores extending to older sediments. It is clear, however, that the reliability of the polarity zonation may be significantly reduced, due to sedimentary and faunal uncertainties.

In principle, once the relation between biostratigraphy and magnetostratigraphy has been established, it should be possible to tie the polarity pattern of marine sediments from land-based sections to the polarity time scale. However, if biostratigraphic datum-levels are diachronous, problems arise. Also, if only or mainly biostratigraphic data or criteria are used to construct a polarity pattern, determination of the polarity zones seems superfluous (e.g. Cita and Ryan, 1973, 1979; Ryan and Flood, 1973; Ryan, 1973; see also Kenneth and Watkins, 1974).
Further confusion is introduced when a polarity zonation is given, but no direct paleomagnetic determinations have been carried out and this zonation is based only on biostratigraphic correlation with an existing magnetobiostratigraphic sequence elsewhere. (e.g. van Gorsel and Troelstra, 1981).
To avoid circular reasoning it is therefore extremely important to examine carefully the various methods by which the various correlations have been made. The most reliable method is to determine directly both the biostratigraphy and magnetostratigraphy of a sequence, either a deep-sea core or a land-based sedimentary section,

and to correlate this sequence with the polarity time scale which is based solely on sea-floor anomalies. This latter polarity time scale can be assumed to represent the most continuous record of the polarity history of the geomagnetic field, since the relative constancy of sea-floor spreading rates has been conclusively demonstrated in the linear relationships found in anomaly versus distance plots of numerous ridge pairs (Ness et al., 1981). Correlation can then be done either by counting from the present (=Brunhes chron) downwards or by recognizing a clear and specific polarity pattern. A good example of such a "fingerprint" is given by Alvarez et al. (1977) for the Gubbio section in Italy, where the Cretaceous long normal zone could easily be recognized, and younger polarity zones could be established by counting upwards. In such a way biohorizons and biozonations can be tied absolutely to the marine magnetic anomaly time scale and a synchrony or diachrony of biohorizons can be demonstrated.
Such a direct correlation can then provide calibration points if the absolute ages of biostratigraphic datum-levels, if known and preferably from the same region, are assigned to the polarity time scale. It should be emphasized, however, that the ages of biostratigraphic and magnetic zones (and magnetic anomalies) ultimately depend on the extent and accuracy of radiometric dating (LaBrecque et al., 1977).

In conjunction with the paleontology and stratigraphy department of the State University of Utrecht and as part of the International Geologic Correlation Program (IGCP) project 74/1/1, "Accuracy in time", a research was started into the usefulness, the potentialities and the restrictions of magnetic stratigraphy in land-based sections of marine sediments in the Mediterranean Area (fig. 1.1).

In the past five years, magnetic polarity stratigraphy of land-based sections has become an important tool for stratigraphic correlation and for relative or even absolute dating of sedimentary sequences. The global and synchronous nature of polarity reversals can be used to check the synchrony of various geological and biostratigraphic boundaries, to correlate marine and non-marine sequences or it can be used to obtain information about tectonic and sedimentologic processes (Ensley and Verosub, 1982).

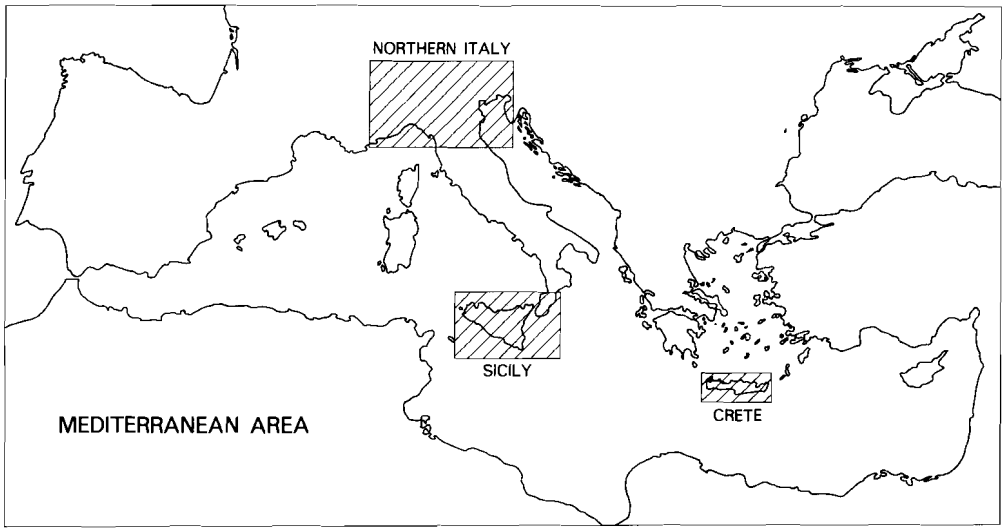

Fig. 1.1 Locations of the regions of interest in the Mediterranean area.

There are many pitfalls associated with magnetostratigraphic methods, which are already used frequently for correlation purposes. Each normal and each reversed polarity zone is identical with other normal and reversed polarity zones and the polarity of the natural remanent magnetization alone is not a distinguishing feature. When there is a high frequency of polarity changes with respect to the biostratigraphic zones, recognition of the individual polarity zones in distributed and restricted outcrops is almost impossible. However, because of differences in the duration of individual polarity zones, polarity reversal sequences can be used for stratigraphic correlations, provided the (magneto)stratigraphic range is long enough for a specific polarity pattern (fingerprint) to be recognized. Furthermore, there must not have been complications in the sedimentary record (unless they can be estimated or are known) such as variation in the sedimentation (accumulation) rate, hiatuses, gaps, faults, erosion, chemical changes, magnetic instability, etc.

Variations in sedimentation rate may alter the original and specific polarity patterns, but the recognition of the pattern will depend on the extent of the variations and on the characteristics of

the pattern.

The effects of faults and hiatuses are evident: parts of the polarity record may be missing or duplicated. In the massive and non-stratified clays studied in this thesis faults are sometime difficult to recognize due to the near absence of distinctly bedded layers. Their existence, however, could sometimes clearly be inferred from the magnetostratigraphic results. For instance, the coincidence of a biostratigraphic datum-level and a polarity reversal horizon may often be due to faulting.

Between original deposition and eventual sampling, sediments may encounter different environments and a range of chemical changes may occur, causing precipitation or alteration of (magnetic) minerals (Watkins et al., 1974), for instance because of weathering. The original magnetization acquired during deposition may then have been overprinted or even superseded by secondary magnetizations of younger (often recent) age. In some cases only distinct lithologic levels may be found to have a natural remanent magnetization of secondary origin, thus giving a false polarity pattern.

Not all kinds of sediments are suited for paleomagnetic research. Magnetic minerals may be near absent or unstable, i.e. may produce magnetizations with (geologically) very short relaxation times. The development of sensitive cryogenic magnetometers has made possible measurement of weakly magnetized samples. Low intensities may also have been caused by oxidation due to weathering of the original magnetic minerals.

It is clear that a careful analysis and interpretation of the magnetic properties is advisable or even necessary. A thorough analysis of changes in direction and intensity during systematic demagnetization is needed (Zijderveld, 1967, 1975) in order to determine the direction of the characteristic and probably original remanent magnetization.

For this study marine clay sections of Late Miocene age were sampled in Crete, Sicily and northern Italy. Crete was chosen because we had detailed information about the Neogene sedimentary-tectonic history (Freudenthal, 1969; Meulenkamp, 1969, 1979; Meulenkamp et al., 1979) and the biostratigraphy (Sissingh, 1972; Zachariasse, 1975). Initial sampling was focused on two Tortonian-Messinian clay sections in western Crete (Langereis and Zijderveld,

1979; Langereis, 1979; Drooger et al.,1979a). Later, more sections were sampled in western and central Crete (Langereis et al., 1984) as well as in eastern Crete, in order to check the initial results, to eliminate local variations in sedimentation rate, to notice (and eliminate) the effect of hiatuses or faults and to extend the stratigraphic range of the initial polarity reversal sequences. To check the Cretan results over a large distance, sections in Sicily and northern Italy were sampled, which were supposed to contain the Tortonian–Messinian boundary. This boundary in the Mediterranean is currently marked by the first occurrence datum (FOD) of *G. conomiozea* (d'Onofrio et al., 1975; Colalongo et al., 1979b).

In addition to the remanence data and the magnetic properties, the magnetic anisotropy of the susceptibility may yield information concerning the magnetic fabric of the sediments and reveal some of their magnetic history since deposition. Sediment transport or water and/or bottom currents may be reflected in the magnetic fabric (Rees, 1961, 1965). A fabric which was originally purely sedimentary may be changed by tectonic activity into a more or purely tectonic fabric (Graham, 1966; van den Ende, 1977). Since tectonic activity and depositional currents may sometimes result in the same magnetic fabric, it is sometimes necessary to determine the anisotropy directions over a larger region and to compare these with paleocurrent or stress directions obtained from indicators other than magnetic ones.

Other correlation data might be provided by changes in the direction and the intensity of the primary natural remanent magnetization. Such directional changes are either a consequence of secular variation or are due to longer term variations, e.g. 10,000 to 100,000 years (van den Ende, 1977). The secular variation has a period which is too short to be of stratigraphic value for the clay sequences studied. Long-term variations which may be related to astronomical parameters can be tentatively established in several sections.

The detailed magnetostratigraphic results from western Crete were also used to locate accurately polarity reversal horizons, which were or still are being studied in detail (Valet and Laj, 1981; Valet et al., 1983) in order to test geomagnetic reversal

models (Hoffman, 1982 and references therein). Because of a favourable sedimentation rate (ca. 4 cm/1000 years), detailed records of transitional remanence directions can be established. Since a typical geomagnetic reversal takes place in 40-50 cm of sediments, detailed sampling is likely to reveal transitional NRM directions. The existence of transitional directions can be used to distinguish a true reversal from a fault or from remagnetized strata. Furthermore, the lowered intensity of the geomagnetic field during a polarity transition is reflected in the lower intensities of the natural remanent magnetization recorded in the sediments. Therefore, a lowered intensity of the characteristic natural remanent magnetization at or near a polarity reversal boundary can be taken as an indication of a true reversal, provided that magnetic properties indicate no (major) change in the magnetic minerals at such a boundary. So far, results of detailed studies of polarity transitions have not indicated that this method is a practical correlation tool, but they are a major source of information about the generation of the magnetic field.

chapter two

THE SECTIONS

INTRODUCTION

The magnetostratigraphic study presented here was started by sampling two pilot sections in Late Miocene marine clays on the island of Crete (Greece), using a large sampling interval of 4 metres. One section with a thickness of 150 metres is situated near the village of Apostoli (Meulenkamp, 1969, 1979a; fig. 2.1) in the province of Rethymnon, another section with a thickness of 40 metres near the village of Potamida (Freudenthal, 1969) in the province of Chania (fig. 2.2). Although both sections are assumed to be partially overlapping in time (Meulenkamp, 1979a), the Apostoli section showed only normal polarities, whereas the Potamida section was found to embrace at least four polarity zones. Apparently the NRM in the Apostoli section has been overprinted by normal polarity and probably (sub)recent magnetizations. Thereupon, attention was focused on section Potamida, which was resampled in detail. Later, more sections in similar Late Miocene marine clays were sampled in the neighbourhood of the first Potamida section (fig. 2.2) and in other parts of western Crete, on central and eastern Crete (fig. 2.1), on Sicily (fig. 2.3) and in northern Italy (fig. 2.4).

Initially we were most interested in sections that contained the first occurrence datum (FOD) of the *G. conomiozea* group and that were situated geographically at an increasing distance from the Potamida section. We wanted to check whether such a datum level could be followed magnetostratigraphically, both in space and time. As our study progressed and a positive magnetobiostratigraphic correlation could be established in western Crete (Langereis, 1979; Langereis and Zijderveld, 1979), we sampled sections for the purpose of extending the stratigraphic range beyond that of the initial

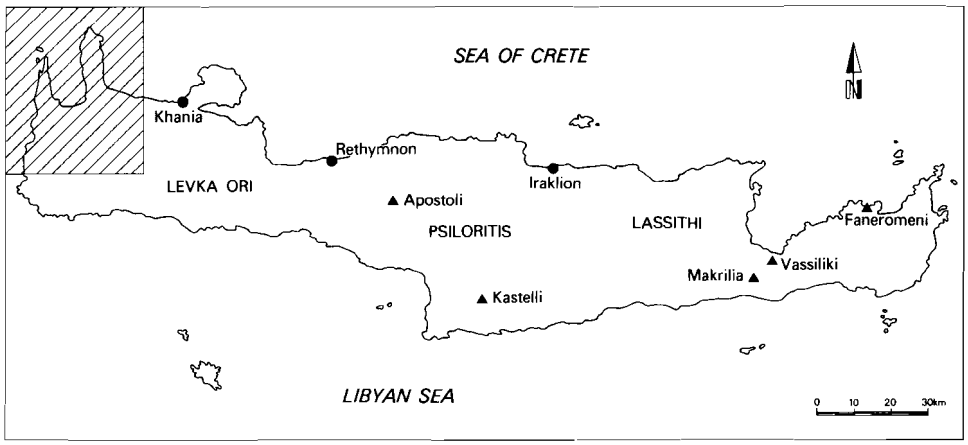

Fig. 2.1 Locations of the Cretan section outside western Crete. For hatched area see detailed map of figure 2.2

sequences and in order to arrive at a detailed geomagnetic polarity stratigraphy for the upper part of the Mediterranean Upper Miocene (see also Langereis et al., 1984). The study reported here is based on more than 20 sections.

In western Crete, four sections are located near the village of Potamida (sections Potamida 1,2,3,4) in the Kissamos district of Chania Province. Two sections are located near the village of Kotsiana, some 2.5 km to the NE (sections Kotsiana 1,2), one is located near the village of Skouloudhiana, 1.5 km SW of Potamida. One more is situated near the village of Episcopi some 4 km east of Kotsiana (section Episcopi, together with 'sections' Episcopi Resampling and Episcopi Extension in the same outcrop) and one near the village of Vasilopoulo, ca. one kilometer south of Episcopi (section Vasilopoulo). The last section in western Crete is located near the village of Makronas (section Makronas) (fig. 2.2).

In central Crete two sections are located near the village of Kastelli (sections Kastelli 1,2; fig. 2.1). A section near the village of Apomarma, several kilometres from the Kastelli sections, could not be sampled in sufficient detail due to the sediment being too friable.

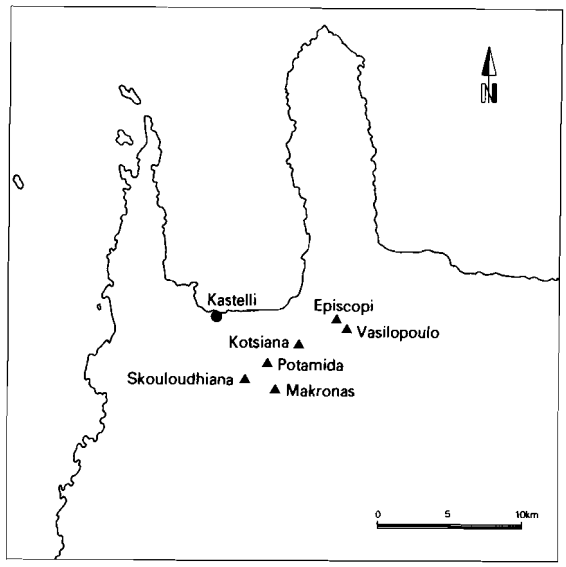

Fig. 2.2 Locations of the western Cretan sections.

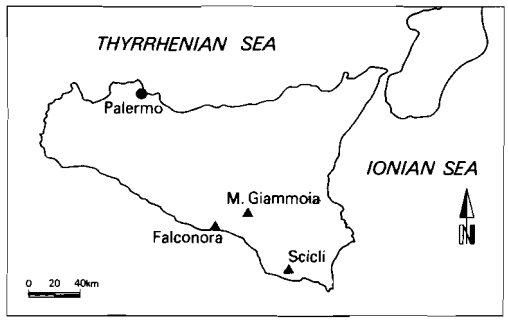

Fig. 2.3 Locations of the Sicilian sections.

In the Ierapetra district of eastern Crete one section was sampled near the village of Vassiliki (section Vassiliki) and one near the village of Makrilia (fig. 2.1).
In the Sitia district of eastern Crete one section was sampled near the monastery of Faneromeni (section Faneromeni) (fig. 2.1).

In Sicily (fig. 2.3) two sections were sampled in the Caltanisetta basin (see also Colalongo et al., 1979a), one near Stazione di Falconara (section Falconara) and one on the southern slopes of Monte Giammoia (section Giammoia). Two more sections were sampled on the Ragusa platform near the village of Scicli (sections Scicli South and Scicli West) (fig. 2.3).

In northern Italy (fig. 2.4) one section is located near the village of Mussotto just north of Alba in Piemonte (section Mussotto) and one more near the village Castellania in the Tortonian type area (section Castellania). A pilot section has been sampled near the village of Luzzena (cf. Borsetti et al., 1975), just south of Cesena (section Luzzena).

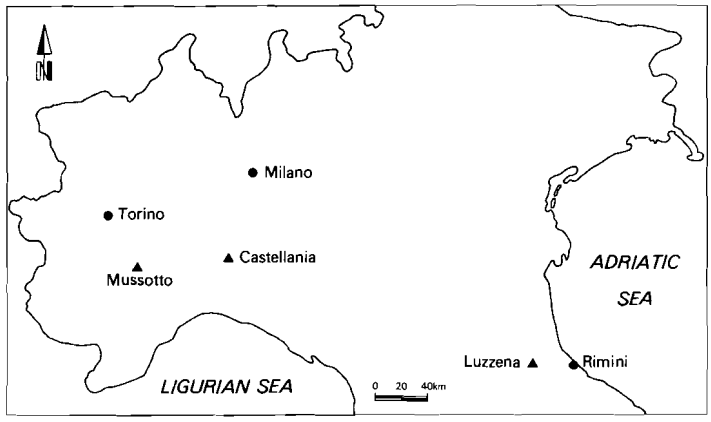

Fig. 2.4 Locations of the northern Italian sections.

GEOLOGY AND LITHOLOGY

Crete

The sedimentary history and the structural development of Crete during the Tortonian and Early Messinian were fundamentally the same all over the island. Paleogeographic configurations and sedimentation during this period were mainly defined by two major tectonic events, one in the Early Tortonian and one during the Tortonian-Messinian boundary interval. The accumulation of terrigenous clastic

deposits in graben-like depressions during the Tortonian was followed by an overall submergence and a more calcareous sedimentation after the transition from the Tortonian to the Messinian (Meulenkamp et al., 1979).

In western Crete coarse clastic sediments and bioclastic limestones of Tortonian Age unconformably overlie pre-Neogene rocks. These deposits accumulated in a narrow strip along the margins of the subbasins and along and on top of submarine ridges; sediment transport was mainly in a northward direction (Meulenkamp, 1979a; Meulenkamp et al., 1979). The sections used for our study in western Crete were in open-marine, homogenous blue-grey clays which had been deposited in the more central parts of those subbasins. The clays are overlain by shallow marine, alternating homogenous-laminated, beige to whitish marls of Messinian Age (see also van der Zwaan, 1982).

In central Crete the basal part of the Upper Miocene consists of a rapidly alternating sequence of marine, brackish and lacustrine sediments from Early Tortonian to Tortonian-Messinian Age. In the upper part of this sedimentary sequence sections Kastelli 1 and 2 were sampled. These sections are composed of open-marine, homogenous and blue-grey clays with some sandy interbeds. Upwards these clays are followed by an alternating homogenous-laminated marl succession of Messinian Age, which in turn is overlain by a thick sequence of evaporites (Meulenkamp et al., 1979).

In the Ierapetra district of eastern Crete the Early Tortonian tectonic phase caused the formation of a deep-water turbidite basin. The northern part of this basin was rapidly filled up by fan-like deposits from the north. In the deepest, more southern part of the basin, sediments with intercalated turbidites were deposited from a western source area (Fortuin, 1977). These sediments were sampled in the Makrilia section and consist of alternating bluish marls/clays and brownish, generally positively graded sands. In section Vassiliki the sediments consist predominantly of blue to purple marls-clays with only a few turbiditic interbeds, but according to Fortuin (1977) they are part of the same formation found in section Makrilia. The sediments overlying the turbidites are composed of

yellow-grey, homogenous or laminated marls alternating with sandy bioclastic limestone, similar to the type of sediments overlying the western Cretan sections, and according to Fortuin (1977) of Tortonian to Messinian Age.

In the Sitia district of eastern Crete the Late Miocene sedimentary history consists of a predominantly terrigenous clastic sedimentation, followed by a mainly calcareous deposition, as observed in the rest of Crete. In the north-western Sitia district the terrigenous clastics are mainly restricted to the western margin and decrease rapidly in thickness to the east; these sediments are of Tortonian Age (Gradstein, 1973). In section Faneromeni 45 metres of these sediments could be sampled, consisting of blue-grey homogenous marls, which were frequently silty.

Sicily

Sections Falconara and Giammoia are located close to the eastern border of the Caltanisetta basin. This basin includes central-southern Sicily and rapidly subsided during the Neogene. Large scale gravity sliding from the north in the Early to Middle Miocene resulted in the deposition of the (allochtonous) "argille scagliose". During the Middle and Late Miocene clastic, open-marine sediments accumulated. Tectonic instability, which began already in the Tortonian, characterized the Tortonian-Messinian boundary interval and resulted in the differentiation of the large Caltanisetta basin. Sediments changed from clay-marl to diatomite-marl sequences. The Messinian is transgressive and fast lateral changes in sediment thickness suggest tectonic differentiation between rapidly and slowly subsiding blocks (Meulenkamp et al., 1981). An overall regression from north to south in the Caltanisetta basin since Pliocene times was connected with a rapid subsidence of the more southern area and an increase of the basin-slope gradient. This caused large scale gravity sliding and intense folding of parts of Neogene sequences. In sections Falconara and Giammoia the "argille scagliose" is overlain by blue-grey marls, regularly interbedded with brown, sometimes laminated clays. These sediments grade into a sequence of white, finely laminated diatomites alternating with light-brown marls in the top of the section (Colalongo et al., 1979a; van der Zwaan,

1979, 1982). The sediments are severely fractured because of the above-mentioned gravity sliding and show gypsum needles along the numerous joints.

Sections Scicli South and Scicli West are located on the Ragusa platform of SE Sicily, the geological history of which differs from that of the Caltanisetta basin. In Early Miocene time mainly carbonates and during the Tortonian mainly open-marine marls and clays were deposited, followed in the Messinian by bioclastic limestones with locally some evaporites. Basaltic intercalations occur in Tortonian-Messinian transitional sediments and in the Pliocene limestones (Meulenkamp et al., 1981).
The lithostratigraphic units in the region of Scicli differ somewhat from this general picture. According to diGrande (1975) they are associated with a single sedimentary cycle of Late Eocene to Late Miocene Age. Messinian deposits show a mainly marly facies of normal open-marine environment, not very different from the Tortonian deposits. Section Scicli South corresponds to the "Ex Cava A.B.C.D." described by diGrande and Romeo (1975). The lower part of the section consists of blue-grey clayey marls and is overlain by distinctly bedded light-coloured marls. According to diGrande and Romeo (1975) the Tortonian-Messinian boundary is present approximately at the transition between these two sedimentary units. However, Zachariasse (personal communication) reports the occurrence of the *G. conomiozea* group throughout the section, which is therefore clearly of Messinian Age according to the proposal of d'Onofrio et al. (1975; see also Colalongo et al., 1979b). Section Scicli West was sampled in a still actively exploited claypit west of Scicli and consists of homogenous, dark-green clays, interbedded with brown-black clay levels at irregular intervals. Towards the top of the section the clay becomes more calcareous and light coloured. The section appeared to be of Serravallian to Early Tortonian Age (fig. 2.5).

Northern Italy

Both the Castelliana and the Mussotto sections are located in the Piedmont basin, which is one of the main depositional areas forming a single, large basin parallel to the Apennines axis (for a

general paleogeographic picture, see Borsetti et al. 1975). The Castellania section is located in the south-eastern part of the Tertiary basin of Piedmont in the type area of the Tortonian Stage (Rio Mazzapiedi; Gianoti, 1953; see also Cita, 1969). The section runs parallel to the Ripa dello Zolfo section of Colalongo et al. (1979a). The sedimentary sequence consists of blue-grey clayey marls overlying sandy marls.

In the western part of the Piedmont basin, the Mussotto section corresponds to the lower part of the Mussotto section as described by Sturani and Sampo (1973; see also d'Onofrio et al., 1975). The sediments are of Tortonian Age and consist of homogenous and open-marine clays rapidly alternating with laminated marls and clays and are overlain by mainly silts and silty marls.

The Luzzena section is described by Borsetti et al. (1975) and is located in the Peradriatic basin, another of the main depositional areas along the Apennines. The section consists essentially of clays and finely laminated silts. Sandy layers with a turbiditic character occur. The section consists of sediments of the post-evaporitic phase (Lago Mare phase in italian literature) and at the base of the section gypsum is present, which is (or has been) quarried.

BIOSTRATIGRAPHY

The sections used for designing a detailed polarity stratigraphy for the Upper Miocene of Crete were selected on the basis of biostratigraphic correlations made by Zachariasse (personal communication). Figure 2.5 shows the position of the sections sampled for this study with respect to major biostratigraphic datum levels in the Mediterranean Upper Miocene.

Intra-Mediterranean biostratigraphic control in the Upper Miocene is rather poor, compared to the Middle Miocene and Pliocene. Commonly three planktonic foraminiferal biohorizons are used to subdivide the Mediterranean Upper Miocene. The first occurrence datum (FOD) of *N. acostaensis* corresponds with a level slightly above the base of the Tortonian and the FOD of *G. conomiozea* is cur-

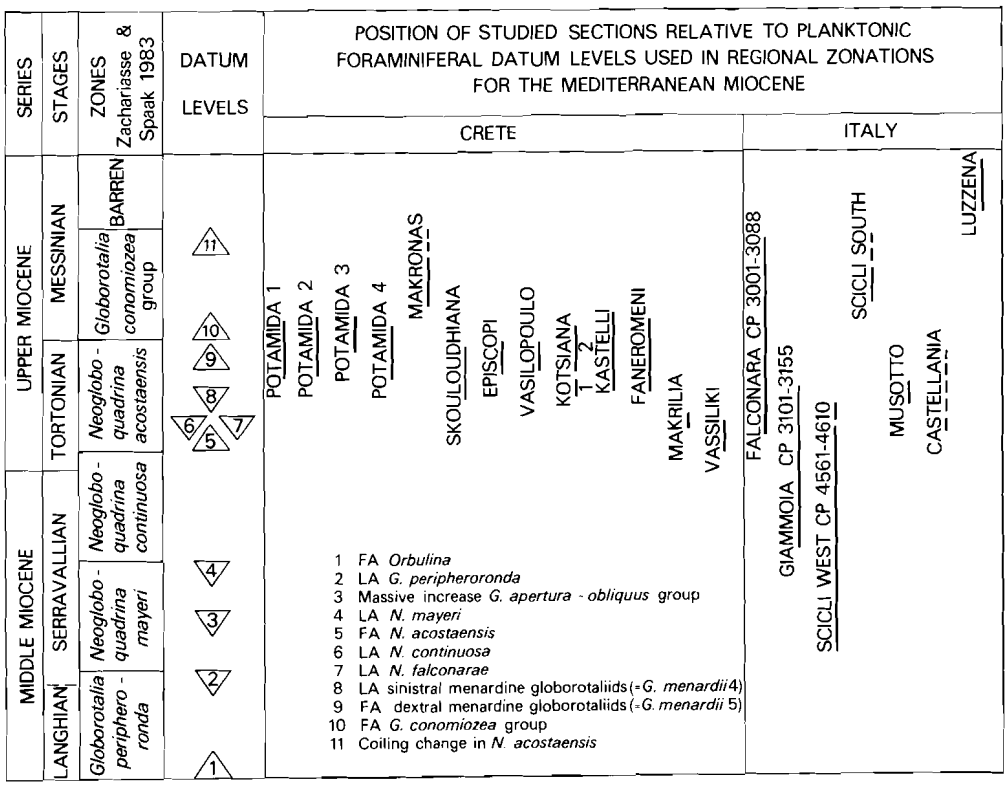

Fig. 2.5 Position of the sections with respect to some important biostratigraphic datum levels in the Late Miocene.

rently used to recognize the base of the Messinian (d'Onofrio et al., 1975; Colalongo et al., 1979). In a strict sense the FOD of *G. conomiozea* refers to the first occurrence of *G. conomiozea* types in the Mediterranean. If interpreted more broadly, this biostratigraphic event corresponds to the sudden spreading of left-coiled, planoconvex, keeled globorotaliids having on the average 4.5 crescent-shaped chambers (Zachariasse, 1979a, 1979b). This group of globorotaliids is labeled here and earlier as the *G. conomiozea* group and includes, in addition to the high-conical *G. conomiozea* type, forms such as the low-convex *G. miotumida* type and the 5-6 chambered *G. mediterranea* type.

The FOD of the *G. conomiozea* types, however, fluctuates relative to the entry level of the calcareous nannoplankton taxon *Reticulo-*

fenestra rotaria (Theodoridis, 1983) and is either coeval or to a certain extent younger than the FOD of the *G. conomiozea* group.

The sudden spreading of the *G. conomiozea* group in the Mediterranean most probably represents a migrational event (Zachariasse, 1979a, 1979b; Wernli, 1980) and constitutes a definite marker level in Late Miocene Mediterranean biostratigraphy.

The youngest biostratigraphic event in the Mediterranean Upper Miocene is a shift, from sinistral to dextral, in the coiling of *N. acostaensis*; this occurred in the Messinian sometime close to the beginning of the main evaporitic phase. All sections, with the exception of section Luzzena, are older than this coiling shift.

Generally, keeled globorotaliids occur in low frequencies and are distributed rather discontinuously in the Mediterranean Upper Miocene. Sinistral assemblages disappear somewhere in the Tortonian and, following a prolonged period of absence of keeled globorotaliids, dextral assemblages reappear in the record. The sinistral and dextral assemblages have been labeled as *G. menardii* form 4 and as *G. menardii* form 5, respectively (Tjalsma, 1971; Zachariasse, 1975, 1979a,b). In the Mediterranean this pattern is very consistent and allows for a subdivision of the Upper Tortonian into a lower zone with sinistral assemblages, an upper zone with dextral assemblages and an intermediate zone in which keeled globorotaliids are absent for a prolonged period.

An abrupt and instantaneous recurrence of sinistral keeled globorotaliids above the FOD of *G. menardii* form 5 was recorded purely by chance in sections Potamida 1 and 3 (fig. 2.5). These sinistral keeled globorotaliids are biometrically intermediate between *G. menardii* form 4 and *G. menardii* form 5 and the *G. conomiozea* group and occur only in a very limited stratigraphic interval of less than 50 cm. Their presence in other sections can therefore easily be missed due to the often larger (paleontologic) sampling interval.

Other major biostratigraphic datum levels which were encountered are, in progressively older sequence, the last occurrence datum (LOD) of *Neogloboquadrina falconarae* (Colalongo et al., 1979a), the LOD of *N. continuosa*, the FOD of *N. acostaensis* and finally, observed only in section Scicli West, the LOD of *N. siakensis*. This latter datum level is only slightly older than the FOD of *N. continuosa*.

Finally, it must be pointed out that although we tried to sample sections gradually extending to older sediments with each older section overlapping a younger one, a possible overlap could only be ascertained after studying the biostratigraphy. Unfortunately, it turned out that there was no overlap between the older sections (fig. 2.5).

SAMPLING

We sampled the homogenous clays and marly clays of all sections (generally) with the help of an electric drill, and took oriented cores of 25 mm diameter and up to 10-12 cm long. The power was supplied by a portable generator and water from a pressure tank was used as a coolant. During the first sampling trip a frame was used, which could be fixed in the clay, since it was assumed that a frame was needed in the friable clay. Later on, we gave up using a frame and cores were drilled by hand.

Generally, four cores were taken at each sampling level and were marked and oriented with a special orientation device, using an ordinary compass. The stratigraphic distances between sampling levels were determined accurately, using vertical (v) and horizontal (h) distance as well as the azimuth (a) between the successive sampling levels. If the strike (s) and dip (d) of the strata are taken into account, the stratigraphic distance (sd) between one sampling level and the next can be calculated according to

$$sd = v * \cos(d) + h * \sin(a-s) * \sin(d)$$

The method described above yields accurate stratigraphic positions of the sampling levels, also in (parts of) sections where the use of a tape measure may give rise to large errors (Langereis and Meulenkamp, 1979). Re-measuring of various parts of sections Potamida 1 and 2 showed that earlier results could be reproduced within one or two per cent. In several cases a theodolite was used to determine the stratigraphic thickness of the whole section as a check on the total of the inter-sample distances or to measure larger gaps in the sampling record (e.g. sections Skouloudhiana and Potamida 4).

Table 2.1 List of the sections and per section the number of sampling levels, the number of cores, the stratigraphic length in metres, the average sampling interval in cm and the sample code. Asterisks denote that paleontologic samples have been taken at every paleomagnetic sampling level, otherwise these samples have been taken independently and calibrated afterwards or sampling was restricted, for instance to every five paleomagnetic sampling levels.

section	levels	cores	length	interval	code
Potamida 1	96	374	38.90	40	KP
2	69	219	35.95	52	KP 100
3	45 *	178	24.95	55	KP 200
4	43 *	136	52.95	123	KB
Skouloudhiana	39 *	117	53.00	135	KS
Kotsiana 1	39	152	20.60	53	KO
2	71	282	35.90	51	KH
Episcopi 1&2	47	186	22.90	49	KE,KL
Res.	12 *	48	6.80	57	KE 100
Ext.	18 *	74	11.50	64	KE 200
Vasilopoulo	18 *	72	20.90	116	KV
Makronas	16 *	47	37.60	220	KG
Kastelli	66 *	267	45.80	69	KT
Vassiliki	42	163	18.40	44	KW
Makrilia	106 *	405	126.80	112	KM
Faneromeni	41 *	162	44.40	108	KF
Falconara	59	284	71.90	122	SF
Giammoia	67	286	78.70	117	SG
Scicli West	79 *	237	36.80	47	SW
South 1	23 *	67	10.50	46	SZ
South 2	16 *	48	5.90	37	SZ 100
Castellania	95 *	285	116.70	123	IC
Mussotto	12 *	36	13.60	113	IM
Luzzena	12 *	12			IL

Table 2.1 lists the sampling details of the sections used for this study. During the first sampling trips the sections were sampled in considerable detail, e.g. sections Potamida 1 and 2, sections Kotsiana 1 and 2, sections Episcopi 1 and 2 and section Vassiliki. This was done so that we could obtain a high enough resolution for determining the exact length of the polarity zones, and so that we would not miss short polarity subzones ("events"). On the basis of the results of the pilot sections, we decided to use a sampling distance which would yield a resolution of 10,000 years.

With some exceptions, later sections were sampled using a wider spacing, especially when it could be assumed that accumulation rates were higher, e.g. in sections Makrilia and Makronas. This was mainly done for reasons of economy in order to be able to sample more sections, both to validate the polarity zonation already found as well as to extend the magnetostratigraphy. From the initial results (Langereis, 1979) it was known that even if a somewhat wider spacing was used not too much magnetostratigraphic resolution would be lost.

As has been noted above, initially we were most interested in sections containing the FOD of *G. conomiozea*. In addition to the FOD of *G. conomiozea*, we found that the FOD of *G. menardii* form 5 and the FOD of *G. menardii* form 4 were useful for relative positioning of the sample series. However, generally the biostratigraphy was not known before, and paleontologic samples were taken as well in order to be able to determine the approximate position of the sections with respect to one another. In such cases sections were chosen on the basis of the geology, lithology and the biostratigraphic data available (Freudenthal, 1969; Meulenkamp, 1969; Gradstein, 1973; Zachariasse, 1975; Fortuin, 1977). It can be seen in figure 2.5 that this procedure was not always successful (sections Makrilia, Vassiliki, Sicli West, Mussotto).

In the sections Potamida 1 and 2 paleomagnetic samples were taken at close intervals (table 2.1); paleontologic samples were taken independently and the sampling levels were calibrated afterwards (Langereis and Meulenkamp, 1979). The sections are on the E and W side of a N-S running valley respectively, and direct lithostratigraphic correlation is not possible. However, thin ferruginous and sandy layers (1-5 cm) are present and a finely bedded clay layer forms the top of both sections. The magnetostratigraphic results confirmed the positive correlation of the layers (Langereis, 1979). The finely bedded clay could be used for direct correlation with section Potamida 3, which lies close (100 metres) to the Potamida 2 section and which was sampled in order to extend the magnetostratigraphy to younger sediments.

Section Potamida 4 is located uphill and to the east of section Potamida 1 (at ca. 500 metres) and is separated from the latter section by a large N-S fault. We decided to try and sample the blue-grey clays up to the overlying homogenous-laminated, beige to

whitish marls. Some parts could not be sampled; one such part had a track running through the section.

Sections Kotsiana 1 and 2 were sampled on the basis of their lithology (homogenous clays) and paleontologic samples were taken every five (paleomagnetic) sampling levels. Section Kotsiana 2 was believed to contain younger sediments than section Kotsiana 1 and lies uphill with respect to the latter section; it is separated from the latter section by olive groves. An attempt was made to determine the stratigraphic distance between the two sections, using a theodolite. A thick sand-layer (80-100 cm) in the lower part of section Kotsiana 1, outcropping at several places in the hillside, served as a reference point, but theodolite measurements showed that (small scale) faulting must have taken place between the two sections.

In sections Episcopi 1 and 2 paleontologic samples were taken at every fifth paleomagnetic sampling level. On the basis of a thin ferruginous level it could be shown that both sections overlap; they were joined to form a single section (the Episcopi section). In the upper part of the section the sampling track contained several joints. We know from experience that the existence of such joints facilitates weathering of the original magnetic minerals and hence may cause a secondary and normal polarity overprint (Langereis, 1979; Drooger et al., 1979b). The upper part of the Episcopi section was therefore resampled in a parallel sampling track without such joints (Episcopi Resampling).
We attempted to extend the upper part of the Episcopi section by sampling one more parallel track (Episcopi Extension) in the same badlands where the other Episcopi sections were taken, but this track came stratigraphically not much higher. The top of section Episcopi Extension is formed by the remains of an iron-rich sandy layer, which must have been thicker than 20-25 cm.

Just one kilometre south of Episcopi, we sampled section Vasilopoulo. The top of the section is formed by a thick (200 cm) and turbiditic sand layer which forms the slightly inclined cover of a "table hill". The magnetostratigraphic results (chapter 4) show that this layer is the lateral equivalent of the top of the Episcopi Extension. Moreover, it can be correlated with one of the (thin) ferruginous levels in the Potamida sections.

Two more sections were sampled in western Crete. The first one is section Makronas which was reported to expose the transition from

the homogenous blue-grey clays to the overlying homogenous-laminated, beige to whitish marls (Spaak, personal communication), but an interval of 13 metres between the two formations could not be sampled due to overgrowth and/or sedimentary properties (sandy). The section contains the youngest sediments sampled in western Crete. The second one is section Skouloudhiana and it is located on the western side of the hill separating the (N-S running) valleys of Potamida and Skouloudhiana (sections Potamida 2 and 3 are located on the eastern side of the hill). This section contains the oldest sediments sampled in western Crete; the underlying coarse clastic sediments (mainly sandstones) were not suited for paleomagnetic sampling. The Skouloudhiana section was sampled in order to extend the (magneto)stratigraphic range to older sediments. Part of the section could not be sampled due to the presence of a road and some small olive groves. The resulting gap in the record has been accurately measured by means of a theodolite.

In central Crete the (bio)stratigraphically long-ranging Kastelli (1) section (see fig. 2.5) is formed by a deep gully in a hillside, the top of which is formed by (sandy) limestones, slightly dipping to the west. Some 250 metres to the south, the sampling of a parallel and seemingly higher ranging section, Kastelli 2, was abandoned because stratigraphic control was impossible due to numerous small faults. Except for the lowermost part of the Kastelli (1) section where joints with gypsum needles were present, it could be ascertained on the basis of thin and undisturbed ferruginous levels, that such small faults were not present in this section. The sediments in the upper part of the section become more and more silty/sandy, indicating an increased sedimentation rate, and cannot be sampled any more from some 20 metres below the (topographic) top upwards.

In the Ierapetra district of eastern Crete section Vassiliki was sampled at close intervals (table 2.1). Biostratigraphic data (fig. 2.5) indicate that this is the oldest section sampled in Crete but unfortunately it does not overlap with any of the other sections.

Although younger than section Vassiliki, section Makrilia does not show an overlap with any of the other sections either (fig. 2.5). Almost 130 metres were sampled; although lithostratigraphi-

cally the longest section on Crete, it may (because of the numerous and intercalated sands of turbiditic origin) represent a (relatively) limited period of time (Fortuin, 1977). Intervals of redeposited sediments and slumping also indicate a much higher sedimentation rate. In the sampled part of the section stratigraphic continuity could be established thanks to the clear layering. Sampling was abandoned when faulting became evident higher up in the outcrop (the badlands just east of the village Makrilia).

In the Sitia region of eastern Crete the biostratigraphically long-ranging Faneromeni section was sampled. It is located some 4 km along the coast west of Sitia; sampling started at sea-level. The hard and often silty clay shows a lighter colour at the surface, indicating weathering to a depth of approximately 5-7 cm. We drilled the longest possible cores (12 cm with the available drills) in order to obtain specimens with (almost) no weathering.

Sections Falconara and Giammoia in the Caltanisetta basin (Sicily) show a partial overlap (fig. 2.5); in section Giammoia only the clay-marl sequence was sampled, whereas in section Falconara sampling was extended to the diatomite-marl sequence. Paleontologic samples were taken independently (see van der Zwaan, 1979, 1982) and calibrated afterwards. The calibration was facilitated by marks inserted by the team of paleontologists. In order to try and take fresh samples, up to 1 metre of weathered surface had to be removed. The sediments in both sections are jointed and fractured all the way through, probably because of large scale gravity sliding in the Pliocene (Meulenkamp et al., 1981), and gypsum needles have formed along the numerous joints present throughout the section.

The Scicli sections on the Ragusa platform (Sicily) were sampled in detail. On the basis of the biostratigraphy section Scicli West is considered to be by far the oldest section we sampled, and it does not overlap with any other section in this study. In section Scicli South a second and (partly) duplicate set was taken parallel to the first sampling track at a distance of some 100 metres (section Scicli South 2), since the marly clays appeared less weathered in that part of outcrop. Due to the topography only a small part of the total exposed section could be sampled; the upper part was an almost vertical wall.

In northern Italy one section was sampled in the Tortonian type area (section Castellania) and one near Mussotto (section Mussotto). In section Castelliana more than 115 metres could be sampled. However, the scarcity of the fauna and possible reworking suggest a very rapid sedimentation (Zachariasse, personal communication). No positive biostratigraphic control is possible for this section

Only the lowermost part of the Mussotto section (Sturani and Sampo, 1973) could be sampled. The rest of the section was overgrown and/or the sediment was too sandy. The sampling spacing is very irregular and is dictated by the presence of the somewhat thicker (more than 5 cm) clay-layers which showed an unweathered (i.e. blue-gray coloured) part in the middle of the layer.

Finally, in the Luzzena section, located in the Peradriatic basin just south of Cesena, fourteen pilot (oriented) hand-samples were taken. Since the section is younger than the Messinian evaporitic phase, and all other sections in this study are older than the Messinian evaporites, there is no overlap with any of the other sections.

chapter three

LABORATORY TREATMENT

INTRODUCTION

In the early days of paleomagnetism it was soon realized that the total natural remanent magnetization (total NRM) of rocks hardly ever reflects the primary magnetization acquired at the time of formation of the rocks. It was found that secondary magnetizations often disturbed the determination of this original magnetization. Subsequently, alternating field and thermal progressive demagnetization methods were introduced as a standard technique to remove secondary magnetizations (As and Zijderveld, 1958). The analysis of directional components during systematic progressive demagnetization has become essential in current paleomagnetic research. The orthogonal projection method commonly known as Zijderveld diagrams (Zijderveld, 1967, 1975) has proved to be especially useful in the analysis of multicomponent NRM (Dunlop, 1979) and it has been used throughout this study.

In recent years it has become increasingly important to identify the magnetic minerals responsible for remanent magnetization components. This work is being done in order to obtain a better understanding of the origin and significance of these remanences (Zijderveld, 1975). Methods for identifying these minerals have (or should) become standard procedure in paleomagnetic research and much work has been done recently on the magnetic properties of sedimentary rocks (e.g. by Lowrie and Heller, 1982) and on the rock-magnetic properties of natural iron-titanium oxides, e.g. by Dankers (1978) and Hartstra (1982a,b,c, 1983) at the paleomagnetic laboratory in Utrecht.

The identification of the magnetic minerals carrying the natural remanent magnetization depends upon their coercivity and blocking temperature characteristics, which can be derived from demagnetiza-

tion data. Most paleomagnetic studies show only decay curves of the total intensity during progressive demagnetization. However, the use of Zijderveld diagrams permits the decay curves (and thus the coercivity or blocking temperature spectra) of the various and differently directed natural magnetization components to be determined separately. The maximum unblocking temperature, close to the Curie temperature which is diagnostic for the mineral concerned, can thus be established and considerably more information concerning the remanences and their associated magnetic minerals can be obtained (Zijderveld, 1975).

Another useful method is coercivity spectrum analysis (Dunlop, 1972). The curve representing the isothermal remanent magnetization (IRM) acquired in progressively higher direct magnetic fields, and the field at which the saturation IRM (SIRM) is reached (or not reached) are indicative of or may be diagnostic for the magnetic mineralogy of the sample. The presence of the most common magnetic minerals such as magnetite, hematite and goethite, and possibly maghemite and pyrrhotite, can thus be inferred (cf. Lowrie and Heller, 1982).

In sediments the original or primary remanent magnetization has been produced by mainly detrital magnetic minerals, which already have a thermal remanent magnetization (TRM) or a chemical remanent magnetization (CRM). Such a depositional remanence is acquired by the settling and statistical alignment of those magnetic minerals, either at the time of deposition (depositional remanent magnetization or DRM) or shortly afterwards (post-depositional remanent magnetization or pDRM; Irving, 1957).
Chemical changes, including oxidation or reduction of magnetic minerals due to diagenesis and weathering, may produce a CRM whose age lies between (shortly after) deposition and subrecent times. Such a secondary CRM may then partly overprint or even replace the original magnetization.

Generally, the identification of magnetite or titanomagnetite as the carrier of the characteristic remanent magnetization (ChRM; see Zijderveld, 1967) in sediments is taken as an indication that this ChRM represents the primary remanent magnetization. Further indications that the ChRM is of primary origin may be inferred from field tests such as the reversal test or fold test (Strangway, 1967), from

the presence of an inclination error (Laj et al., 1982) or from the decrease in intensity during a polarity transition, provided the magnetic properties, such as susceptibility and SIRM, indicate that this decrease is not due to lithologic factors.
Magnetite in sediments may have a number of origins, but terrigenous detrital magnetite plays a major role in most marine sediments as the carrier of the remanence, and is transported either by wind or water. Magnetite may also have formed authigenically in marine environments (Henshaw and Merril, 1980), although Lowrie and Heller (1982) assume that authigenic magnetite plays a minor role. Biogenic magnetite of single domain size produced by magnetotactic bacteria may contribute to the remanence as well (Kirschvink, 1982; Chang and Kirschvink, in press). Other sources, which can be volcanic, cosmic or hydrothermal, are believed not to be very common.

Other magnetic minerals that may contribute to natural remanences are hematite, maghemite, goethite and pyrrhotite. These minerals are often of secondary origin and may be the carriers of a secondary remanence acquired some time between deposition and eventual sampling. Hematite may have a detrital origin or may be formed diagenetically or because of weathering. Goethite is often a product of the weathering of iron minerals; it may also form authigenically or by precipitation from sea-water. Maghemite may form diagenetically as a product of maghemization, i.e. the low-temperature oxidation of magnetite (or titanomagnetite) to maghemite (see Henshaw and Merrill, 1980).
Finally, part of the magnetite may have very short relaxation times and hence produce secondary and viscous magnetizations.

TOTAL NATURAL REMANENT MAGNETIZATION

In the present study remanent magnetization measurements were carried out initially on astatic magnetometers (As, 1960) and on a JR-3 spinner magnetometer (Jelinek, 1966). Since the acquisition of a ScT cryogenic magnetometer (Goree and Fuller, 1976) by the paleomagnetic laboratory Fort Hoofddijk, this was the instrument that was generally used to measure the numerous specimens. In order to gain a first impression, the total natural remanent magnetization (total NRM) of one specimen per core was measured and the directions and

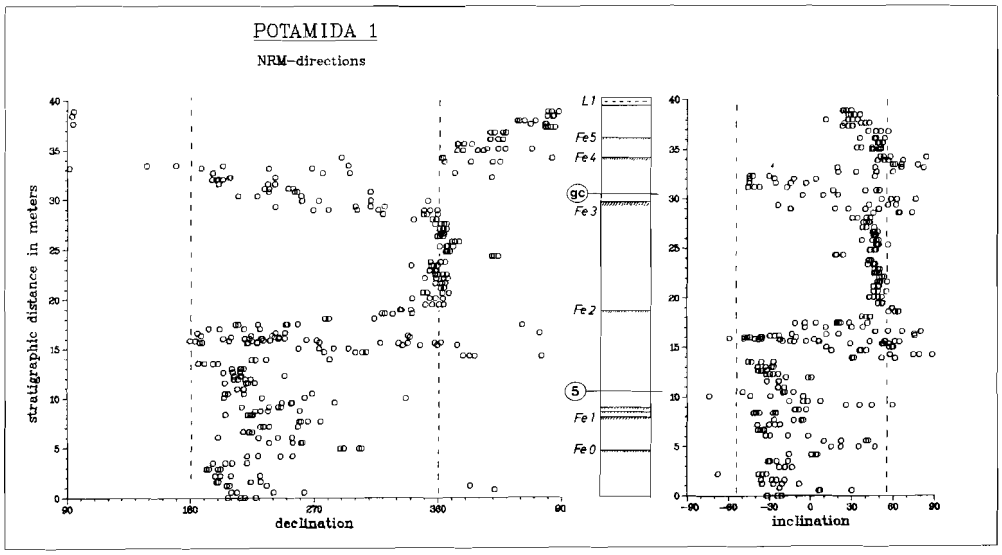

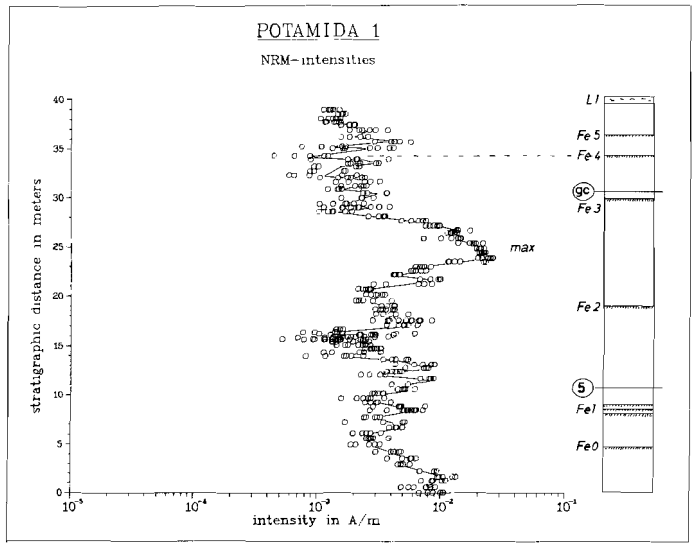

Fig. 3.1 a) Declination and inclination of the total NRM vs. stratigraphic position in section Potamida 1. Vertical dashed lines denote the direction of the geocentric axial dipole field at the present latitude; gc = FOD of the *G. conomiozea* group, 5 = FOD of *G. menardii* form 5. Ferruginous levels are labeled Fe 1–5; L1 denotes layer of finely bedded clay. b) Intensities of the total NRM in section Potamida 1. Horizontal dashed lines indicate intensity decreases corresponding with the ferruginous levels due to increased weathering close to such layers. A maximum in the intensities is noted between Fe 2 and Fe 3 (max).

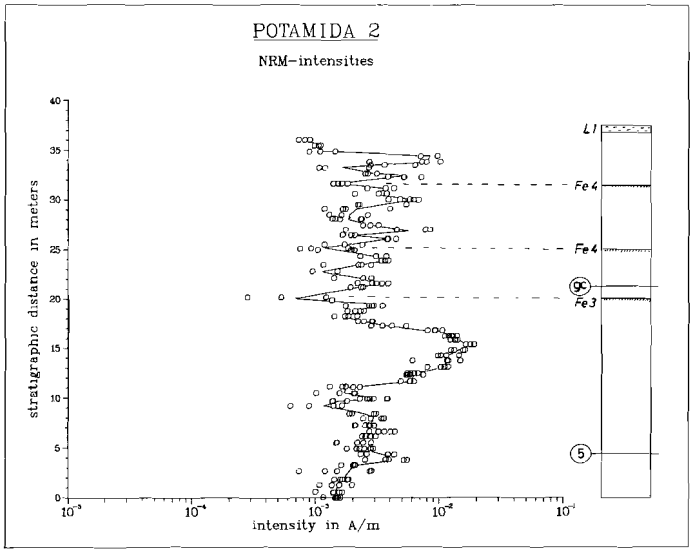

Fig. 3.2 Intensities of the total NRM in section Potamida 2. The same maximum (max) is present as in section Potamida 1 (fig. 3.1). A fault (f) is present, causing a doubling of part of the section. See also fig. 3.1 caption.

intensities of the total NRM were plotted versus the stratigraphic position. Since the total NRM may represent the resultant vector of two or more magnetizations, a further analysis of the total NRM is necessary to remove possible viscous (laboratory induced) and recent normal polarity overprinting. Therefore, the plots of directions and intensities of the total NRM allow for preliminary conclusions only and in view of their limited value, only a few selected examples will be shown in order to give a general impression.

The NRM directions of section Potamida 1 (fig. 3.1a) show that reversed as well as normal polarity directions are present, but polarity zones cannot be delimited reliably with these preliminary data. The NRM intensities (fig. 3.1b) ranging 1.0 - 20.0 mA/m, which is the common range for most Cretan sections. A clear maximum in the NRM intensities between two ferruginous layers, Fe 2 and 3, can be seen. This correlates with a similar intensity maximum in section Potamida 2 (fig. 3.2), indicating that this is a regional feature.

In many cases a decrease in intensity is found close to the ferruginous layers. Remanent coercive forces and saturation remanences of the samples (see chapter 5) close to these levels indicate oxidation of the original magnetic minerals. Since these ferruginous sandy layers are more permeable than the dense clay, oxidation and the resultant drop in intensity are most probably induced by weathering. Not all the data around ferruginous layers show a clear decrease in intensity. This is due either to the sample having been taken too far from such a layer or to the fact that the layer was too thin or discontinuous. The existence of several other levels at which an intensity decrease is observed might indicate the presence of several more and unnoticed discontinuous layers. However, it should be noted that a decrease in intensity may also be due to a polarity reversal horizon.

In section Potamida 3 the stratigraphic range could be extended to some nine metres above the lower layer of finely bedded clay (L1) which forms the top of the former Potamida sections. The NRM directions (fig 3.3a) show clearly reversed and normal polarities, and apparently reversed polarities are present in the very top of the section. The greater scatter in the upper part of the section corresponds with lower intensities (fig. 3.3b) approximately from layer L1 upwards. The intensity variations are matched by variations in magnetic susceptibility and saturation remanence (chapter 5), suggesting that lithology is responsible for these lower values. In the field it was already observed that the clay from one metre below L1 towards the top is less dense and homogeneous and more silty-sandy intervals are present, representing a higher accumulation rate. It is probable that a higher sedimentation rate is accompanied by the deposition of fewer fine-grained magnetic minerals. This would correspond to the lower intensities observed and to more scatter in the NRM directions due to more viscous or less stable magnetization components. In addition, the less dense sediment is more susceptible to weathering and hence to the concomitant oxidation of magnetic minerals. The oxidation results in lower intensities as well as in lower values of the magnetic susceptibility and saturation remanence. The higher remanent coercive forces observed in the upper part of the Potamida 3 section indicate that oxidation did indeed take place as well (see chapter 5).

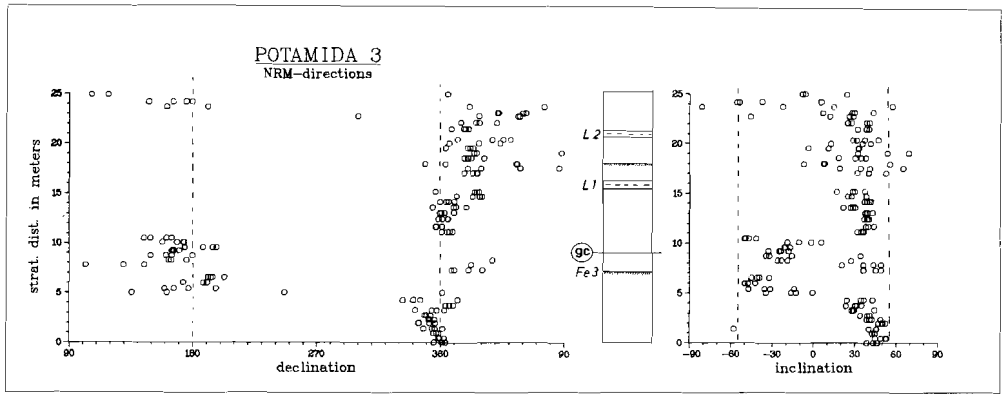

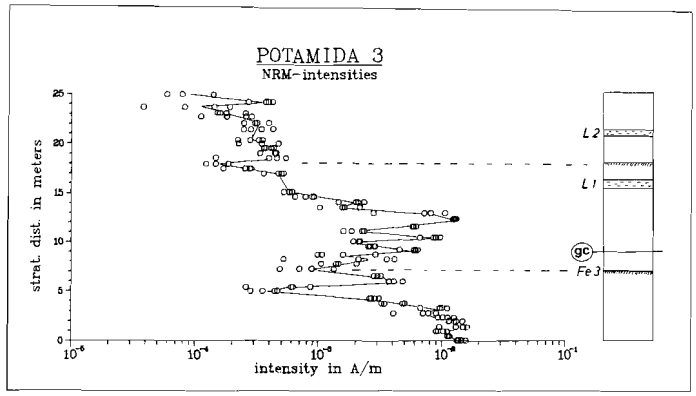

Fig. 3.3 a) Declination and inclination of the NRM vs. stratigraphic position in section Potamida 3. Fe 3 and L1 correspond with the same levels in sections Potamida 1 and 2; a second layer of finely bedded clay (L2) is present. b) Intensities of the total NRM in section Potamida 3. Lower intensities in the upper part of the section correspond with a change in lithology towards less homogenous clays with more silty/sandy intervals. See also fig. 3.1 caption.

The Faneromeni section in eastern Crete is biostratigraphically long-ranging (fig. 2.5), but NRM directions show appreciably more scatter in than in the western Cretan sections (fig 3.4a). The scatter in NRM directions corresponds with lower intensities (fig. 3.4b) ranging 0.05 - 0.50 mA/m. Only in the middle part of section Faneromeni are (mainly reversed) NRM directions well grouped per sampling level and intensities appreciably higher, up to 2.0 mA/m.

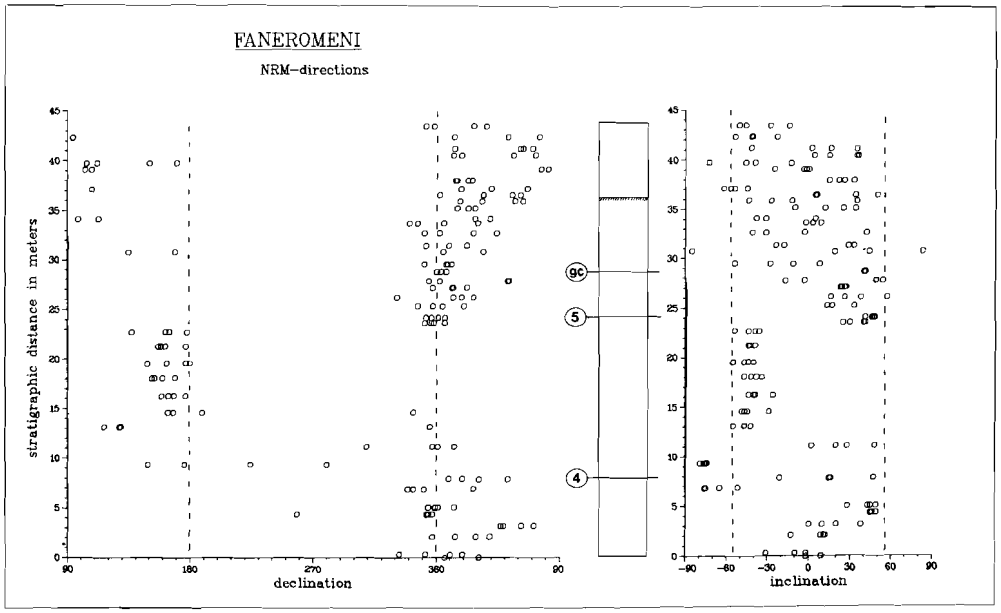

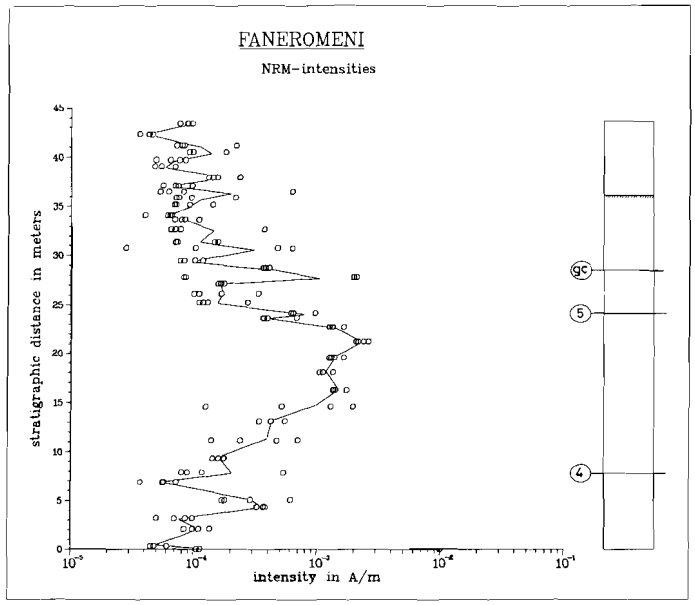

Fig. 3.4 a) Declination and inclination of the NRM in section Faneromeni; 4=LOD of *G. menardii* from 4. In the upper and lower part directions are rather scattered, whereas the middle part shows consistent, reversed polarity directions. b) Intensities of the total NRM in section Faneromeni. See also fig. 3.1 caption.

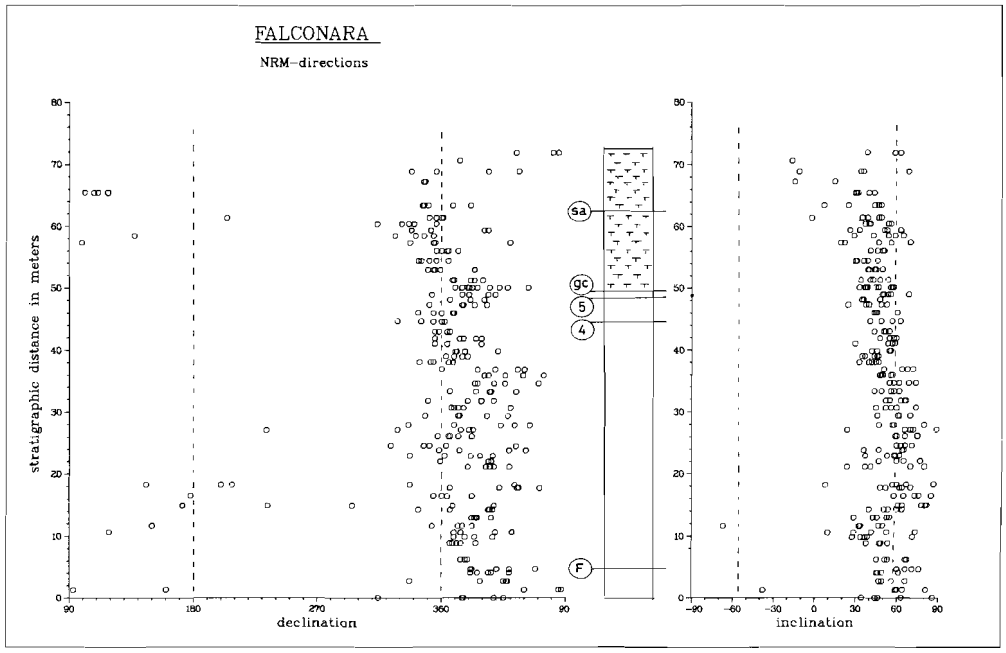

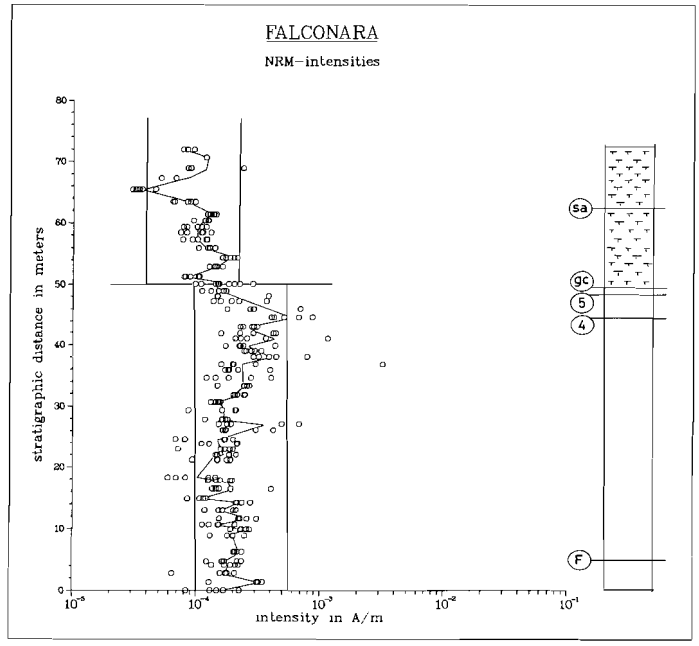

Fig. 3.5 a) Declination and inclination of the total NRM in section Falconara; sa = coiling shift of *N. acostaensis*, f=LOD of *G. falconarae*. NRM directions are scattered around the geocentric axial dipole field direction. b) Intensities in the upper part of the section are lower due to lithology (diatomite-marl). See also fig. 3.1 caption.

Section Falconara in Sicily is biostratigraphically the longest ranging section that was sampled. However, for the present latitude of the locality the NRM directions are scattered around the geocentric axial dipole field (fig. 3.5a) and intensities are low (fig. 3.5b), ranging 0.10 - 0.50 mA/m. Intensities of the overlying diatomite-marl sequence are even lower (0.04 - 0.20 mA/m). This section is unlikely to yield positive magnetostratigraphic data. The Giammoia section shows a very similar picture; the Scicli sections on the Ragusa platform show also very low intensities and scattered directions. Section Scicli West shows intensities that are the lowest recorded in the present study, ranging 0.02 - 0.20 mA/m. For the analysis of the total NRM the specimens have to be demagnetized and if initial intensities have such low values, the accuracy level and the noise level of even the most sensitive magnetometers is quickly reached.

The total NRM intensities of the northern Italian sections are generally somewhat lower than in the average Cretan section, but higher than in the Sicilian sections.

DEMAGNETIZATION AND IRM ACQUISITION

At least one specimen per sampling level was demagnetized progressively in alternating fields increased stepwise up to a maximum of 300 mT (milliTesla) peak value. At least one more specimen was treated thermally by stepwise heating in a non-magnetic furnace up to temperatures of 600 - 650 oC.

Initially it was assumed that the marine clays could not be heated without being destroyed and samples were only treated with alternating magnetic fields. Alternating field demagnetization clearly revealed the polarity of the characteristic remanent magnetization (ChRM), but at first the direction of this remanence could not be determined with sufficient accuracy. It appeared that disturbing remanences were introduced during treatment in alternating fields higher than 50 mT. This phenomenon is clearly seen in figure 3.6: the remanence remaining after demagnetization in higher fields does not decrease to zero, but bypasses the origin of the

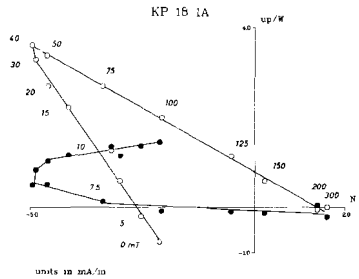

Fig. 3.6 Alternating field (AF) demagnetization of a specimen from section Potamida 1. The end points of the changing resultant remanent magnetization vector are projected on the vertical plane (open circles) and on the horizontal plane (solid circles), having the N-S axis in common. Numbers denote alternating field in milliTesla (mT). A secondary component is removed after treatment in fields of 40-50 mT. A characteristic remanent magnetization component does not decrease towards the origin, but is disturbed by a remanence which increases in higher alternating fields.

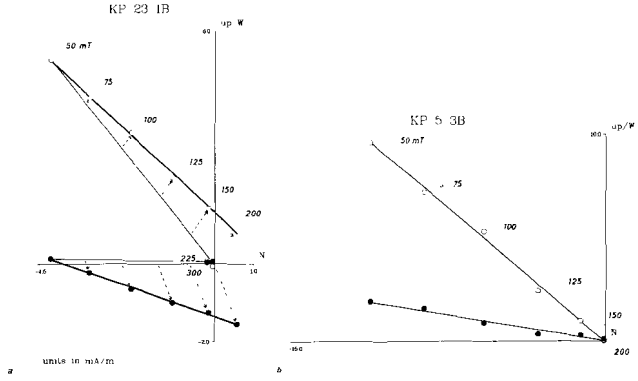

Fig. 3.7 Partial AF demagnetization of two specimens from section Potamida 1. a) The decreasing resultant remanent magnetization vector bypasses the origin of the axes system because of the introduction of disturbing remanences in the alternating field. At the 225 and 300 mT points these disturbing remanences have been avoided by using a special method (see text). b) Special method applied to all demagnetization steps.

vector diagram because of the increasing influence of the disturbing remanence in higher fields. This disturbing remanence has been noted earlier by Zijderveld (1975) and in these clays by Langereis (1979). Its direction proved to lie in the plane perpendicular to the demagnetization coil axis and this fact can be used to prevent this remanence from interfering with the natural remanence. At each demagnetization step the specimen is then treated three times with the same field strength, each time with one of the three orthogonal components parallel to the coil axis, and after each treatment only that component is measured. This method, described in more detail by Langereis (1979), yields good results (see fig. 3.7) and was used during subsequent alternating field demagnetizations.

It is clear, however, that the application of this method to the numerous samples from all sections is a laborious task. Therefore, pilot specimens were treated thermally and it was found that progressive thermal demagnetization was not only possible, but it also gave more consistent results than alternating field demagnetization. In order to investigate whether the prevention of oxidation by the addition of argon gas within the furnace had any influence on the decay of the natural remanent magnetization of the clay, pairs of specimens from several cores were heated with and without argon gas (Langereis, 1979). Since the results were not notably different, subsequent thermal treatment was performed in air. Originally, specimens were heated in a laboratory-built furnace, but later a Schonstedt furnace was used for routine heat treatment; this resulted in more rapid heating and cooling cycles specimens (half hour heating and cooling cycles instead of half-day cycles).

The general picture, especially for the Cretan sections, that emerges from the progressive demagnetizations of the samples, both thermally and in alternating fields, is as follows: a small, viscous component which is easily removed in low fields or at low temperatures and is randomly directed; a secondary, normal polarity component with a present-day direction which has intermediate coercivities and unblocking temperatures; a characteristic magnetization component which has high coercivities and unblocking temperatures typical for magnetite. These various components will be described below in more detail.

Viscous component

In most cases the samples contain a small, randomly directed component, apparently acquired in the laboratory. This viscous component can generally be removed in a peak field of 5–10 mT or at temperatures of 80–110 oC (see all examples of demagnetization diagrams in this chapter).

For instance in section Episcopi a relatively strong viscous component is present. This viscous component is virtually removed at temperatures higher than 100 oC. Using alternating field demagnetization, however, it appears that the coercivities of the viscous and secondary component overlap (fig. 3.8a).

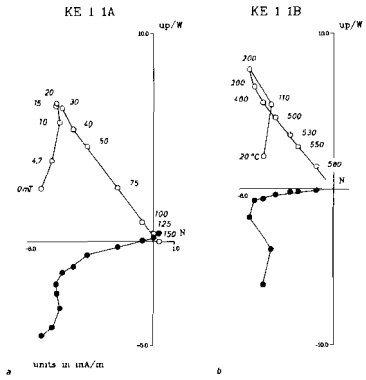

Fig. 3.8 Alternating field and thermal demagnetization diagrams of specimens from section Episcopi. The viscous, secondary and characteristic magnetization components can be more easily distinguished by thermal demagnetization (b), whereas AF demagnetization shows a much more gradual change in the respective magnetization components (a).

This indicates that the magnetic fractions responsible for these two components have overlapping coercive spectra and more distinct blocking temperature spectra. The viscous component in this section has a rather constant direction instead of being randomly directed. This need not cause surprise: if samples have similar orientations due to sampling (drilling) in a straight gully with a constant topo-

graphic dip, a viscous and laboratory-induced magnetization acquired during storage and with the specimen axis vertical (as is usual) is likely to have more or less the same direction.

In section Makrilia the viscous (and secondary) component in many samples is often very large with respect to the ChRM (fig. 3.9a). In part of this section (e.g. KM 31 2A in fig. 3.9b) the total remanent magnetization is almost entirely of viscous origin. Almost all of the NRM is removed after 100 oC and demagnetization with higher temperatures results only in scatter.

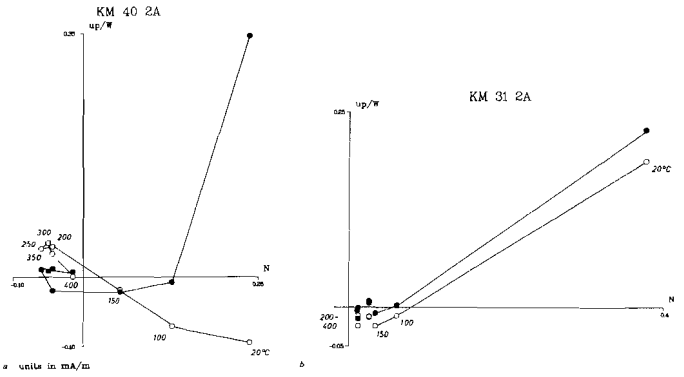

Fig. 3.9 Thermal demagnetization diagrams of specimens from section Makrilia which show a) a large viscous and secondary magnetization component with respect to the (reversed) characteristic component and b) an entirely viscous magnetization.

Secondary component

A secondary normal polarity component can easily be recognized in samples with a characteristic remanent magnetization of reversed polarity (figs. 3.10 and 3.11). This secondary component generally has an inclination which is up to 10 or even 15 degrees steeper than the inclination of the ChRM (figs. 3.6, 3.10b, 3.11). Most probably this secondary normal polarity component is of (sub)recent origin, since its average inclination is close to the present day inclination (51 degrees) or the geocentric axial dipole field inclination (ca. 55 degrees) at the present latitude of the sampling locality.

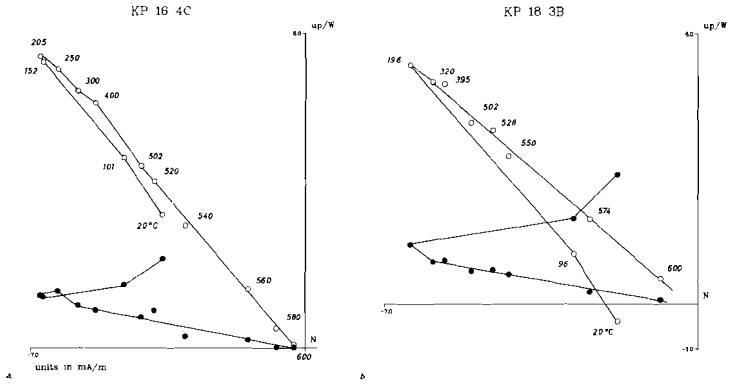

Fig. 3.10 Thermal demagnetization diagrams of specimens from section section Potamida 1. The secondary magnetization component seems to be entirely removed at 200 °C.

From two examples in the lower part of section Potamida 1 it would appear that the secondary component is removed after 200 oC (fig. 3.10). However, from other samples in the same section (fig. 3.11b,d) it can be deduced that the secondary component is only totally removed at temperatures as high as 500 oC; nevertheless, at 200 oC more than 80% of the secondary remanence is removed. This is illustrated more clearly in the decay curves of the thermal demagnetizations (fig. 3.12b).
Alternating field demagnetization also clearly reveals the secondary and magnetization component. The secondary normal polarity component can be removed entirely by alternating fields up to 100 mT (figs. 3.11a,c) and a median destructive field of ca. 20 mT can be deduced from the alternating field decay curves (fig. 3.12a).

In samples containing a normal polarity ChRM, the secondary component is less distinct, but it can sometimes be recognized by a change in the direction of the resultant remanence component during the demagnetization procedure (figs. 3.13, 3.15). Since the secondary and characteristic magnetization components differ only slightly in direction, decay curves for each component separately cannot be reliably constructed. From the total thermal decay curve, i.e. the decay curve of the algebraic sum of the difference vectors between successive steps, it is clear that two components with diffe-

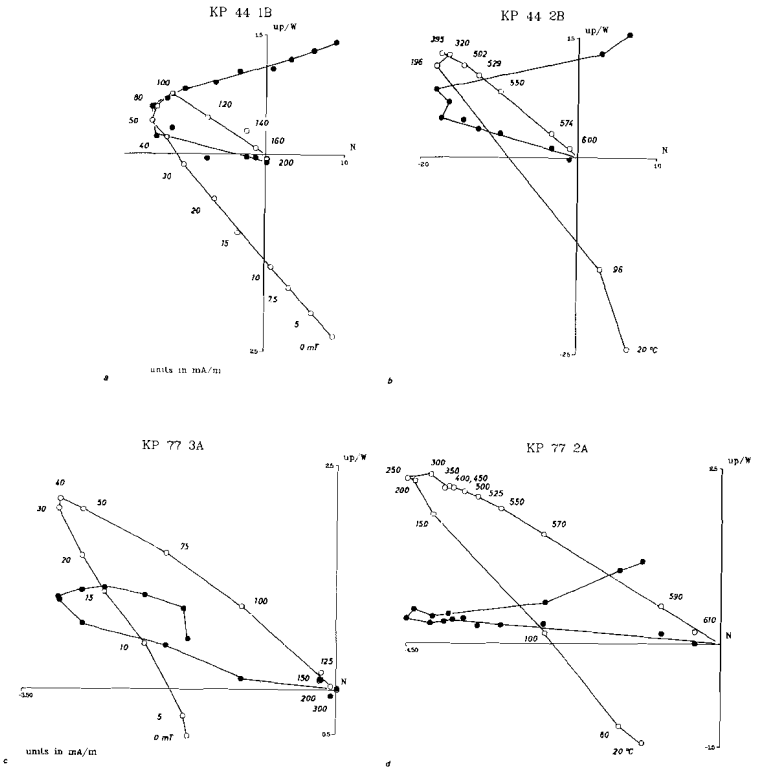

Fig. 3.11 AF and thermal demagnetization diagrams of specimens from section Potamida 1. The secondary magnetization component seems to be entirely removed at 100 mT (a,c) or at temperatures as high as 500 °C (b,d).

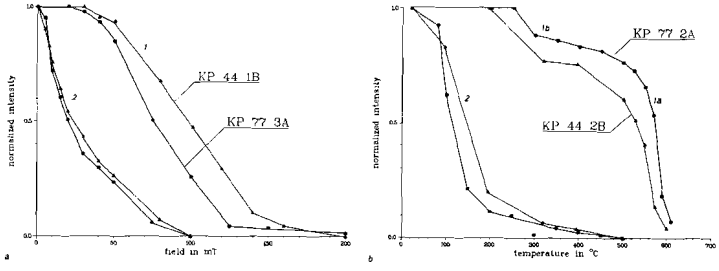

Fig. 3.12 Decay curves of the AF (a) and thermal (b) demagnetizations from figure 3.11; the secondary component (2) is only entirely removed at 100 mT or at 500 °C. The thermal decay curve of the characteristic component shows an initial, slight decay (1b) followed by a rapid decay (1a) at temperatures above 500 °C.

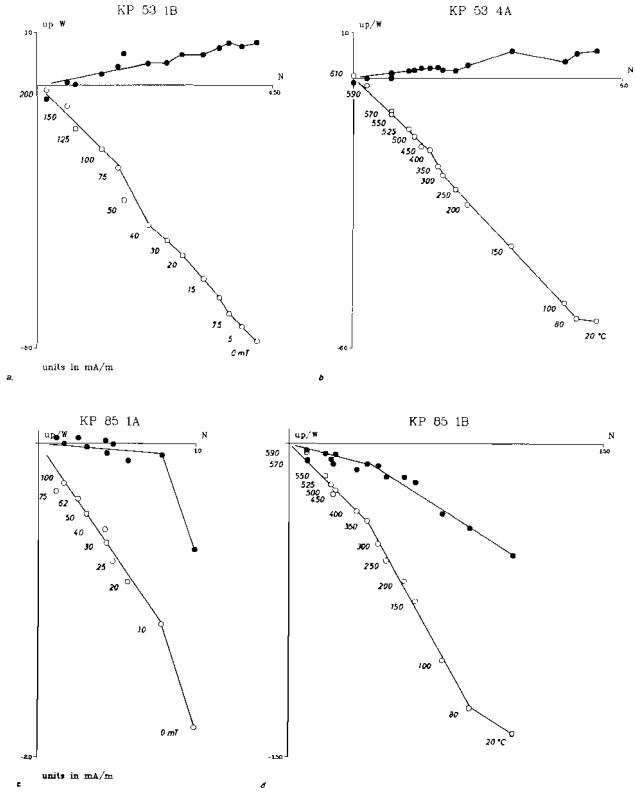

Fig. 3.13 AF and thermal demagnetization diagrams of specimens from section Potamida 1. Since secondary and characteristic components all show normal polarity, it cannot be determined at which alternating field or temperature the secondary component is removed.

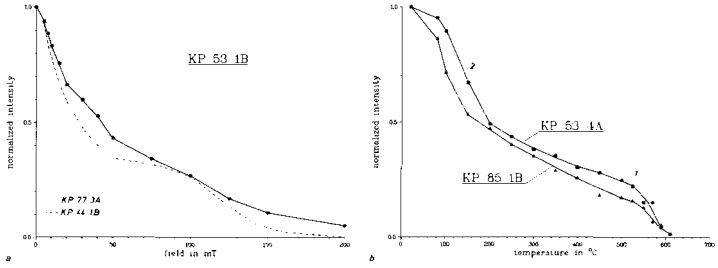

Fig. 3.14 Decay curves of the AF (a) and thermal (b) demagnetizations from figure 3.13; for comparison, the total decay curves of the algebraic sum of the difference vectors between successive steps of the samples from figures 3.11 and 3.12 are shown.

rent blocking temperature spectra can be inferred (fig. 3.14b). From the AF decay curves this is much less evident (fig. 3.14a), but if these are compared with the total decay curves of the secondary and characteristic components of e.g. samples KP 44 1B and KP 77 3A (dashed and dotted lines in fig. 3.14a) it is apparent that the curves of the normal and reversed polarity clay specimens are very similar.

In general, the secondary component shows very similar characteristics in almost all Cretan sections (see further examples of demagnetization diagrams in this chapter). Thermal demagnetization results in a clear separation of this component from the characteristic (original) magnetization, whereas alternating field demagnetization shows that the secondary component has overlapping coercivities with the viscous component on the one hand and with the characteristic magnetizations on the other hand (see e.g. the thermal and alternating field decay curves: figs. 3.12, 3.14, 3.16).

Characteristic component

A stable and characteristic magnetization component can usually be determined by thermal demagnetization at temperatures of 500 oC and higher (figs. 3.11b,d, 3.17b,d and others). Since most of the characteristic NRM is removed between temperatures of 500 and 600 oC the main magnetic mineral carrying the remanence is magnetite. The residual magnetization remaining at temperatures above 580 oC can be attributed either to a small amount of hematite or to insufficiently accurate calibration of the temperatures (fig. 3.19).

The decay curves of this characteristic component (figs. 3.12b, 3.18b) show an initial small decay between 250 and 350 oC and a final strong decay at temperatures higher than 500 oC, suggesting two magnetic phases; these are indicated in the decay curves as 1b and 1a, respectively. These two magnetic phases are especially clear when the secondary magnetization component can be separated from the characteristic magnetization component, as is the case when the two components have different polarities (see figs. 3.12b, 3.18b, 3.20b). If the secondary and characteristic components have the same (normal) polarity the initial magnetic phase (1b) is masked, because of the partly overlapping unblocking temperature

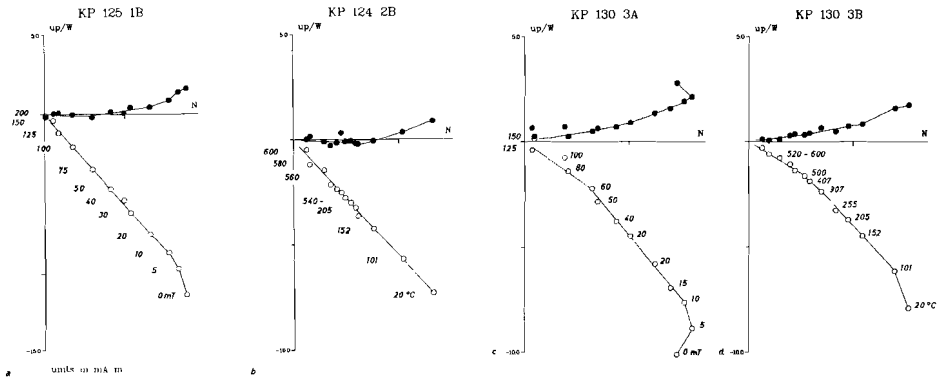

Fig. 3.15 AF and thermal demagnetization diagrams of specimens from section Potamida 2. A slight change can be seen between the secondary and characteristic components both in the AF (in a at 50 mT, in c at 60 mT) and in the thermal demagnetization diagrams (in b at 150–200 °C, in d at 400 °C).

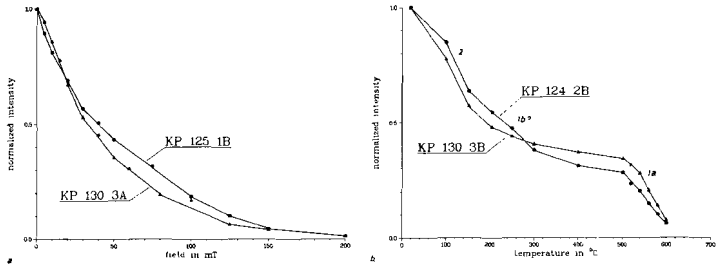

Fig. 3.16 Decay curves of the AF (a) and thermal (b) demagnetizations from figure 3.15; the initial decrease of the characteristic component (1b) can tentatively be recognized in the thermal decay curve of specimen KP 124 2B. In both specimens the rapid decay at temperatures above 500 °C (1a) is evident.

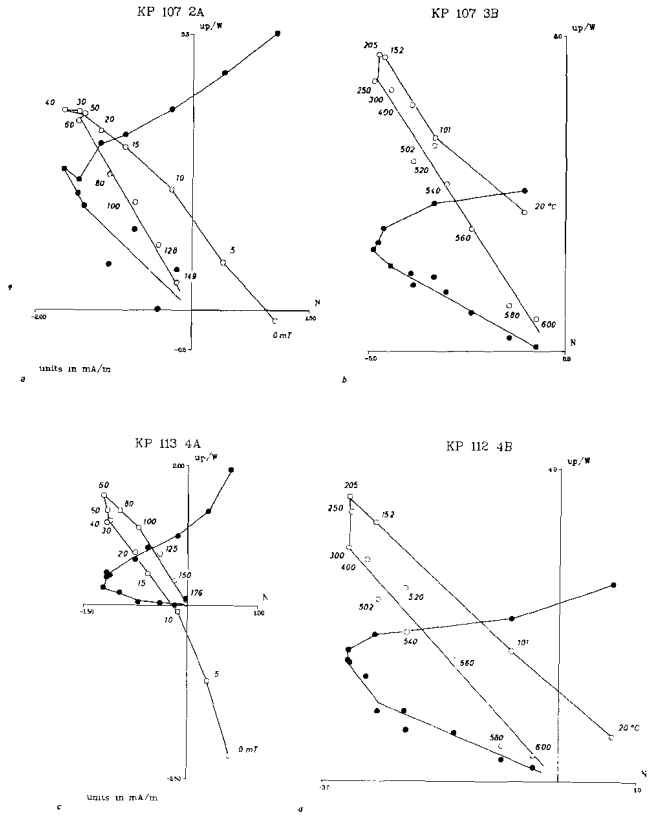

Fig. 3.17 AF and thermal demagnetization diagrams of specimens from section Potamida 2.

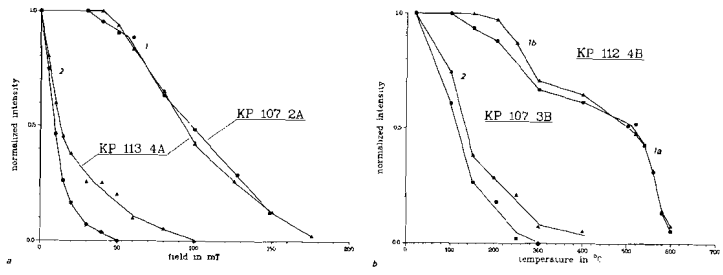

Fig. 3.18 Decay curves of the AF (a) and thermal (b) demagnetizations from figure 3.17; the initial decay (1b) of the characteristic component is somewhat more pronounced than in figure 3.12.

spectra of the secondary component and the initial magnetic phase of the characteristic component (figs. 3.14b, 3.16b). Nevertheless, the presence of this phase is sometimes still clearly indicated in such cases (fig. 3.20a).
The features described here are strongly connected to the magnetizations as found in the homogenous and dense clays. If the clays are less dense, for instance in the top of section Potamida 3, viscous magnetizations arise at temperatures higher than ca. 500 oC (figs. 3.21b,d; see also fig. 3.22b). Although the demagnetization diagram shows more scatter than in the previous examples, the polarity of the characteristic magnetization can be recognized unambiguously.

The low temperature magnetic phase (1b) of the characteristic remanent magnetization is sometimes more pronounced: compare for instance figures 3.12b (Potamida 1) and 3.20b (Potamida 3) with figure 3.18b, (section Potamida 2). This relatively pronounced decay agrees with the fact that section Potamida 2 is an outcrop consisting of gullies which are in places covered with scrub and a crust of weathered clay. This would point to more severe weathering in this section, possibly causing oxidation (maghemization) of the original magnetic minerals (magnetite).

Origin of the characteristic remanent magnetization

The ChRM in the clays is most probably a DRM carried by detrital magnetite grains already having a TRM. From the decay curves it can be seen that the ChRM unblocks at high temperatures and close to the Curie temperature of magnetite (578 oC). Since the blocking temperature increases with decreasing grain-size (Neél, 1955), the decay curves suggest that a very fine-grained magnetite is the carrier of the ChRM (cf. Hartstra, 1983). The small and initial decay of the characteristic remanent magnetization component (1b) may be due to the presence of some maghemite. Maghemite may form as a result of low-temperature oxidation of magnetite, e.g. following burial (diagenesis) or because of weathering. It is metastable and reverts to hematite at temperatures higher than 200-350 oC.

The characteristic component can be removed by alternating fields up to 200 mT (see the figures shown so far) and has a median destructive field of 80-100 mT (see the alternating field decay

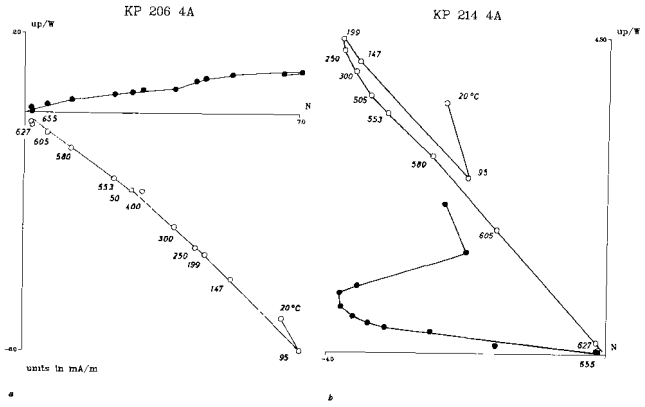

Fig. 3.19 Thermal demagnetization diagrams of specimens from section Potamida 3.

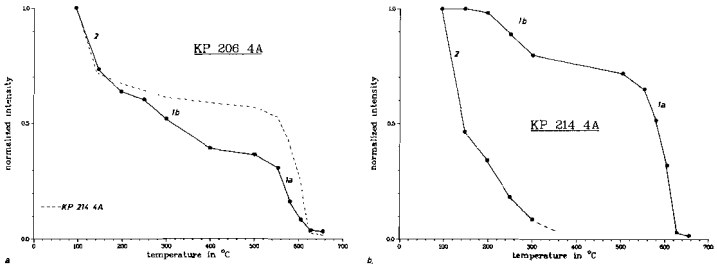

Fig. 3.20 Decay curves of the thermal demagnetizations from figure 3.19; the initial decay (1b) of the characteristic component can also be inferred from the decay curve of the algebraic sum of the two components of KP 206 4A.

curves). The high coercivities support the conclusion from the thermal demagnetization data that very fine-grained magnetite is the main magnetic carrier of the ChRM. In the alternating field decay curves of the characteristic component two distinct magnetic phases, such as can be seen in the thermal decay curves, are not apparent (figs. 3.12, 3.14, 3.16, 3.18). Since maghemite has coercivities very similar to those of magnetite, the coercive spectra of the two magnetic phases would indeed overlap, resulting in decay curves as shown.

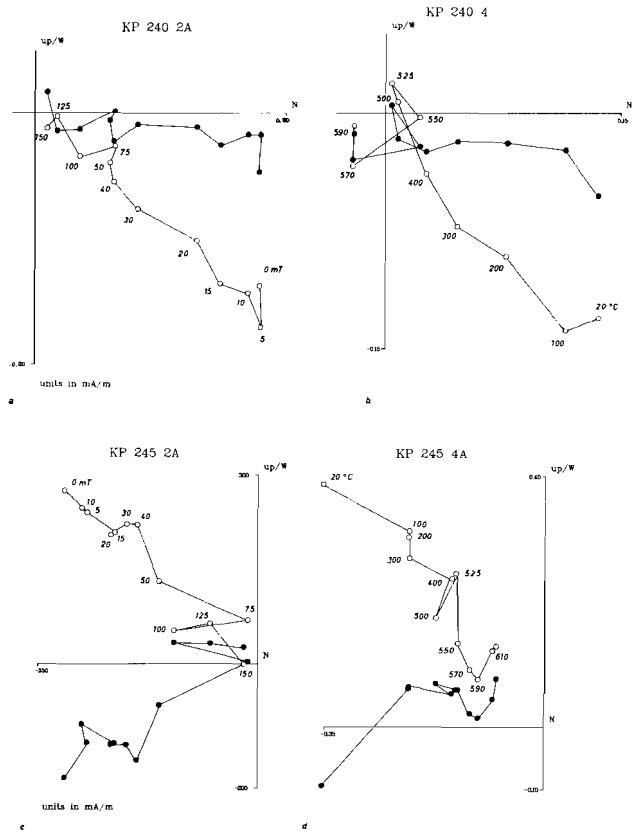

Fig. 3.21 AF and thermal demagnetization diagrams of specimens from section Potamida 3. Although the demagnetization results are more scattered than in the Potamida 1 and 2 sections, the polarity can be determined unambiguously. The magnetization becomes disturbed at temperatures above 500 °C.

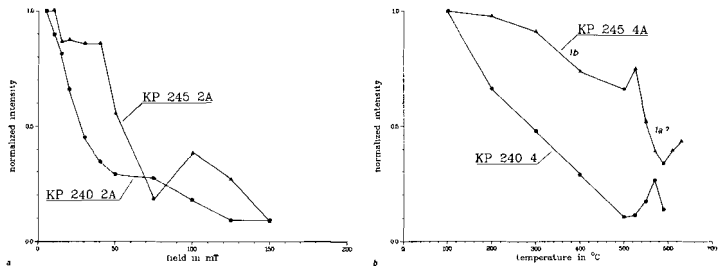

Fig. 3.22 Decay curves of the AF (a) and thermal (b) demagnetizations from figure 3.21.

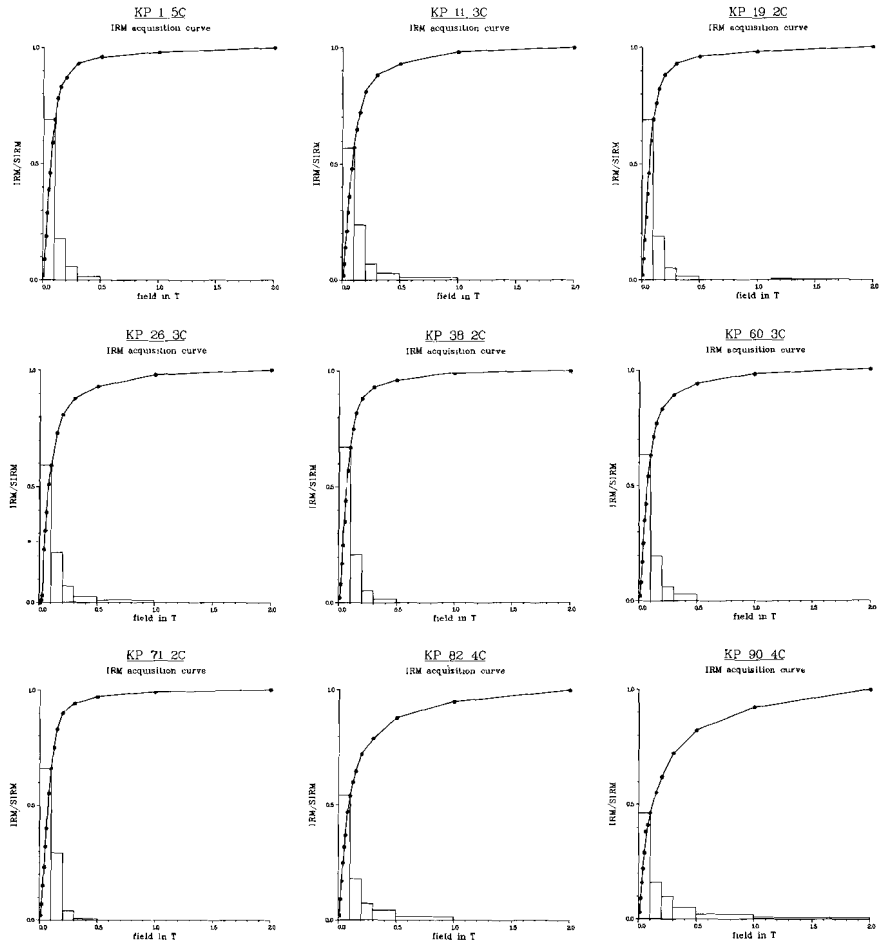

Fig. 3.23 Isothermal remanent magnetization (IRM) acquisition curves from section Potamida 1. Generally some 90% of the saturation IRM (SIRM) is reached at 300 mT, indicating that the main magnetic mineral is fine-grained magnetite. In specimens KP 82 4C and KP 90 4C a high coercivity mineral is present.

A further indication that the main magnetic carrier of the ChRM is magnetite is provided by the IRM acquisition curves (fig. 3.23). Generally, most of the SIRM (or rather the IRM acquired in a field of 2 Tesla, the maximum obtainable field in our laboratory) is acquired at 300 mT (ca. 90%); the majority of the specimens are saturated in fields of 1-2 Tesla. Some exceptions are found in the top of section Potamida 1 (KP 82 4C and especially KP 90 4C in fig.

3.23), where the steady increase in IRM intensity in higher magnetic fields up to 2 T clearly indicates the presence of a high coercivity mineral (hematite). Since the top of the section consists of more silty and less dense clay, weathering may occur more easily, resulting in oxidation of the magnetic minerals.

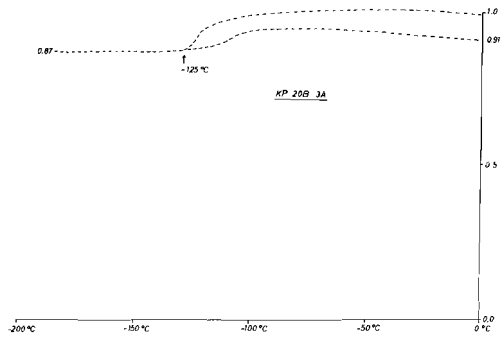

Fig. 3.24 Low temperature cycle of the SIRM of a specimen from section Potamida 1. The high ratio of original and regenerated magnetization indicate that most of the IRM is carried by single-domain magnetite (cf. Hartstra, 1982c).

An example of a low temperature cycle of the SIRM of a specimen from section Potamida 1 shows clear evidence of the presence of very fine-grained, probably single domain magnetite (fig. 3.24). Upon cooling, only a small part of the remanence is lost (13%) and re-heating results in a partial regeneration of the lost remanence. In the case of single domain magnetite there is no loss in remanence upon cooling down below its transition point (-155 oC), whereas for multi-domain grains the remanence will decrease strongly (Kobayashi et al., 1975; Dankers, 1978). Therefore, the curve of figure 3.24 indicates that a major part of the SIRM is carried by very fine-grained, single domain magnetite. The ratio of the remanence at -196 oC and the original remanence (0.87) and the ratio of the re-generated remanence and the original remanence (0.91) support this assumption (cf. Hartstra, 1983).

Two magnetic phases of the ChRM

The initial decay (1b) and the final decay (1a) of the characteristic remanent magnetization as shown in the thermal decay curves indicate two different magnetic phases. As has been noted above, this could be a maghemite and a magnetite phase, respectively. The maghemite phase could have been formed in an initial stage following burial (diagenetic maghemite) or it may have been formed as a low-temperature oxidation "skin" around magnetite grains due to weathering.

If the maghemite has been formed shortly after deposition it will probably acquire a magnetization with the same polarity (and direction) as the magnetization resulting from the alignment of the magnetite grains, except perhaps close to a polarity reversal. In the latter case the direction of the maghemite will depend on the time at which it was formed after deposition. If this is longer than the duration of a polarity reversal (say 5,000 - 10,000 years), the maghemite will have a polarity opposite to that of the magnetite. Alternatively, if the maghemite results from weathering, it may form a "maghemite skin" which would probably acquire a chemical remanent magnetization (CRM) with the same direction as the remanence carried by the magnetite grains, since the magnetic field at the surface of the magnetite grains is stronger than the geomagnetic field by more than one order of magnitude. The latter theory would explain the greater initial decay (of the maghemite phase, 1b) in sections which have been exposed to more intensive weathering. However, the experiments of Johnson and Merrill (1972, 1973) may indicate that an alternative mechanism is responsible for the same observation. Their results show that the original direction of the ChRM remains the same when a single domain magnetite grain is completely oxidized to single domain maghemite, even in the presence of an external magnetic field, whereas this external field dominates in the case of maghemization of multi-domain grains, thus yielding a chemical remanent magnetization which is (or may be) different from the original remanence of the magnetite. This might be explained by a positive exchange coupling between maghemite and magnetite in single-domain grains, whereas the presence of domain walls in multi-domain grains yields an effective decoupling (Henshaw and Merrill, 1980).

Secondary versus characteristic component

The first (1b) and second (1a) magnetic phase can generally not be recognized in the coercivity spectrum of the ChRM since they largely overlap. The coercivity spectrum of the secondary component in turn overlaps the coercivities of the ChRM, resulting in a major overprint by the secondary component close to a polarity transition or where weathering occurs (e.g. fig. 3.25a). It is clear from fig. 3.25b that thermal demagnetization on the other hand results in a clear separation of the normal secondary and the reversed characteristic component. The above described phenomenon is frequently observed and in sections Potamida 1 and 2, for instance, the original polarity zone boundaries had to be slightly adjusted when thermal demagnetization data became available.

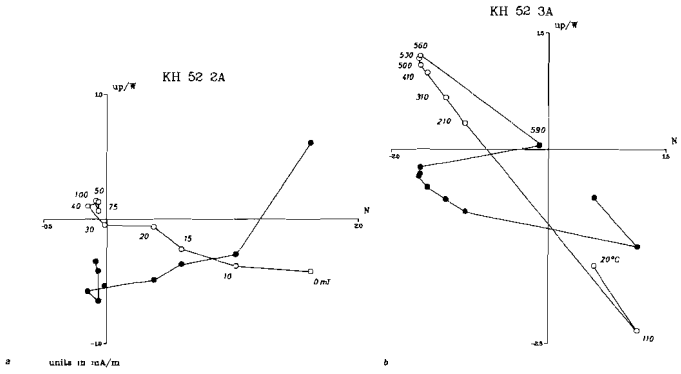

Fig. 3.25 AF and thermal demagnetizations diagrams of specimens from the top of section Kotsiana 2. A major overprint by the secondary component because of weathering cannot be separated by AF demagnetization because of overlapping coercivities (a). Thermal demagnetization on the other hand results in a clear separation of the secondary and characteristic components (b).

Usually the secondary component decays quickly up to 200 oC; after heating up to 200 oC some 80% of the secondary component has decayed and the remaining 20% decays slowly up to 400-500 oC. After 200 oC the low temperature magnetic phase (1b) of the ChRM decays up

to ca. 350 oC, followed by the high temperature phase (1a), which decays rapidly at temperatures higher than 500 oC. At a polarity transition the ChRM is smaller due to the decreased aligning geomagnetic field and the secondary component (unblocking totally at temperatures up to 400-500 oC; cf. figs. 3.12, 3.18, 3.20) predominates the (low temperature magnetic phase (1b) of the) ChRM until ca. 400-500 oC. After that the (high temperature magnetic phase (1a) of the) ChRM starts unblocking rapidly at temperatures higher than 500 oC. In places where weathering has taken place the same happens, but this time due to a larger secondary component rather than to a smaller ChRM.

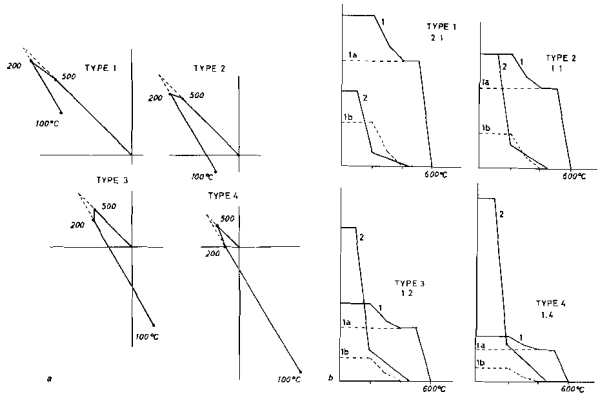

Fig. 3.26 a) Synthetic demagnetizations diagrams (only the projection on the vertical plane is shown) in which the ratio secondary/characteristic component is (a) 1:2, (b) 1:1, (c) 2:1 and (d) 4:1; the inclination difference is taken at 15 degrees. b) Corresponding decay curves for secondary and characteristic components. Stippled lines denote the individual decay curves for the low (1b) and high (1a) temperature magnetic phases of the characteristic component. For further explanation see text.

In figure 3.26a four types of synthetic demagnetization diagrams pare shown, in which the ratio secondary/characteristic component changes from 1:2 to 4:1. The corresponding decay curves are shown in figure 3.26b. It is assumed that at 200 oC 80% of the secondary com-

ponent has decayed, and that the remaining 20% is decaying linearly to zero at 450 oC. Furthermore, it is assumed that between 200 and 500 oC 30% of the characteristic component decays, mainly due to the decay of the low temperature phase. The remaining 70% decays between 500 and 600 oC. These values are based on the real values as determined from the demagnetization diagrams. Although this is a simplification, it can be shown that the resulting synthetic demagnetization diagrams closely resemble the observed diagrams. Some examples will be discussed below; one has already been shown in figure 3.25b which corresponds to type 4 from figure 3.26a.

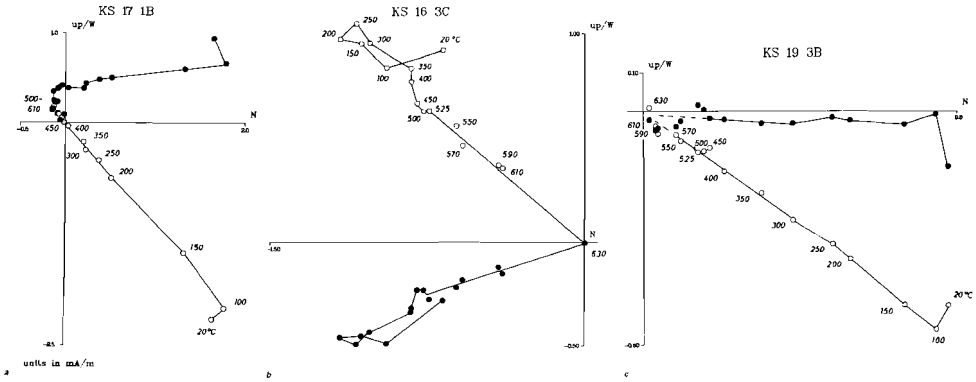

Fig. 3.27 Thermal demagnetizations diagrams of specimens below, close to and above a polarity reversal horizon in section Skouloudhiana. The secondary component is relatively larger than the characteristic component close to this horizon.

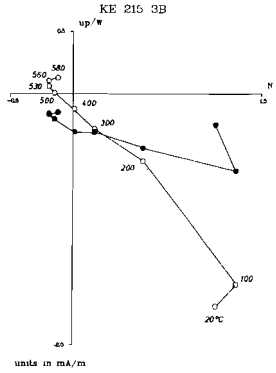

Fig. 3.28 Thermal demagnetizations diagram of a specimen from section Episcopi Extension, taken close to the top of the section, which is intensively weathered. Nevertheless, the characteristic remanence has clearly reversed polarity.

Figure 3.27 shows some demagnetization diagrams of samples below, close to and above a polarity reversal horizon in section Skouloudhiana. The secondary normal polarity component has approximately the same intensity in all samples, but it is relatively larger with respect to the intensity of the ChRM which is lower close to the polarity reversal horizon. The demagnetization diagram of KS 16 3C (fig. 3.27a) corresponds closely to type 1, and that of KS 17 1B (fig. 3.27b) to (an even more advanced) type 4 of figure 3.26a.

Another example of these types can be seen in section Episcopi Extension, where reversed polarities are present in the top of the section. From the demagnetization diagram it could be inferred that sample KE 215 3B (fig. 3.28) is either close to a polarity transition or close to the top of the section. Indeed, this sample was taken close to the top, where intensive weathering had taken place and numerous joints with tan-coloured clay were present. In addition, the sample was taken close to a polarity reversal horizon. Nevertheless it can be seen that the ChRM has a clearly reversed polarity, although a direction cannot be determined reliably. The temperatures needed to reveal the presence of the reversed, characteristic component are even higher than shown in the example denoted as type 4 in figure 3.26a.

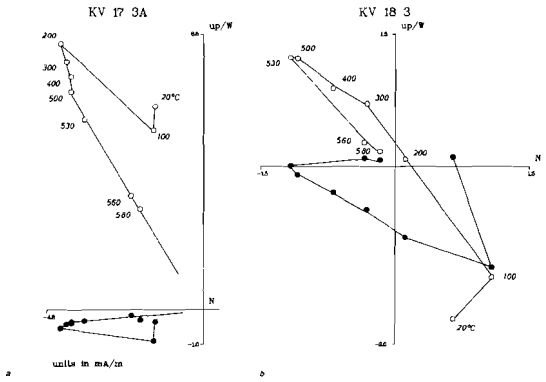

Fig. 3.29 Thermal demagnetizations diagrams of specimens from section Vasilopoulo. Sample KV 18 is taken close to the top of the section, whereas sample KV 17 is taken well away from it. Specimen KV 18 3 closely resembles type 4 of fig. 3.27.

In section Vasilopoulo, close to the Episcopi sections, very similar characteristics are seen in the demagnetization diagrams. Figure 3.29 shows a sample well away from the top, containing a relatively small secondary component (KV 17 3A) as well as a sample taken ca. 50 cm below the thick, sandy turbidite layer which forms the top of the section (KV 18 3). The latter sample again shows a relatively large secondary component, while a major directional change occurs at temperatures higher than 500 oC. Sample KV 17 3A corresponds to type 1, whereas sample KV 18 corresponds to type 4 of fig. 3.26a.

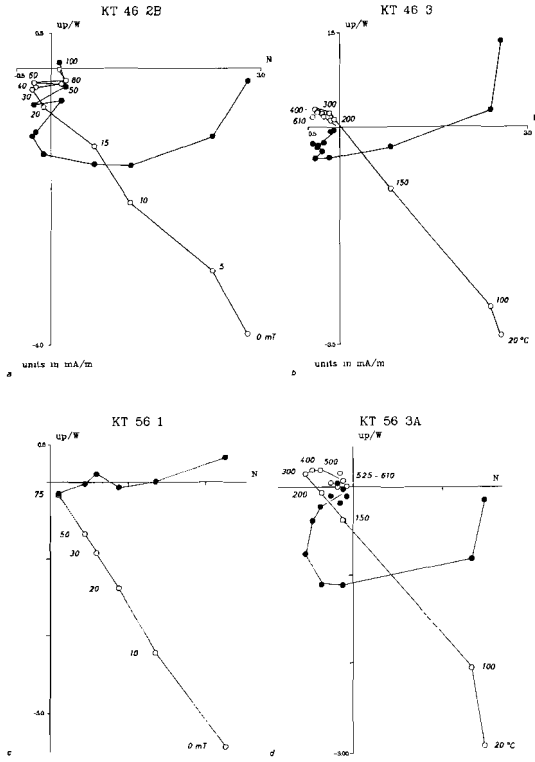

Fig. 3.30 AF and thermal demagnetizations diagrams of specimens from section Kastelli. Sample KT 46 is taken close to the top of a polarity reversal horizon and KT 56 is taken close to the top of the section: AF demagnetization does clearly fail to reveal the characteristic component, whereas thermal demagnetizations does not, despite the very large normal overprint.

The Kastelli section illustrates clearly the phenomena observed at polarity transitions and weathered parts (see fig. 3.30). For instance, in the demagnetization diagrams close to the transition near or at KT 46 or at the top of the section (KT 56) alternating field demagnetization fails to show the characteristic component, whereas thermal demagnetization clearly reveals this component. A major directional change is only observed at higher temperatures (400-500 oC); it can be seen that KT 46 and 56 correspond to type 4 of fig. 3.26a Alternating field demagnetization does not succeed in separating the normal and reversed components. Apparently processes that have played a role in this section are the same as or similar to those observed in the western Cretan sections.

The various components in the individual sections

So far the various characteristics of the total natural remanent magnetization have been discussed. Below, the individual sections will be discussed shortly with some emphasis on the features described above.

Examples of demagnetization diagrams of samples from section Potamida 1 have already been extensively shown in figures 3.10-3.14, as well as IRM acquisition curves (fig. 3.23) and an example of a low temperature cycle (fig. 3.24).

Examples for section Potamida 2 are shown in figures 3.15-3.18. The decay curves show that the initial decay (1b) of the characteristic component is somewhat more pronounced than in section Potamida 1 and may even be inferred from samples with a normal polarity ChRM (see fig. 3.16b).

In section Potamida 3 the decay of the secondary component as well as the initial (1b) and final (1a) decay of the characteristic component can clearly be recognized in the thermal decay curves, (fig. 3.20), not only in the samples with a reversed polarity ChRM, but also in samples with a normal polarity ChRM. The ChRM seems to unblock at temperatures appreciably higher than 600 oC. Although the presence of some hematite cannot be excluded, this is more probably

due to insufficiently accurate calibration of the temperatures.

In the top of section Potamida 3 the clay is less dense and contains more sandy intervals. Intensities are much lower and demagnetization data are less consistent (fig. 3.21). Apart from a viscous remanent magnetization (VRM) which is removed at 100 oC, sample KP 245 does not seem to contain a secondary normal polarity component such as that seen in the previous samples. The thermal decay curve is rather similar to the curves for sections Potamida 1 and 2, however, and the two magnetic phases (1b and 1a) can be recognized tentatively (fig. 3.22). This is not the case for sample KP 240, which seems to contain a single component, seemingly unblocking at 500-550 oC. The thermal decay curve suggests less fine-grained magnetite, which is not surprising considering the lithology of the upper part of the Potamida 3 section, i.e. less fine-grained (more silty) sediments. Although the directions of the ChRM in the upper part of this section cannot be determined accurately, the polarities are unambiguous.

The IRM acquisition curves of samples from sections Potamida 2 and 3 are shown in figure 3.31. The lowest two samples from section Potamida 2 have been shown to be remagnetized due to weathering along numerous joints (Langereis, 1979; Drooger et al., 1979b) and the IRM acquisition curve of the lowermost sample (KP 101 in fig. 3.31a) does indeed suggest the presence of hematite: in a magnetic field up to 300 mT, less than 70% of the maximum IRM is acquired, whereas in other samples this is approximately 90%. For the major part of the section it can be inferred that the main magnetic carrier is magnetite.
The same applies to the lower part of section Potamida 3 (KP 201-220 in fig. 3.31b): approximately 90% of the SIRM is acquired at 300 mT, the maximum coercivity for (single domain) magnetite. In the upper part of section Potamida 3 a greater amount of a high coercivity mineral is present (KP 229-245 in fig. 3.31b). Since the less dense clay in the upper part of the section facilitates weathering, the resulting oxidation may form a high coercivity mineral such as hematite (or goethite: see for instance the initial decrease upon heating to 100 oC of KP 245 4A in figure 3.21).

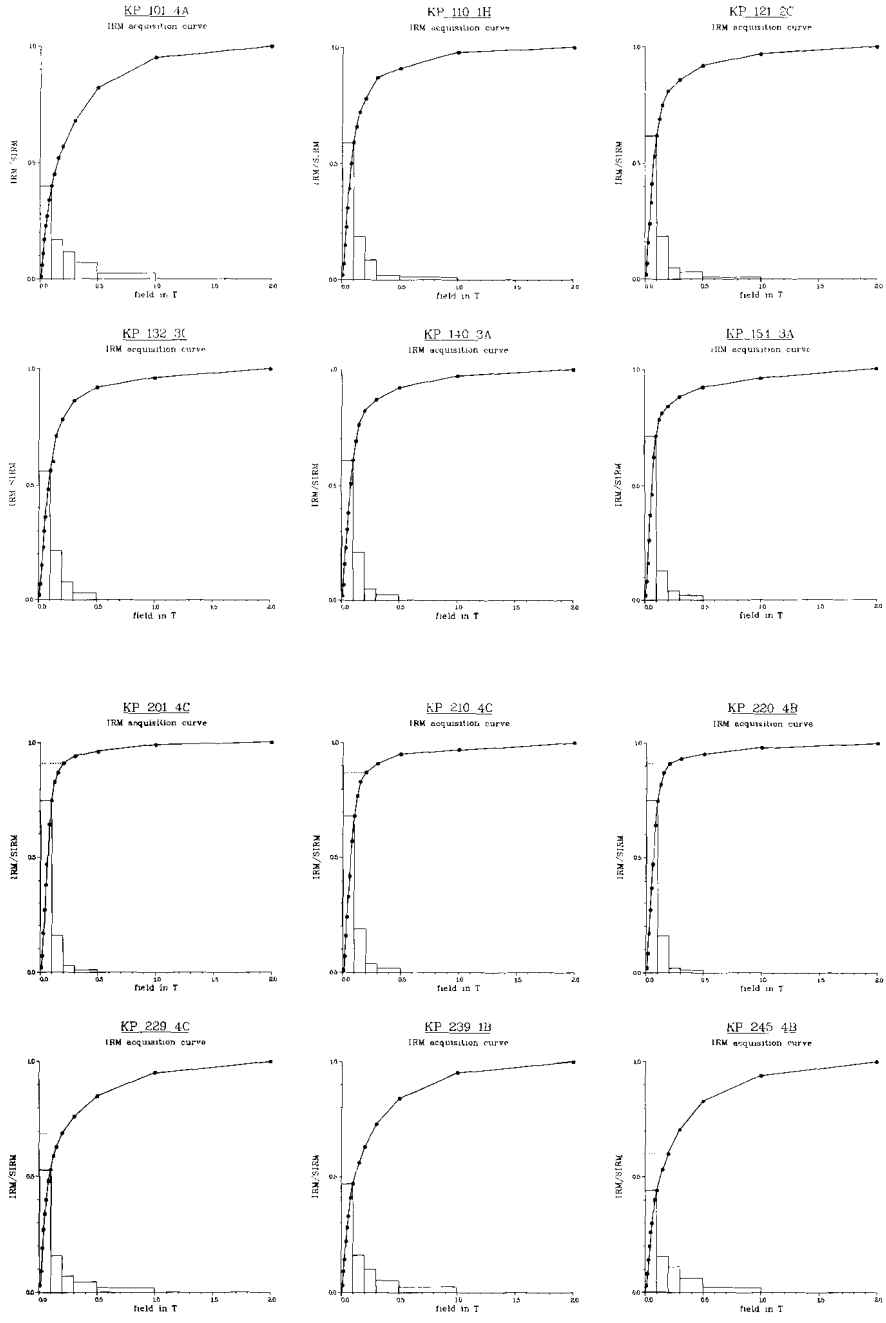

Fig. 3.31 IRM acquisition curves of specimens from section Potamida 2 (KP 101 - 154) and from section Potamida 3 (KP 201 - 245). See also text and see caption to figure 3.23

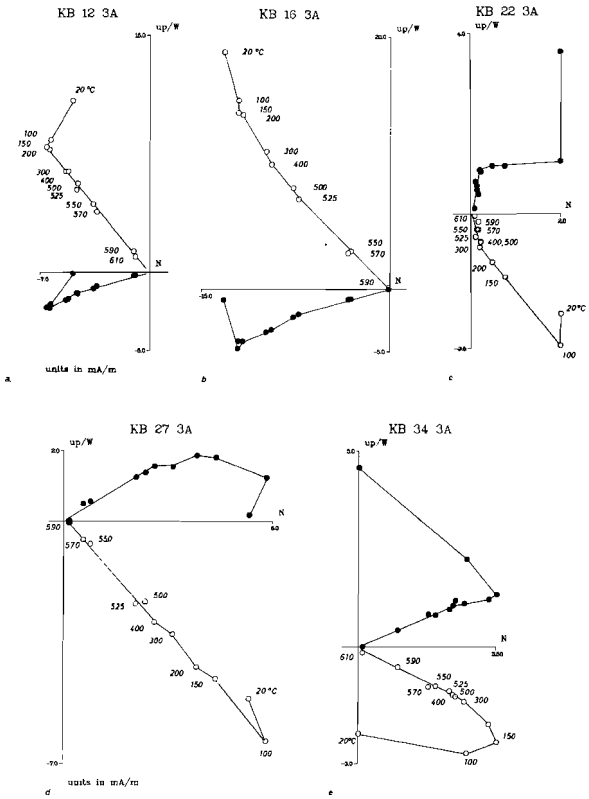

Fig. 3.32 Thermal demagnetizations diagrams from section Potamida 4, below, close to and above a polarity reversal horizon, approximately at the level of KB 22. Note the relatively large secondary component in specimen KB 22 3A.

Figure 3.32 shows some examples of thermal demagnetizations from section Potamida 4. There is a slight but distinct directional change of the characteristic remanent magnetization at 500-525 oC, both in the normal and reversed polarity ChRM. This can be seen most clearly in the declination of these components; the change in direction can be explained by a secondary normal polarity component with a mainly northern declination and only unblocking totally at approximately 500 oC. Its strong usual initial decrease at 150-200 oC (see for instance figures 3.12, 3.18, 3.20) may be masked in the demagnetization diagrams of KB 12 3A and KB 16 3A by a somewhat harder viscous component.

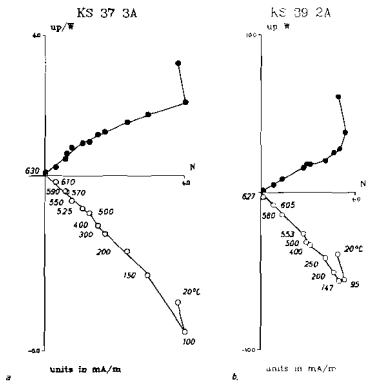

Fig. 3.33 Thermal demagnetizations diagrams of specimens from section Skouloudhiana; see also figure 3.27

Some examples below, close to and above a polarity transition in section Skouloudhiana have been shown in fig. 3.27. In sample KS 19 3B (fig. 3.27c) no directional change is observed between the secondary and characteristic component, both having a normal polarity. In most other samples, however, a slight change can be detected at temperatures of 500-525 oC (fig. 3.33).

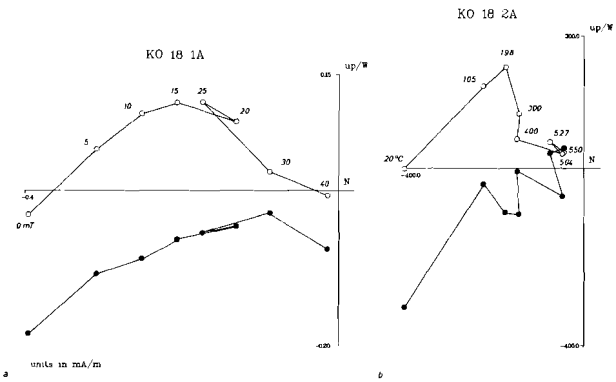

Fig. 3.34 AF and thermal demagnetizations diagrams of specimens from section Kotsiana 1. Due to low NRM intensities, directions of the characteristic remanent magnetization cannot reliably be determined, but (in this case reversed) polarities can be established reliably.

The NRM intensities in section Kotsiana 1 are substantially lower than in the other western Cretan sections. Directions of the ChRM cannot be determined reliably, but polarities can be established unambiguously throughout the section, except in the lowermost part below a thick sand layer (see also chapter 4). The example shown in figure 3.34 clearly shows a reversed polarity of the characteristic component, although the demagnetization diagram shows considerable scatter. Unblocking alternating fields are much lower than in the former sections: in fields higher than 40-50 mT the ChRM is removed entirely and at temperatures higher than 500 oC the magnetization generally becomes viscous. The carrier of the ChRM may be a "softer" magnetic mineral, e.g. less fine-grained and multi-domain magnetite or titanomagnetite (cf. Dankers, 1978).

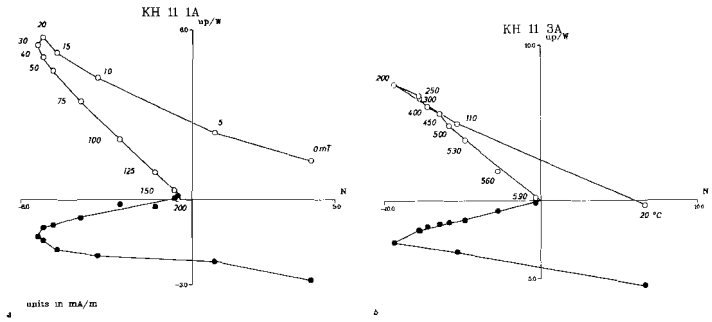

Fig. 3.35 AF and thermal demagnetizations diagrams of specimens from section Kotsiana 2. A relatively large intensity secondary component can be recognized, resembling type 3 of figure 3.26

Section Kotsiana 2, on the other hand, shows characteristics very similar to those of the previous sections. A rather large intensity secondary normal polarity component can be recognized in a type 2 demagnetization diagram and the characteristic component has coercivities and unblocking temperatures suggesting fine-grained (probably single-domain) magnetite (fig. 3.35).

Section Makronas was sampled partly in the open marine clays identical to those of the former sections and partly in the overlying beige-whitish, homogenous-laminated marls. From preliminary

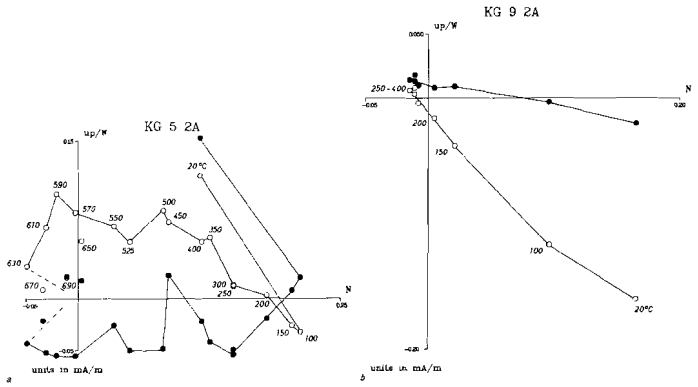

Fig. 3.36 Thermal demagnetizations diagrams of specimens from section Makronas. Samples from the lower part of the section (e.g. KG 5 2A) show clearly a reversed polarity characteristic remanent magnetization, probably carried by hematite (a). In the middle and upper part of the section results are more ambiguous (e.g. KG 9 2A), but still suggest reversed polarities of the characteristic remanent magnetization (b). See also text.

results it was assumed that the overlying formation contained only a secondary normal overprint. From figure 3.36 it can be seen that careful and detailed thermal analysis shows that a predominant secondary component is indeed present, but a reversed characteristic component can still be recognized. The lower part of the section may correspond with the uppermost part of the Potamida 3 section but an overlap cannot be proved. The clay is correspondingly less dense, and numerous sandy intervals occur. An example from the lower part (KG 5 2A in fig. 3.36) shows that a reversed ChRM is revealed at temperatures higher than 600 oC. Although the results are largely scattered, the demagnetization steps up till 690 oC indicate that the carrier of the ChRM is hematite. Samples from the marl sequence of the middle and upper part of the section have been carefully measured, even taking account of (and correcting for) the sample holder of the cryogenic magnetometer. Although intensities at temperatures higher than 200 oC are in the order of 0.020 mA/m (the sample holder has an intensity of 0.003 - 0.005 mA/m, the noise level is ca. 0.001 mA/m), a reversed ChRM can be inferred (fig. 3.36b).

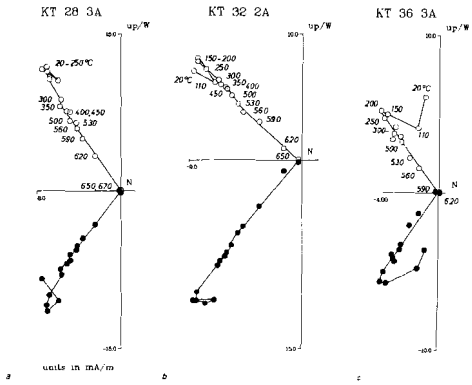

Fig. 3.37 Thermal demagnetizations diagrams from section Kastelli. Declinations of the characteristic remanent magnetization deviate strongly from N-S, by some 40 degrees.

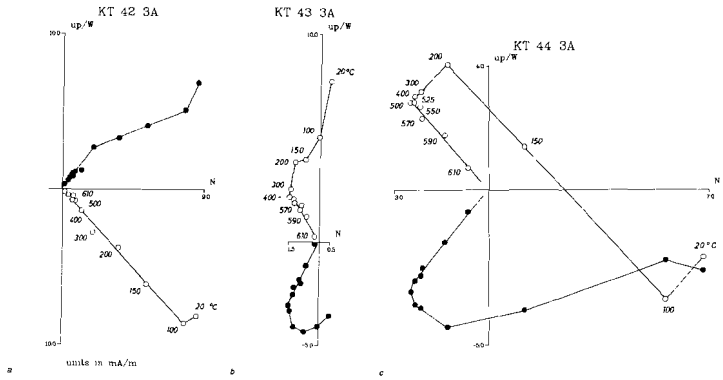

Fig. 3.38 Thermal demagnetizations diagrams of specimens from section Kastelli below and above a polarity reversal horizon (between KT 42 and KT 43).

The Kastelli section in central Crete shows in general demagnetization characteristics similar to those of the sections in western Crete. In the lower-middle part of the section (fig. 3.37) the secondary normal polarity component is small compared with the characteristic component, which in this section has the highest intensities observed in Crete. A very slight directional change at 530 oC indicates that the secondary component only unblocks totally at such

temperatures. A small viscous component disturbs the secondary component in its turn and is removed at ca. 150 oC. The characteristic component seems to show a gradual change in the temperatures at which it totally unblocks, from more than 620 oC in KT 28 to 590 oC in KT 36. This could be due to a gradual change of the magnetic mineralogy, but a small temperature gradient in the furnace could also have been the case.
Examples of demagnetization diagrams below and above a polarity transition occurring between sampling level 42 and 43 are shown in figure 3.38. Although a directional change between secondary and characteristic component is generally observed at 300 oC, sample KT 44 3A (fig. 3.38c) shows that the secondary component only unblocks totally at temperatures of ca. 500 oC. The ChRM directions deviate strongly from N-S, more than in the sections in western Crete and up to some 40 degrees.

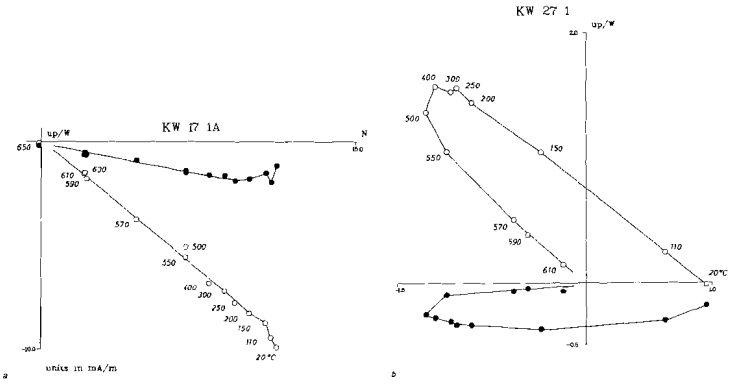

Fig. 3.39 Thermal demagnetizations diagrams of specimens from section Vassiliki.

Section Vassiliki is older than any other section in Crete and there is no overlap according to the biostratigraphy (fig. 2.5). Routine demagnetizations were carried out and show that levels with normal normal as well as reversed characteristic remanent magnetizations are present (fig. 3.39). Demagnetization shows characteristics similar to those of the younger sediments, except that the secondary component is only removed totally at 550 oC. Some hematite appears

to be present, in view of the temperatures needed to remove the ChRM (up to 650 oC). The demagnetization diagram of KW 27 1 (fig. 3.39b) closely resembles a type 2 rather than a type 1 demagnetization (cf. fig. 3.26a).

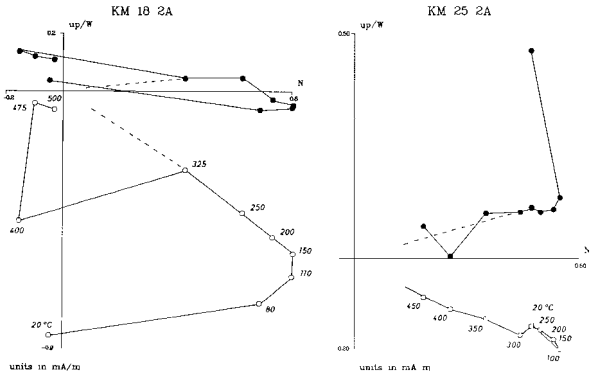

Fig. 3.40 Thermal demagnetizations diagrams of specimens from section Makrilia. Often the magnetization becomes viscous at temperatures of 400 ^{o}C or higher. See also figure 3.9

Section Makrilia, though younger than section Vassiliki is older than the other Cretan sections and again there is no overlap (fig. 2.5). The lithology of the section suggests rapid sedimentation and because of numerous turbiditic (and non-lithified) sand layers weathering may easily occur. The demagnetization results are rather mixed: natural remanent magnetizations are encountered which consist of a single, viscous component (fig. 3.9b). A large viscous component is always present, both in specimens with a reversed polarity ChRM (fig. 3.9a) and in specimens with a (probably) normal polarity ChRM (fig. 3.40). Often the magnetization becomes highly viscous at temperatures higher than 400 oC (fig. 3.40a)). Important parts of the section contain magnetizations of which the polarity cannot be determined reliably.

Section Faneromeni in the Sitia district of eastern Crete has a biostratigraphic range similar to that of the Kastelli section in central Crete (fig. 2.5) and should therefore produce the same magnetostratigraphic results as found for western and central Crete.

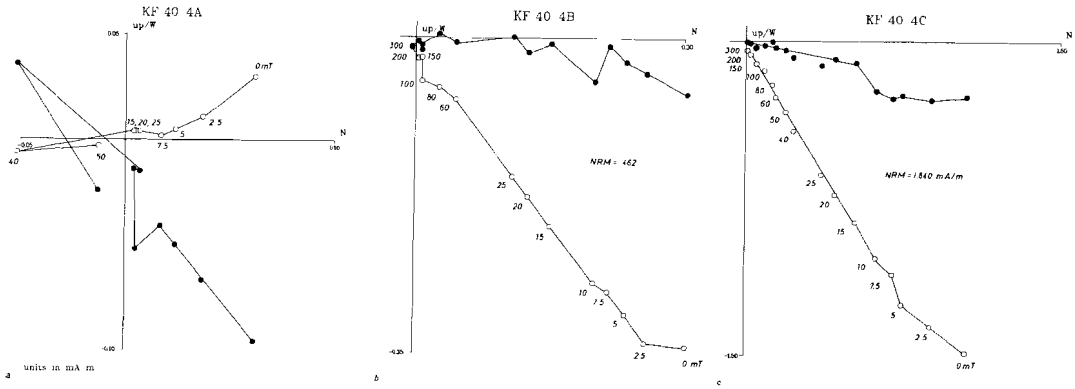

Fig. 3.41 AF demagnetizations diagrams of three specimens from the same core in section Faneromeni. The A - specimen is least weathered and furthest from the surface of the outcrop; the direction of the magnetization is neither normal nor reversed, whereas the more weathered specimens (B and C) show a normal polarity magnetization and higher total NRM intensities.

Unfortunately, the demagnetization results are generally not very encouraging. The longest possible cores were drilled in order to try and obtain fresh (unweathered) specimens. All specimens have been demagnetized from a number of cores; an example is shown in figure 3.41. The fresh, unweathered specimen (the A specimen) has a low initial intensity (.12 mA/m), whereas the specimens closer to the surface of the outcrop have increasingly higher intensities (.46 and 1.84 mA/m for the B and oC specimen, respectively). Apparently the intensity increases with an increasing amount of weathering due to the acquisition of a CRM. The magnetization of the fresh (or least weathered) specimen can only resist alternating fields up to 25 mT, after which the magnetization becomes erratic (fig. 3.41a). The direction of the magnetization is neither normal nor reversed, having an easterly declination and a slightly negative inclination. The magnetization may be viscous and laboratory induced, since at 7.5 mT most of the remanence is removed. The weathered specimens show magnetizations with coercivities up to 300 mT and have a normal polarity, almost certainly of (sub)recent origin (fig. 3.41b, c).

In the middle part of the section NRM intensities are appreciably higher and a clearly reversed polarity ChRM is present. Both

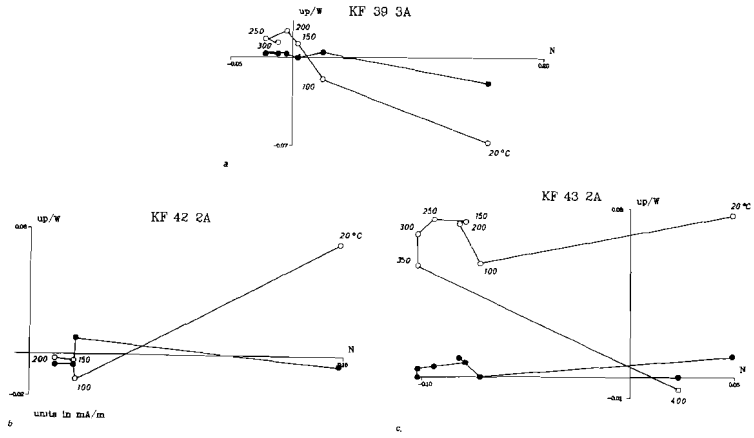

Fig. 3.42 Thermal demagnetizations diagrams of specimens from the middle-upper part of section Faneromeni. Reversed polarity ChRM is clearly present, except in sample KF 42 2A which shows only viscous magnetizations.

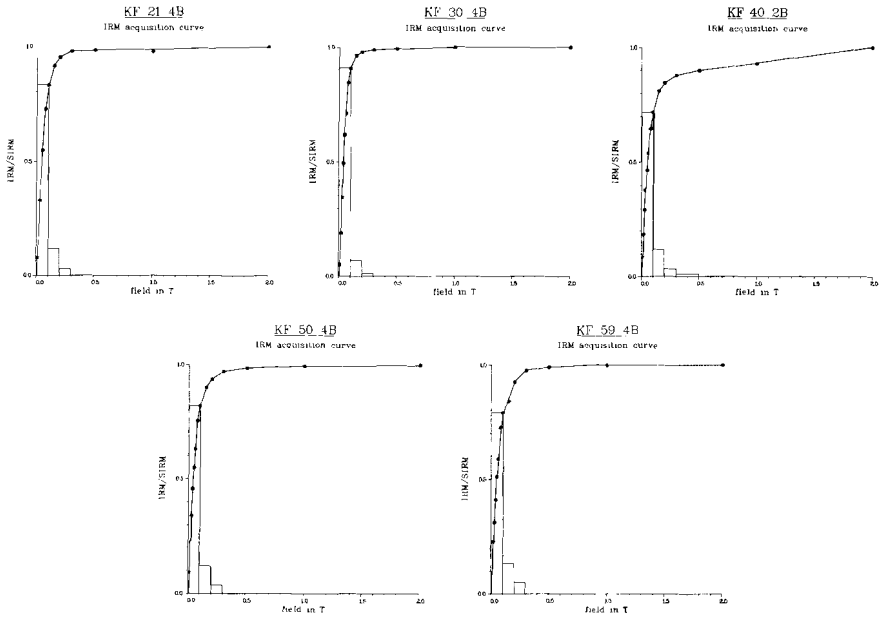

Fig. 3.43 IRM acquisition curves of specimens from section Faneromeni. Except in sample KF 40 2B, most of the SIRM (80-90%) is acquired in a field of 100 mT, indicating that large-grained (multi-domain) magnetite is the carrier of the IRM.

below and above the FOD of the *G. conomiozea* group in this section reversed polarities are present (fig. 3.42a,c), whereas close to this datum only viscous magnetizations can be found (fig. 3.42b).

The IRM acquisition curves (fig. 3.43) indicate the presence of magnetite as the main carrier of the remanence; only in sample KF 40 2B does there seem to be a small amount of hematite. It appears that, except in the middle part of the section with higher NRM intensities, the magnetic mineralogy (of the least weathered specimens) often yields viscous (laboratory induced) magnetizations, suggesting that large grained, multi-domain magnetite is the predominant iron oxide. This is corroborated by the shape of the IRM acquisition curves and the remanent acquisition coercive force, i.e. the field needed to magnetize a specimen to half its SIRM (cf. Hartstra, 1982b).

In general the results of the Cretan sections indicate that the characteristic magnetizations are of primary origin. The main magnetic carrier of the ChRM has been shown to be magnetite, most probably very fine grained and of single domain size. The average ChRM has an inclination which is lower than the inclination of the geocentric axial dipole field at the present latitude of Crete, whereas the secondary normal polarity magnetization generally has an average inclination close to the latter value. This supports the (sub)recent origin of the secondary magnetization, which consists probably of a chemical remanence acquired during the Brunhes chron. The lower inclination of the ChRM may be due to an inclination error (King, 1955), which has been frequently observed in magnetizations of depositional origin. Valet and Laj (1981) note that the lower inclination of these clays may be due to compaction of the sediment, although they do not elaborate on the mechanism involved. Laj et al. (1982) argue that both explanations suggest that the ChRM has been acquired at an early stage and support its primary origin. Further support for the primary origin of the ChRM is provided by the transitional directions and lowered intensities occurring at or close to polarity reversal horizons. Having established the primary origin of the characteristic remanent magnetization, it can be inferred that the polarities of the ChRM accurately reflect the polarity of the geomagnetic field at the time of deposition.

Whereas the results of the Cretan sections yield reliable magnetostratigraphic sequences, the results of the Sicilian sections are less satisfactory.

Section Falconara has a stratigraphic range encompassing most Cretan sections, but nevertheless only normal polarity magnetizations are found. Intensities of the total NRM are generally very low (see fig. 3.5) and very often a large component is removed by heating up to 100 oC, indicating either a large viscous magnetization or a secondary magnetization resulting from a (sub)recently acquired CRM which is carried by goethite. After removal of the viscous c.q. goethite component the intensities decrease quickly to 0.020 mA/m or lower (fig. 3.44). Demagnetization at higher temperatures results in scatter or in a normal polarity remanent magnetization.

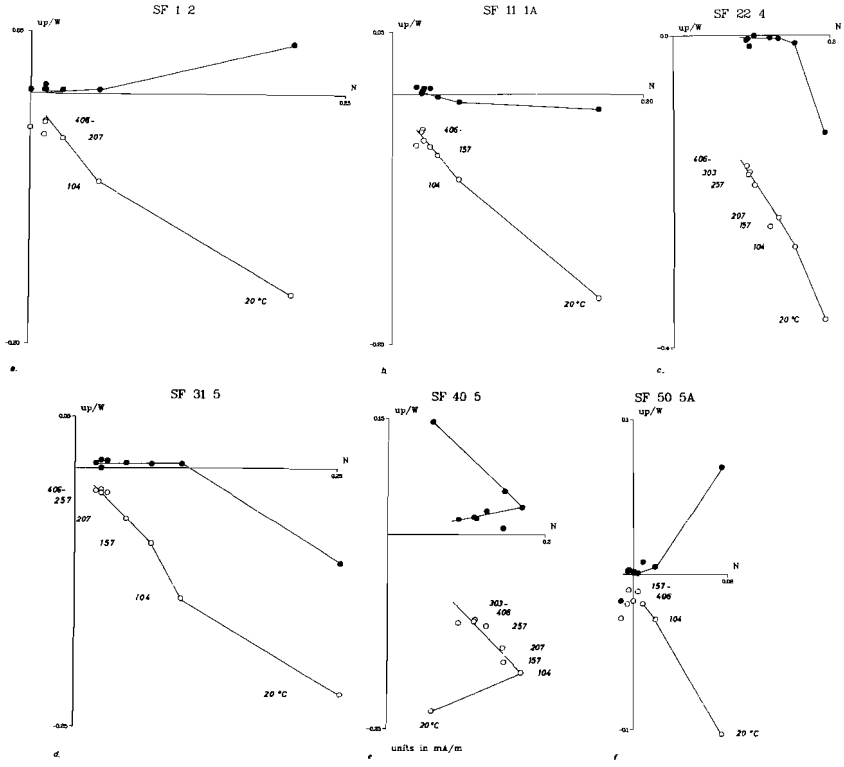

Fig. 3.44 Thermal demagnetization diagrams of specimens from section Falconara, showing only normal polarity magnetizations throughout the section. Often a large component is removed by heating up to 100 ^{o}C, possibly due to the presence of goethite.

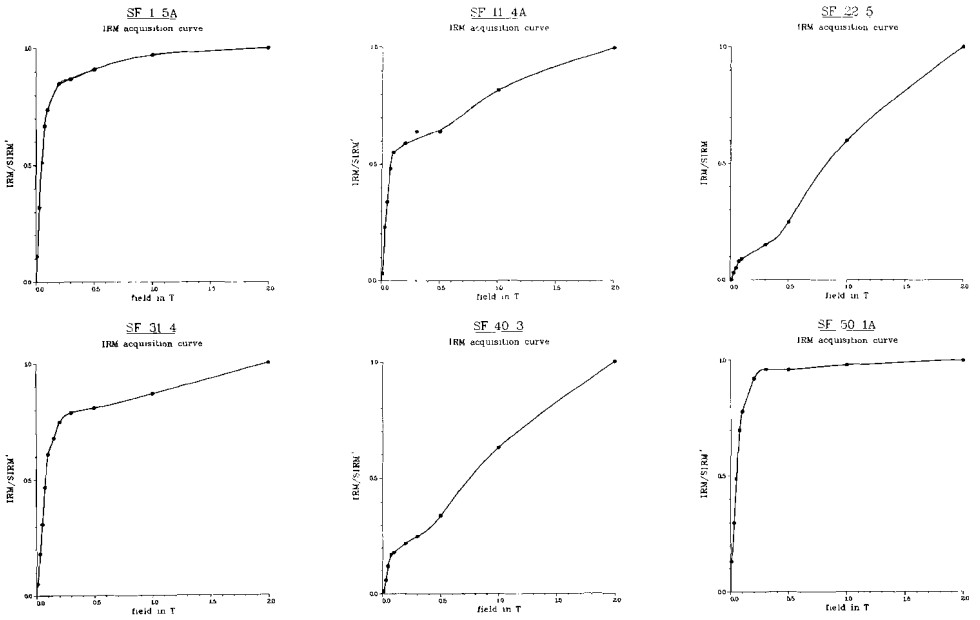

Fig. 3.45 IRM acquisition curves of specimens from section Falconara, indicating the presence of both a low coercivity mineral and a high coercivity mineral (goethite or hematite).

Furthermore, IRM acquisition curves (fig. 3.45) not only indicate the presence of a low coercivity mineral (magnetite or maghemite), but also indicate very clearly the presence of a high coercivity mineral. The shape of the curve may indicate the presence of goethite: it is initially flat and rises steeply at fields higher than 0.5 Tesla. Lowrie and Heller (1981) show similar curves, indicating goethite as the magnetic mineral carrying the IRM, but they note that these curves are often indistinguishable from hematite. Also, both goethite and hematite may be present.
It is obvious that the whole section has been remagnetized due to weathering, which caused oxidation of the original magnetic minerals. Section Giammola shows very similar results.

In section Scicli South 1 results are rather mixed. In the lowermost part of the section reversed polarities can be inferred from the demagnetization diagrams (fig. 3.46). A viscous component is removed at temperatures of 100 oC; demagnetization at higher

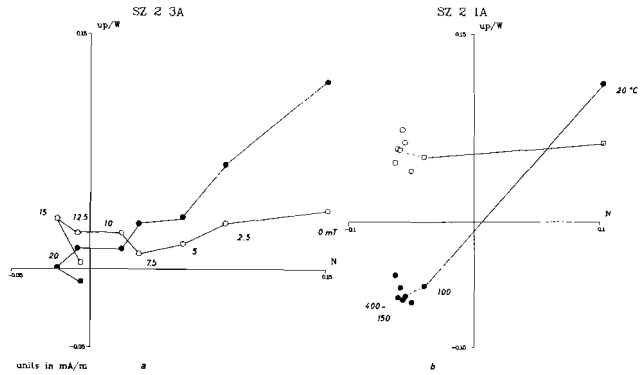

Fig. 3.46 AF and thermal demagnetizations diagrams of specimens from the lower part of section Scicli South 1. A viscous component is removed at fields of 10 mT or 100 °C; a reversed polarity component can clearly be recognized in the thermal demagnetizations diagrams.

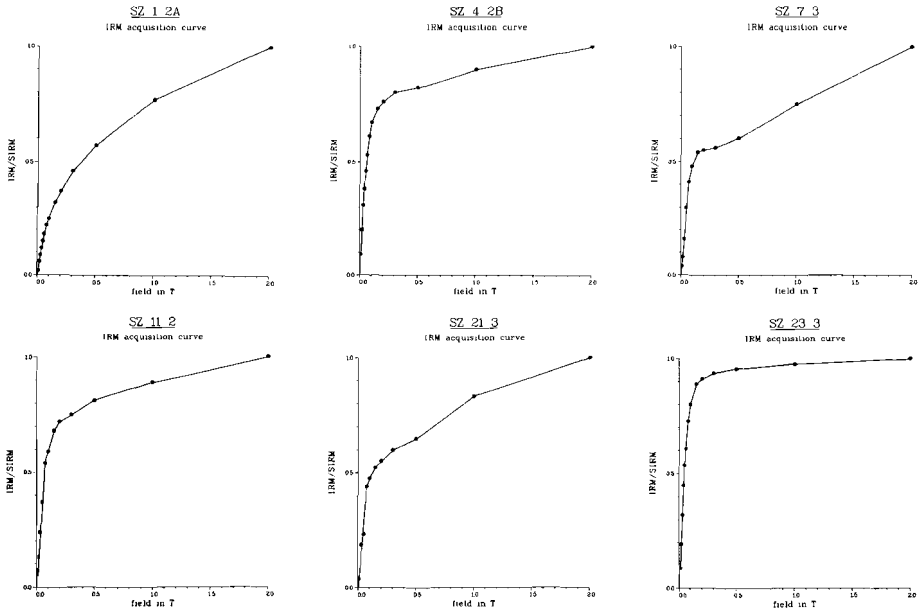

Fig. 3.47 IRM acquisition curves of specimens from section Scicli South 1, revealing the presence of both low and high coercivity minerals.

temperatures reveals the presence of a reversed polarity ChRM, whereas results from alternating field demagnetization are less conclusive (fig. 3.46a). A major part of this section, however, shows considerable normal polarity overprinting and polarities cannot be established unambiguously. The IRM acquisition curves of section Scicli South 1 reveal the presence of various magnetic minerals (fig. 3.47). In the lowermost sample (SZ 1 2A) hematite is the predominant mineral, whereas in the remaining samples magnetite appears to be present, as shown by the initial curve, as well as goethite and/or hematite.

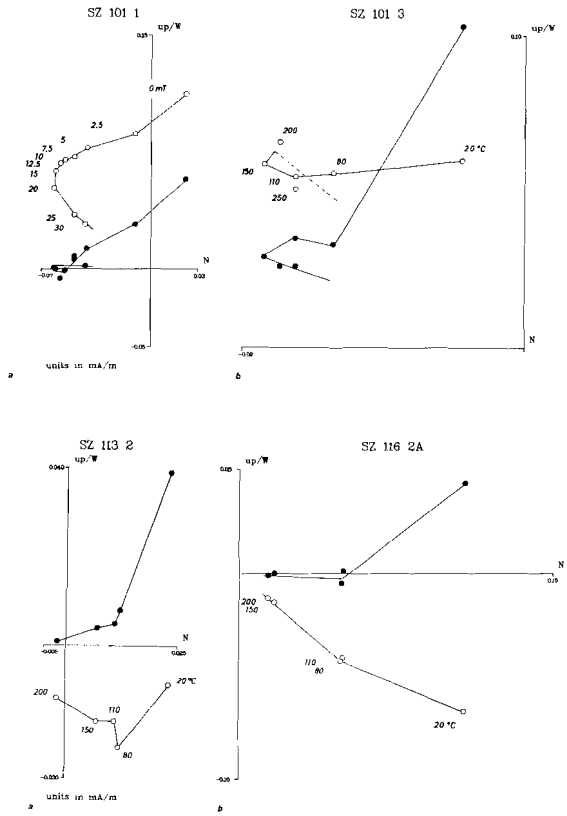

Fig. 3.48 AF and thermal demagnetizations diagrams of specimens from section Scicli South 2. In the lower part of the section (e.g. SZ 101) polarities of the characteristic remanence are clearly reversed, in the middle-upper part (e.g. SZ 113, 116) results are not conclusive due to extreme low intensities.

A parallel sampling track, section Scicli South 2, has been sampled close to the original track, since the clay looked less weathered. Results are correspondingly slightly better. In the lower part of this section, which corresponds to the lower part of the former section, both alternating field and thermal demagnetization reveal the presence of a reversed polarity ChRM (fig. 3.48a,b). In the middle and upper part of the section, however, intensities become extremely low after demagnetization at temperatures higher than 200 oC (fig. 3.48c,d). It cannot be ascertained whether only a normal polarity magnetization is present or whether a reversed polarity magnetization is masked because the accuracy level of the magnetometer has been reached. The magnetization vector of sample SZ 113 2 (fig. 3.48c) seems to bypass the origin, pointing to a reversed polarity, but intensities are down to 0.010 mA/m and no reliable conclusions can be made. The IRM acquisition curves indicate mainly the presence of magnetite (fig. 3.49); goethite and/or hematite appear not to be as dominant as in the former section cf. figure 3.47).

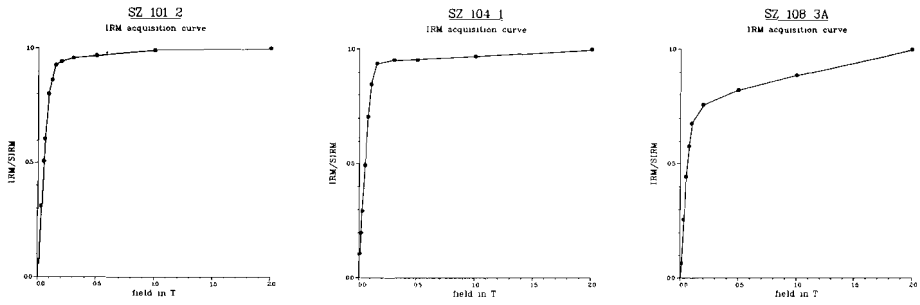

Fig. 3.49 IRM acquisition curves of specimens from section Scicli South 2. The magnetic minerals responsible for the IRM are mainly large-grained (multi-domain) magnetite.

Section Scicli West shows demagnetization diagrams all of which are similar throughout the section; some examples are shown in figure 3.50. After heating to 100 oC a large, viscous magnetization component is removed and at higher temperatures magnetizations are

revealed with predominantly northwest declinations and inclinations which are positive or near zero. Intensities are again extremely low and generally less than 0.010 or 0.020 mA/m after heating to 100 oC. The IRM acquisition curves (fig. 3.51) indicate that the main magnetic mineral is magnetite; practically no higher coercivity mineral is present. The magnetizations found in this section may be entirely due to a viscous remanence carried by a low coercivity mineral such as (large grained) magnetite.

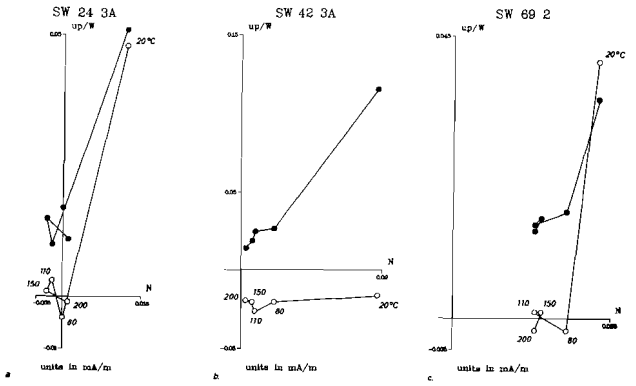

Fig. 3.50 Thermal demagnetizations diagrams of specimens from section Scicli West. Results are similar throughout the section and indicate that the NRM consists of viscous magnetizations only.

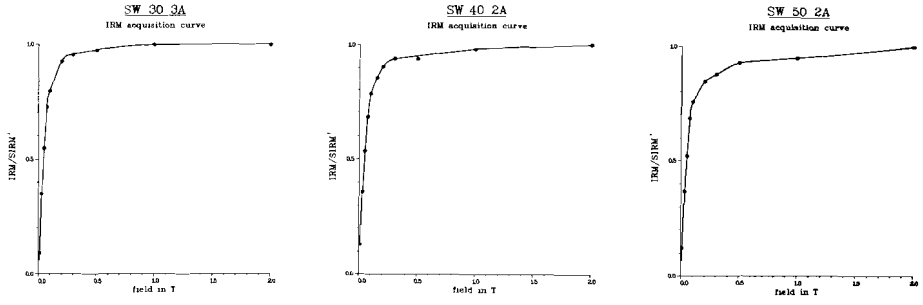

Fig. 3.51 IRM acquisition curves of specimens from section Scicli West, indicating that large-grained magnetite is the main mineral carrying the IRM.

The Mussotto section in northern Italy shows both normal as well as reversed polarities (fig. 3.52). A large variation of the coercivities may be the result of the variable lithology of the section (see chapter two). A very large viscous component is present which in several samples is removed in fields of 5 mT: the total NRM in sample IM 2 2A, for instance, has an initial intensity of 13.2 mA/m, which decreases to 1.6 mA/m at 5 mT. This first step has therefore been omitted from the diagram (fig. 3.52a).

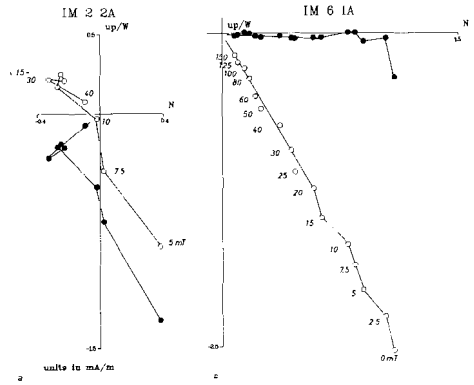

Fig. 3.52 AF demagnetizations diagrams of specimens from section Mussotto. An extremely large viscous component is present in specimen IM 2 2A, which decreases from 13.2 mA/m at 0 mT to 1.6 mA/m at 5 mT.

Section Castellania near the Rio Mazzapiedi in the Tortonian type area shows normal as well as reversed polarity ChRM's. A viscous component is removed after 100 oC and a secondary component is removed after heating up to temperatures of 200–300 oC. The characteristic component often becomes viscous after 350–400 oC (fig. 3.53), but its polarity, though not its direction, can be determined reliably. The lithology of the section is rather constant, which is reflected in the similar behaviour of the magnetizations during thermal demagnetization (see fig. 3.53).

In the Luzzena section only pilot samples were taken. The section consists of post-evaporitic sediments, whereas all other sections in Crete, Sicily and northern Italy consist of pre-evaporitic deposits. All pilot samples throughout this section show clearly reversed polarities, although directions of the ChRM show a large variation (fig. 3.54). This may be due to the fact that parts of the section have rotated due to gravity sliding (frana).

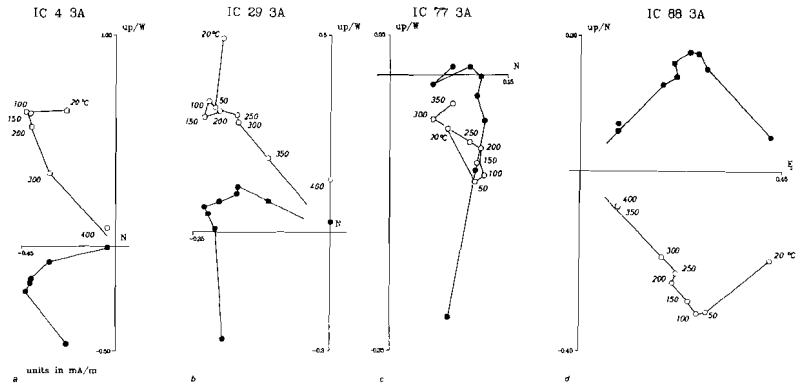

Fig. 3.53 Thermal demagnetizations diagrams of specimens from section Castellania.

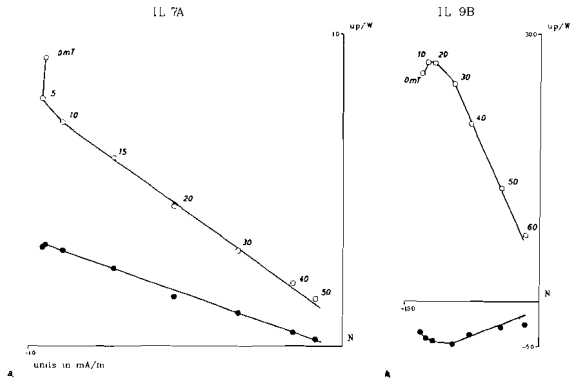

Fig. 3.54 AF demagnetizations of two pilot specimens from section Luzzena, showing a reversed polarity characteristic remanent magnetization.

chapter four

M A G N E T O S T R A T I G R A P H Y

INTRODUCTION

The characteristic remanent magnetization (ChRM) directions of at least two specimens per sampling level were determined and are plotted as the declination and the inclination versus the stratigraphic position. In general ChRM directions vary by less than ca. 5 degrees per sampling level in most Cretan sections. Largest differences occur in the top part of the sections and close to lithologic discontinuities such as ferruginous levels, sandy layers or layers of finely bedded clay. These differences are thought to be induced by weathering processes causing a (partial) overprint by a secondary remanence due to oxidation. Such a secondary magnetization is often relatively large with respect to the characteristic remanent magnetization, the direction of which is then more difficult to determine with accuracy. The polarity of such a ChRM can nevertheless be derived reliably from the demagnetization diagrams (see chapter 3).

It has been established that the characteristic remanent magnetizations are of primary origin and hence the polarities reflect the polarity of the geomagnetic field at the time of deposition. If the remanence consists of a mainly viscous magnetization or if the magnetic properties indicate a secondary origin, remanence directions have either not been plotted or it is indicated that the polarity may not reflect the original polarity.

In general, inclinations of the ChRM are shallower than the inclination of the geocentric axial dipole field for the present latitude of the localities. Deviations in the declination of the ChRM from the geocentric axial dipole field are recorded as well, up to ca. 40 degrees in section Kastelli. A more detailed discussion of

the ChRM directions together with the anisotropy of susceptibility will be given in chapter 6. In the current chapter we shall be concerned with the polarity results and the ensuing polarity patterns of the sections. The established polarity zones are labeled with a letter and a sign, which denotes normal (+) or reversed (–) polarities and this label refers to the position of the polarity zone in the resulting composite polarity sequence determined for western Crete. Polarity zone A– is the oldest complete polarity zone encountered which can reliably be correlated in more than one section, polarity zone F+ is the youngest.

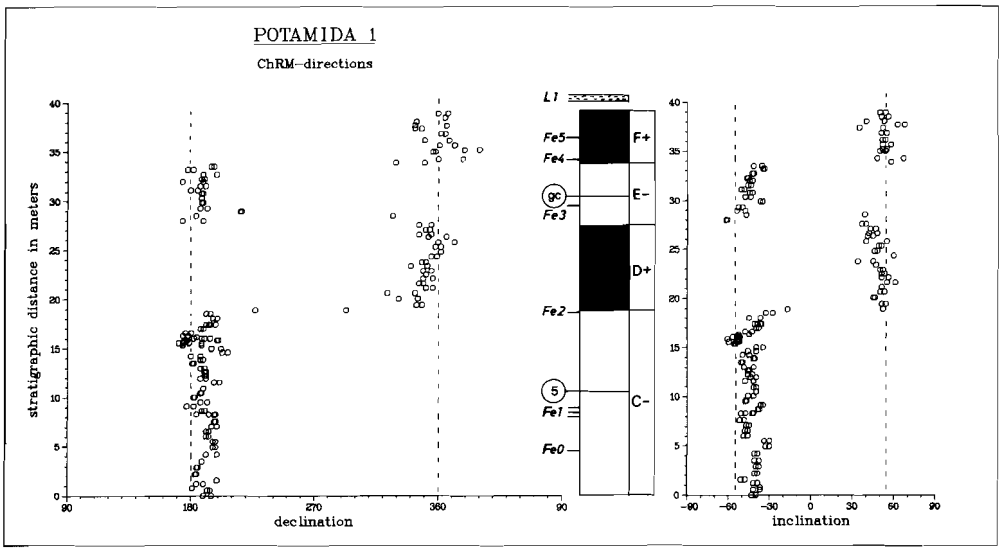

Fig. 4.1 Declination and inclination of the ChRM in section Potamida 1. Black (white) intervals represent normal (reversed) polarities. Dashed lines indicate declination and inclination of the geocentric axial dipole field for the present latitude of the locality. Polarity zones are labeled with a letter; the sign denotes normal (+) or reversed (–) polarity; gc = FOD of the *G. conomiozea* group; 5 = FOD of *G. menardii* form 5; Fe = ferruginous layer; L = layer of finely bedded clay.

MAGNETOSTRATIGRAPHIC RESULTS

The ChRM directions of section Potamida 1 are shown in figure 4.1. The section appears to contain four polarity zones. A conspicuously long, reversed polarity zone (C-) in the lower part of the section, containing the FOD of *G. menardii* form 5, is followed upwards by polarity zones D+, E- and F+. The FOD of the *G. conomiozea* group occurs in the reversed polarity zone E-. Only the lengths of polarity zones D+ and E- are well defined, whereas the lengths of zones C- and F+ are uncertain because their lower and upper reversal boundaries were not recorded.

The same four polarity zones can be recognized in section Potamida 2 (fig. 4.2) on the basis of magnetostratigraphic, lithostratigraphic and biostratigraphic evidence. The lengths of polarity zones D+ and E- are the same in sections Potamida 1 and 2. The positions of the ferruginous levels Fe 3 in zone E- and of Fe 4 in the lower part of F+ and of the biostratigraphic datum levels (the FOD's of *G. conomiozea* in zone E- and of *G. menardii* form 5 in zone

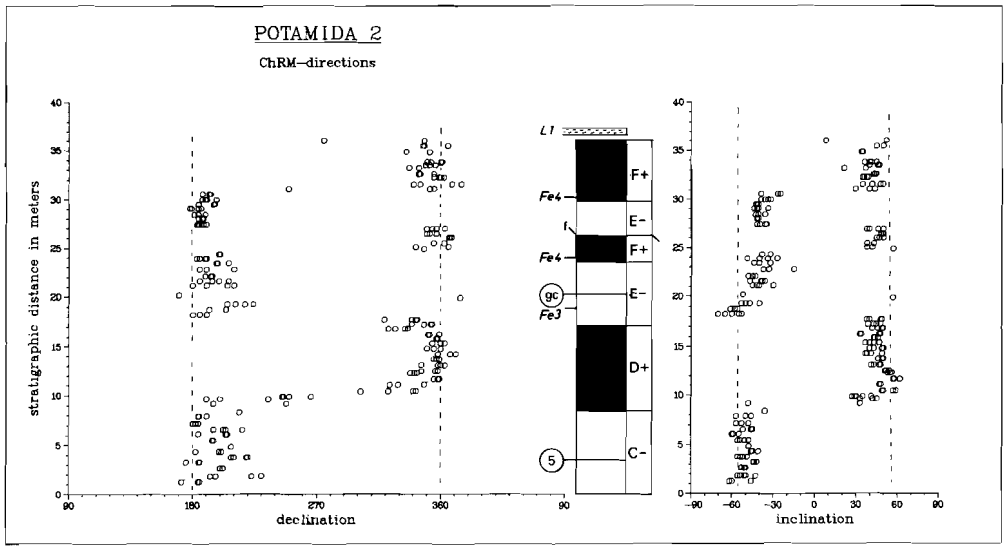

Fig. 4.2 Declination and inclination of the ChRM in section Potamida 2. Doubling of polarity zones E- and F+ is caused by a fault (f). See also fig. 4.1 caption.

C-) are further evidence for a positive magnetostratigraphic correlation. Faulting caused a doubling in the polarity pattern of section Potamida 2 (Langereis, 1979; see also figure 4.2).

Section Potamida 3 was sampled in order to try and establish the upper boundary of polarity zone F+. A relatively thick (10-15 cm) ferruginous level (Fe 3) and a layer of finely bedded clay (L 1) could be used to correlate this section unambiguously to section Potamida 2. As is shown in figure 4.3, the lower reversed polarity zone found in section Potamida 3 contains the FOD of the *G. conomiozea* group and can be correlated with polarity zone E-. Since the uppermost part of section Potamida 3 shows reversed polarities, the upper reversal boundary of polarity zone F+ can indeed be established and its length can be determined. The (part of) polarity zone following F+ (i.e. G-) represents the youngest magnetostratigraphic unit recorded in western Crete.

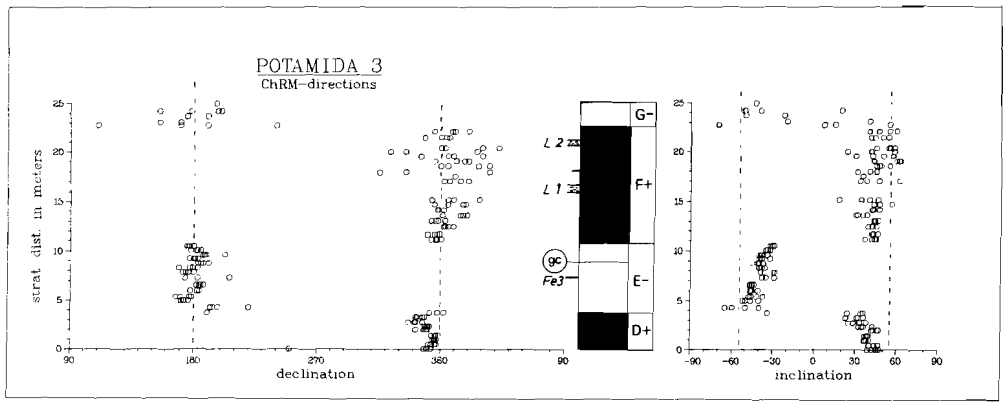

Fig. 4.3 Declination and inclination of the ChRM in section Potamida 3. See also fig. 4.1 caption.

By sampling section Potamida 4 a polarity stratigraphy older than the upper boundary of zone F+ was recorded. The reversed polarity zone in the lower half of section Potamida 4 is relatively very long and contains the FOD of *G. menardii* form 5; it is therefore polarity zone C- (fig. 4.4). Although based on a single sampling level only, normal polarity at the base of the section may

indicate that Potamida 4 contains the lower boundary of polarity zone C-. The true thickness of zone C-, however, is uncertain in this section due to possible faulting in the interval corresponding to the upper gap in the sample record (upper shaded area in fig. 4.4). The thickness of polarity zone E- is notably reduced relative to that measured in the other Potamida sections. Moreover, the FOD of the *G. conomiozea* group coincides exactly with the boundary between polarity zones E- and F+; this position is anomalous relative to its position in the other sections and strongly points to the presence of a fault. On revisiting the section we indeed found that polarity zone E- is tectonically reduced in thickness due to faulting.

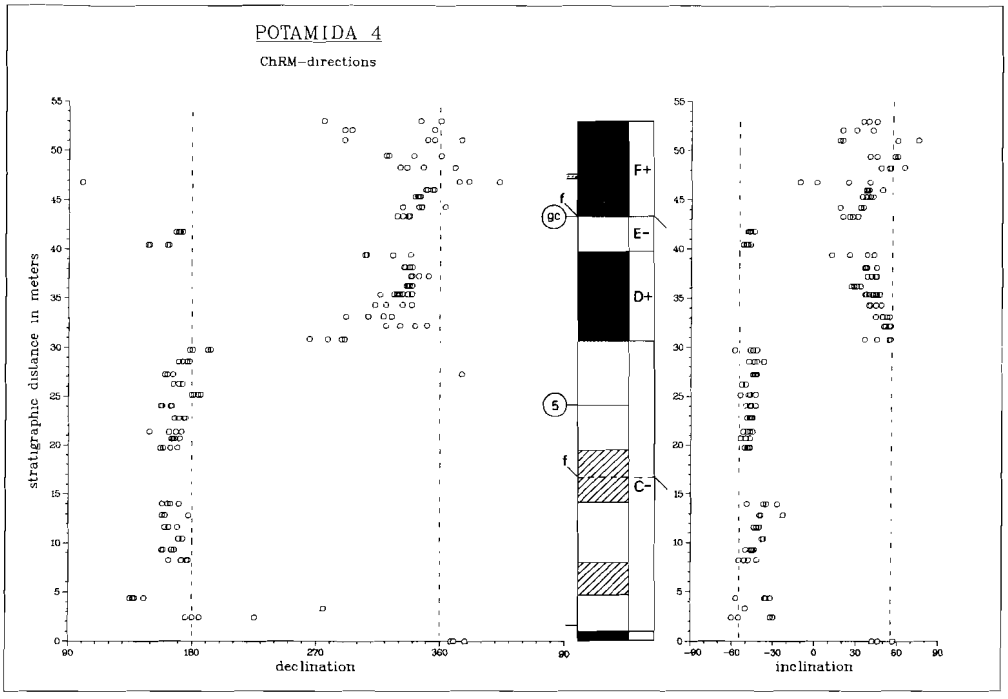

Fig. 4.4 Declination and inclination of the ChRM in section Potamida 4. Hatched intervals refer to gaps in sample record, f indicates faults. See also fig. 4.1 caption.

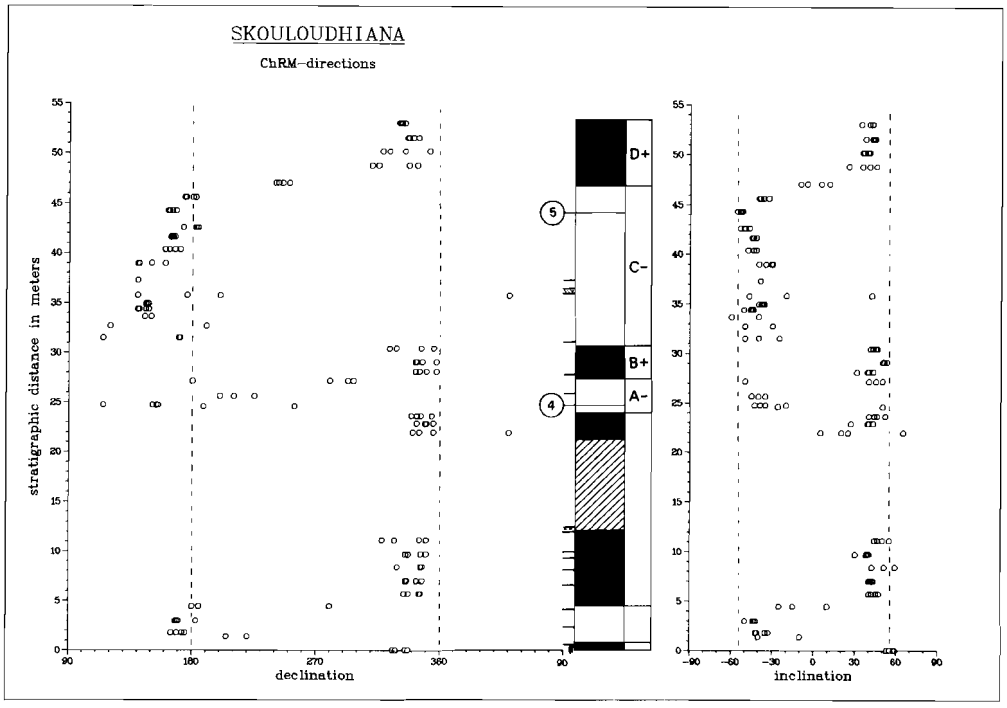

Fig. 4.5. Declination and inclination of the ChRM in section Skouloudhiana. Hatched interval represents gap in sample record; 4 = LOD of *G. menardii* form 4. See also fig. 4.1 caption.

Section Skouloudhiana contains the oldest Tortonian clays we could sample in NW Crete, which was the reason this section was chosen; the underlying formation consists mainly of sands and is not suited for paleomagnetic sampling.

The presence of the LOD of *G. menardii* form 4 indicates that section Skouloudhiana extends to much older levels than do the Potamida sections. As shown in figure 4.4, the upper reversed polarity zone is characteristically long and contains the FOD of *G. menardii* form 5; therefore it correlates to polarity zone C-. The lower reversal boundary of zone C- is documented, as well as the boundaries of two older polarity zones, B+ and A-. The latter zone (A-) contains the LOD of *G. menardii* form 4. The biostratigraphy between the LOD of *G. menardii* form 4 and the FOD of *G. menardii* form 5 is characterized by an absence of keeled globorotaliids. Downwards, at least two more polarity zones occur, but the long non-exposed inter-

val below polarity zone A- does not rule out the possibility that more polarity reversals are present than the ones recorded in the lower part of section Skouloudhiana.

Section Kotsiana 1 shows three distinct polarity zones as shown in figure 4.6. In the upper part of the reversed polarity zone and in the upper normal polarity zone no keeled globorotaliids have been found. The FOD of *G. menardii* form 4 is recorded in the lower normal polarity zone, but considering the scarce number of paleontologic samples taken in this section (at every fifth paleomagnetic sampling level), the position of the LOD of *G. menardii* form 4 in the Skouloudhiana section is certainly more reliable. It is therefore very likely that the actual LOD of *G. menardii* form 4 is somewhat younger than the observed LOD in section Kotsiana 1. Together with the noted absence of keeled globorotaliids in the upper part (half) of the section, this suggest that the reversed polarity zone corresponds to zone A- and hence the upper normal polarity zone to zone B+. The lower part of the section contains magnetizations which may have a viscous origin, the majority of which show indeterminate polarities; only the lowermost level shows clearly reversed magnetizations. Nevertheless, no distinct polarity is assigned to this lower part.

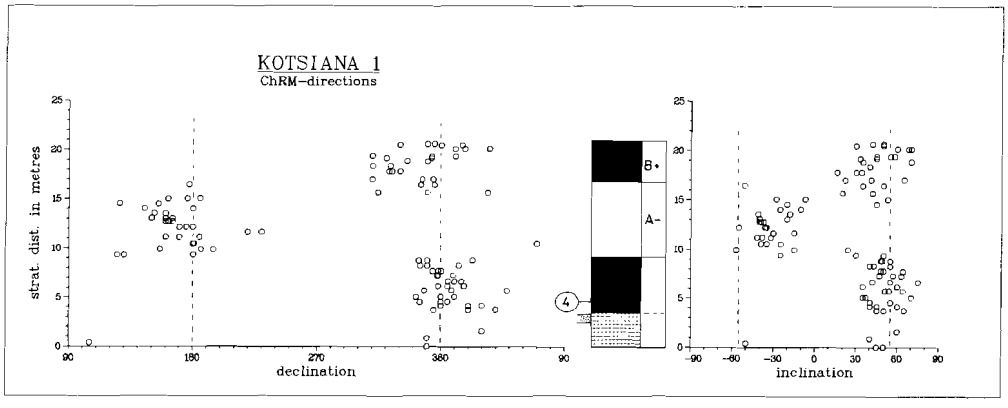

Fig. 4.6 Declination and inclination of the ChRM in section Kotsiana 1. Cross-hatched interval denotes indeterminate polarities. See also fig. 4.1 caption.

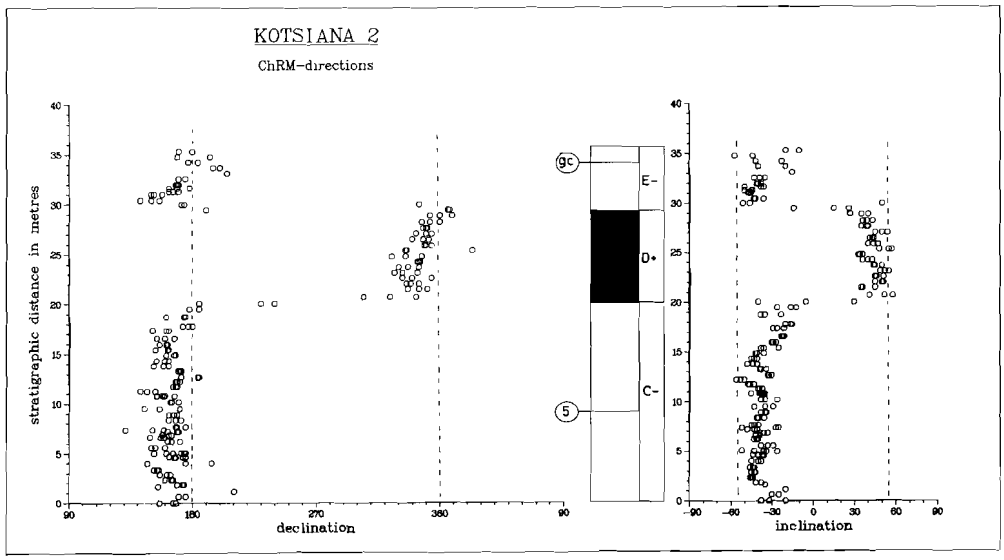

Fig. 4.7 Declination and inclination of the ChRM in section Kotsiana 2. See also fig. 4.1 caption.

Section Kotsiana 2 is younger than section Kotsiana 1 (see also figure 2.5) and the magnetostratigraphic results confirm that there is no overlap between the two sections. The section contains the characteristically long reversed polarity zone which contains the FOD of *G. menardii* form 5 and hence correlates to polarity zone C- (fig. 4.7). The lower reversal boundary of C- is not recorded; this zone is followed upwards by polarity zones D+ and E-, the latter containing the FOD of the *G. conomiozea* group.

The results of the Episcopi section show that the familiar long polarity zone C- is present in this section as well. The upper part of section Episcopi was resampled, since a small fault disturbed the original sampling track. In this part both normal and reversed polarities are derived from thermal demagnetization and no distinct polarity can be assigned (fig. 4.8).

In a parallel sampling track in the same outcrop, Episcopi Resampling, no faulting occurs and the results show unambiguous polarities (fig. 4.9a).

In the same badlands close to the Episcopi section, section Episcopi Extension was sampled in order to try and establish the upper reversal boundary of polarity zone D+. Indeed, the upper part clearly

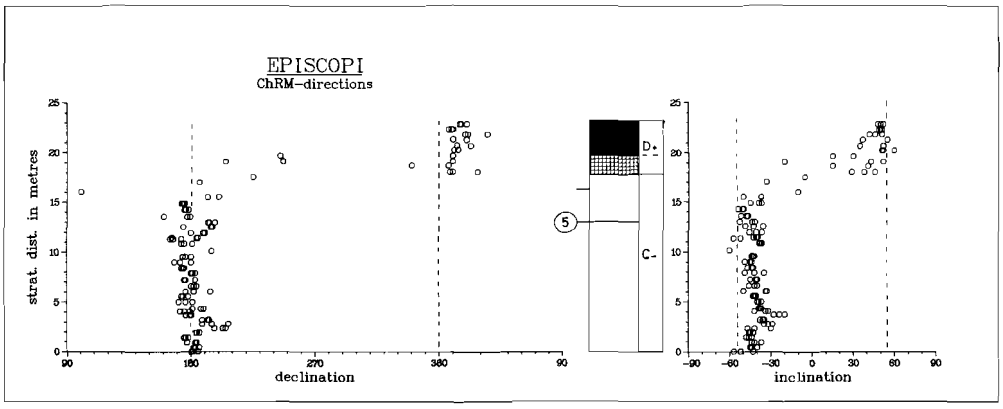

Fig. 4.8 Declination and inclination of the ChRM in section Episcopi. Cross-hatched interval denotes indeterminate polarities. See also fig. 4.1 caption.

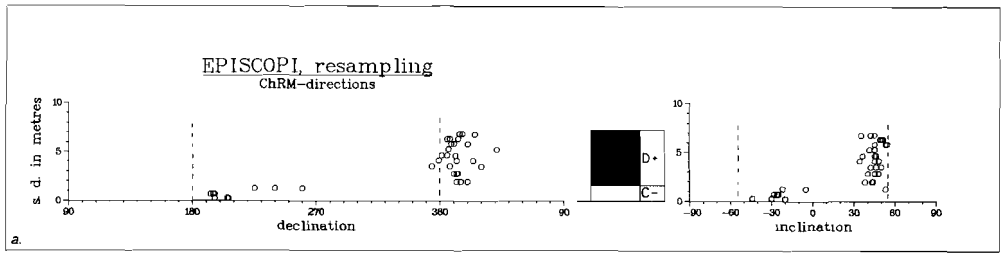

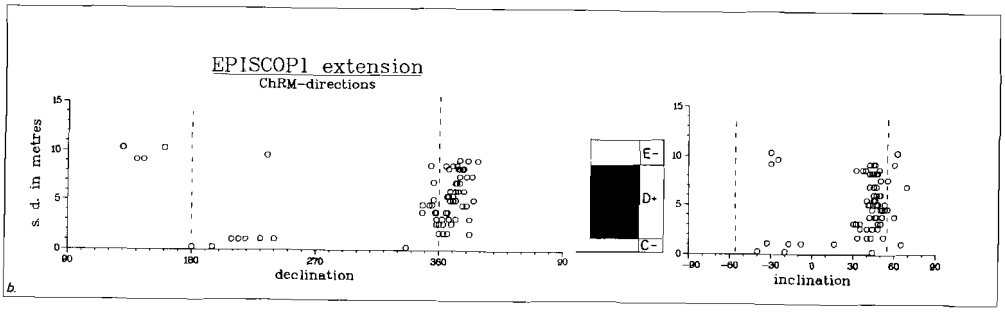

Fig. 4.9 Declination and inclination of the ChRM in section Episcopi Resampling (a) and Extension (b).

shows reversed polarities (fig. 4.9b) and zone D+ is completely defined. The top of the section consists of the remnants of a sandy, ferruginous level with a thickness of at least 20 cm.

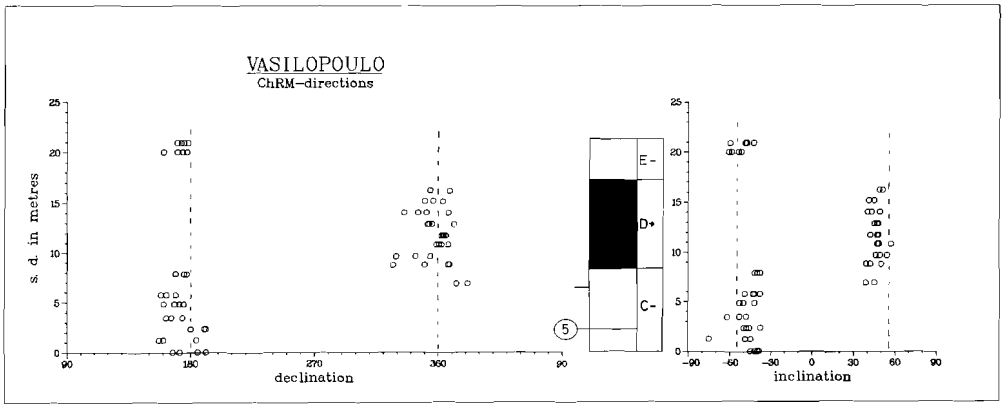

Fig. 4.10 Declination and inclination of the ChRM in section Vasilopoulo. See also fig. 4.1 caption.

The same polarity zones encountered in the Episcopi sections can be found in the nearby section Vasilopoulo (fig. 4.10). Apparently the accumulation rate in section Vasilopoulo is somewhat higher, since polarity zone D+ is longer than the corresponding zone in section Episcopi Extension. The sandy layer, which forms the top of section Vasilopoulo, has a thickness of ca. 2 metres and from the established magnetostratigraphy it can be concluded that this layer corresponds to the sandy layer at the top of Episcopi Extension. The position of this layer in polarity zone E- strongly suggests that it is identical to the ferruginous layer Fe 3 in the Potamida 1, 2 and 3 sections. Furthermore, the position of the ferruginous level just below the polarity transition from polarity zone C- to D+ similarly indicates that this level correlates to Fe 2 in the Potamida 1 section.

The Makronas section is the youngest section sampled in western Crete and contains the transition from the clays of the former sections to the overlying homogenous-laminated marls. The contact between the successive formations is partly covered and no samples could be taken. The clays in the lower half of the section are silty and contain numerous sandy layers. Although the section consists of some 40 metres of sediments, including a gap of 13 metres, it most probably represents only a limited amount of time, since the lithology suggests a rapid sedimentation. In general, intensities of the

ChRM are extremely low and ChRM directions cannot be determined reliably. From the demagnetization diagrams (see chapter 3) reversed polarities are suggested. A tentative interpretation is shown in figure 4.11: the section is assumed to contain (part of) polarity zone G-.

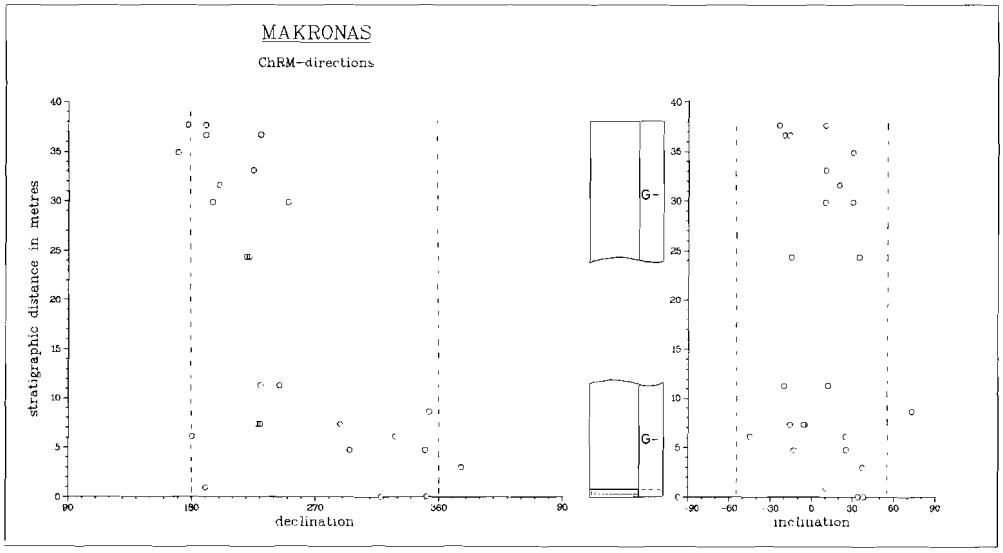

Fig. 4.11 Declination and inclination of the ChRM in section Makronas. See also fig. 4.1 caption.

Some nine polarity reversals were recorded in section Kastelli in central Crete (fig. 4.12). Both biostratigraphically and magnetostratigraphically, section Kastelli can be correlated with the western Cretan sections and allows the polarity zones in section Kastelli to be labeled in terms of the western Cretan polarity succession. As shown in figure 4.12 polarity zones A- through G- are recognizable in this section: the familiar long polarity zone C- is again present, following two short polarity zones, A- and B+, similar to the situation in western Crete (section Skouloudhiana). Furthermore, the various biostratigraphic datum levels occur in the corresponding (reversed) polarity zones. The polarity zones below zone A- cannot be correlated with those in western Crete, or more specifically, with those in section Skouloudhiana, due to the non-exposed interval in the latter section.

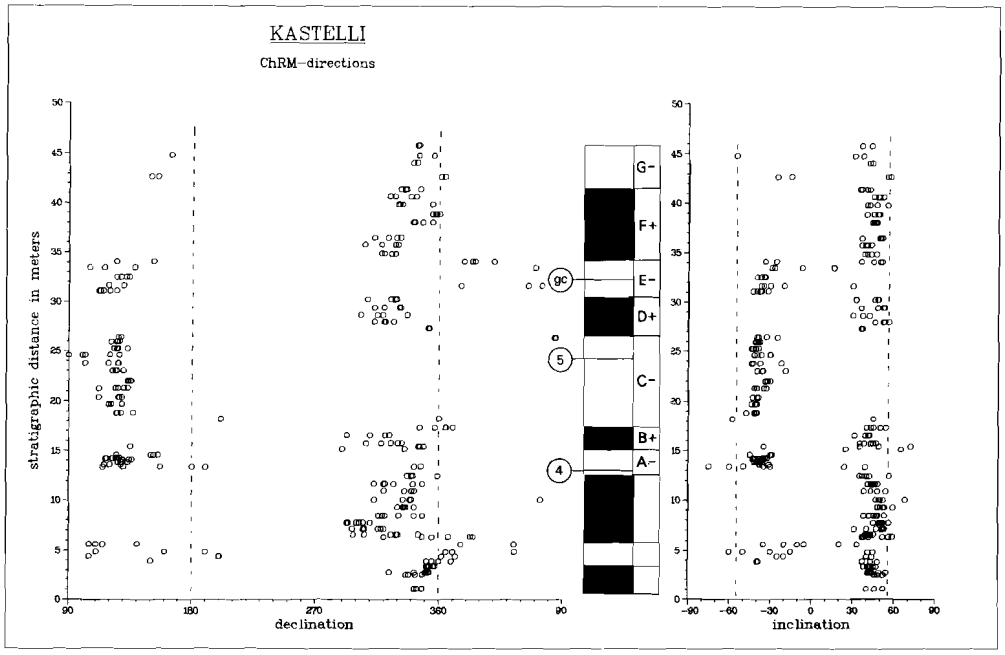

Fig. 4.12 Declination and inclination of the ChRM in section Kastelli. See also fig. 4.1 and fig. 4.5 caption.

In addition, due to limited stratigraphic control it is not certain whether the polarity sequence below polarity zone A- is correct or not. From polarity zone A- upwards (litho)stratigraphic control was possible thanks to (uninterrupted) thin ferruginous levels, whereas the lower part of the section is covered by a crust of (weathered) clay. Moreover, the lowermost part of the section contains gypsum needles along numerous joints. Some faulting can therefore not be ruled out (cf. chapter two). The sediments overlying the Kastelli section are not suitable for paleomagnetic analysis due to their predominantly silty and sandy lithology, and no samples could be drilled.

The samples of the topmost part of the section show a large secondary component and only thermal demagnetization reveals the reversed polarity ChRM (cf. chapter 3). The lithology of the overlying sediments furthermore suggests a higher sedimentation rate, similar to the top of the Potamida 3 section and especially to the lower part of the Makronas section.

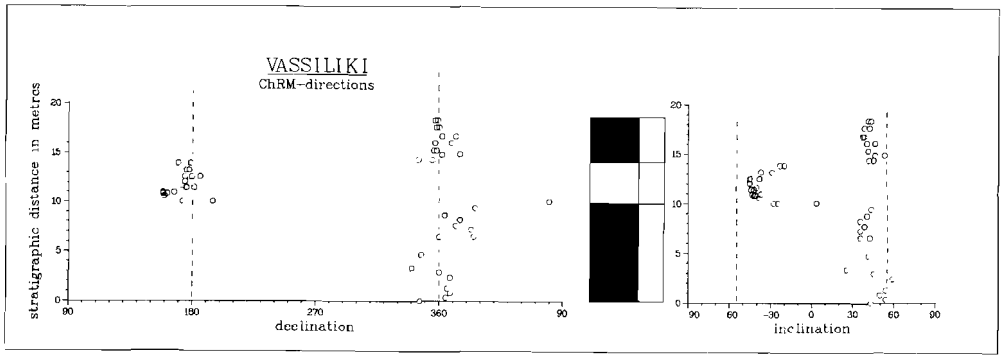

Fig. 4.13 Declination and inclination of the ChRM in section Vassiliki. See also fig. 4.1 caption.

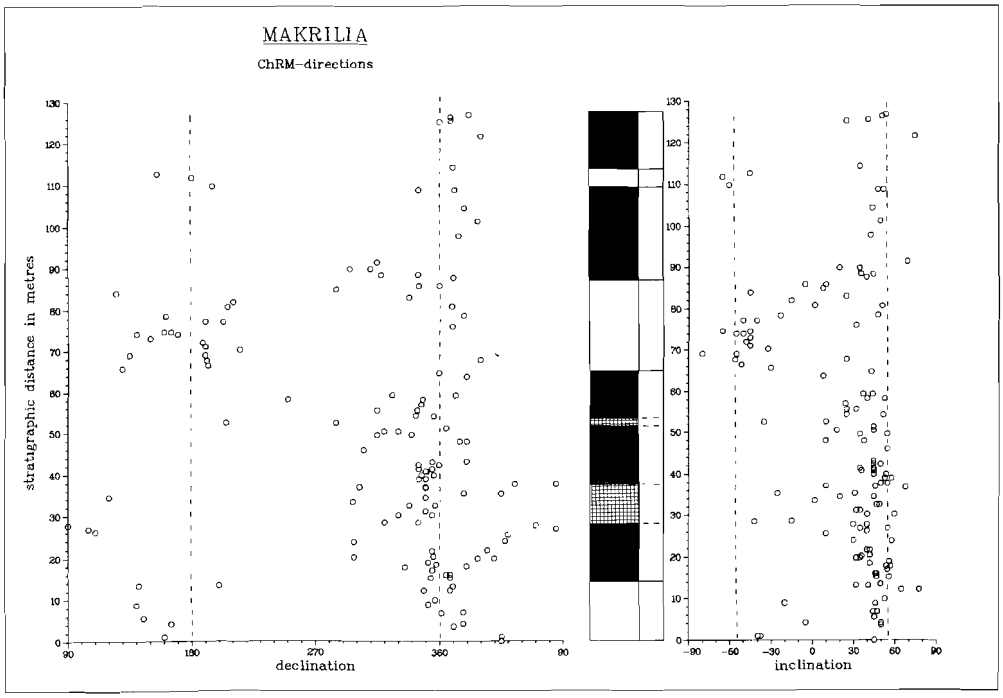

Fig. 4.14 Declination and inclination of the ChRM in section Makrilia. Cross-hatched interval denotes indeterminate polarities. See also fig. 4.1 caption.

In the Ierapetra district of eastern Crete two sections have been sampled which are older than all other Cretan sections (cf. fig. 2.5). In section Vassiliki three polarity zones can be recognized (fig. 4.13). Although the lower part of the section contains several distinctly sandy layers, the homogenous clays suggest a rather constant sedimentation rate.

In section Makrilia, which is younger than section Vassiliki and older than the other Cretan sections, results are rather equivocal often due to viscous or secondary remanences. A tentative interpretation of the polarity zonation is given in figure 4.14. Several reversed polarity zones are present, but the section shows predominantly normal polarities. Since no sections of similar age have been sampled, the polarity zonation cannot be validated. Furthermore, the section contains numerous sandy turbidites as well as layers where slumping has taken place. This suggests rapid sedimentation and possibly rapid changes in the accumulation rate, which may yield a false polarity pattern.

In the Sitia district of eastern Crete the biostratigraphically long-ranging Faneromeni section has been sampled. As shown in figure 4.15 results are rather ambiguous. In the central part the characteristically long, reversed polarity zone can be recognized, which correlates most probably with polarity zone C-, although the FOD of *G. menardii* form 5 seems to occur in the normal polarity zone D+. It should be noted that polarity zone B+ is based upon a single sampling level with sufficiently reliable ChRM directions, and its length is therefore not accurate. The length of polarity zone D+ on the other hand, is more accurately defined (fig. 4.15).
No reliable polarities could be derived in the lowermost part of the section around the FOD of the *G. conomiozea* group and in the upper part of the section. It is not certain whether or not the LOD of *G. menardii* form 4 occurs in a reversed polarity zone, although a sampling level just below this datum shows an intermediate ChRM direction. Below this level some normal polarity levels are present. Below and above the FOD of the *G. conomiozea* group reversed polarity characteristic remanent magnetizations are present (see previous chapter), and reversed polarities could be derived in the top of the section as well. In general, several of the characteristic features

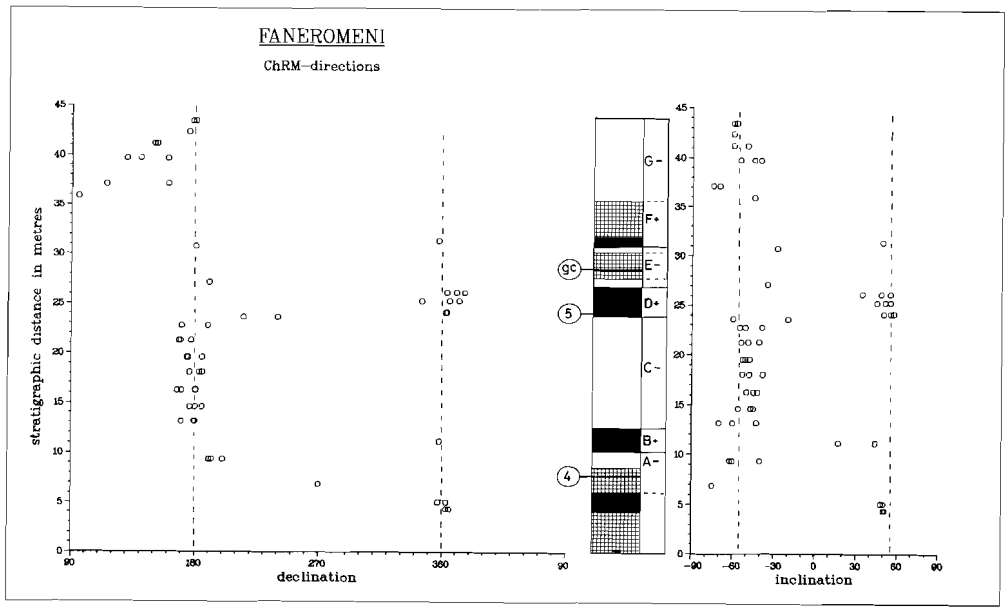

Fig. 4.15 Declination and inclination of the ChRM in section Faneromeni. Cross-hatched interval denotes indeterminate polarities. See also fig. 4.1 and fig. 4.5 caption.

seen in western and central Crete can be observed: the short intervals of reversed (A-) and normal polarities (B+) followed by a characteristically long interval (C-) closely resemble the corresponding sequence in western Crete and Kastelli. If it is furthermore assumed that the indeterminate polarities around the *G. conomiozea* datum were originally of reversed polarity and the indeterminate interval in the top of the section of normal polarity, then the picture is complete, especially in combination with the positions of the LOD of *G. menardii* form 4 and the FOD of the *G. conomiozea* group. The anomalous position of the FOD of *G. menardii* form 5 is obviously due to the fact that the relevant fauna in lower sampling levels was not observed. Originally the FOD of *G. menardii* form 5 was observed even higher. On the basis of the magnetostratigraphic results, the paleontologic samples were re-examined, resulting in the present position of this first occurrence datum. On this basis the polarity zonation, consisting of polarity zones A- through G-, is proposed in figure 4.15.

The results of section Falconara in southern Sicily are unambiguous: considering the appreciable time-span as evidenced by the biostratigraphic results in combination with the western Cretan results, it is clear that the normal polarities are due to remagnetization of the original remanence (chapter 3). The remanence directions without correction for the bedding tilt are scattered around the geocentric axial dipole field for the present latitude of the section (fig. 4.16), whereas bedding tilt correction results in a significant deviation from this field direction. This indicates that the remanence observed was acquired (sub)recently, after the tilting of the section. Since demagnetization of a number of specimens throughout the Giammoia section yielded the same results as in the Falconara section, we refrained from demagnetizing specimens from each sampling level in this section.

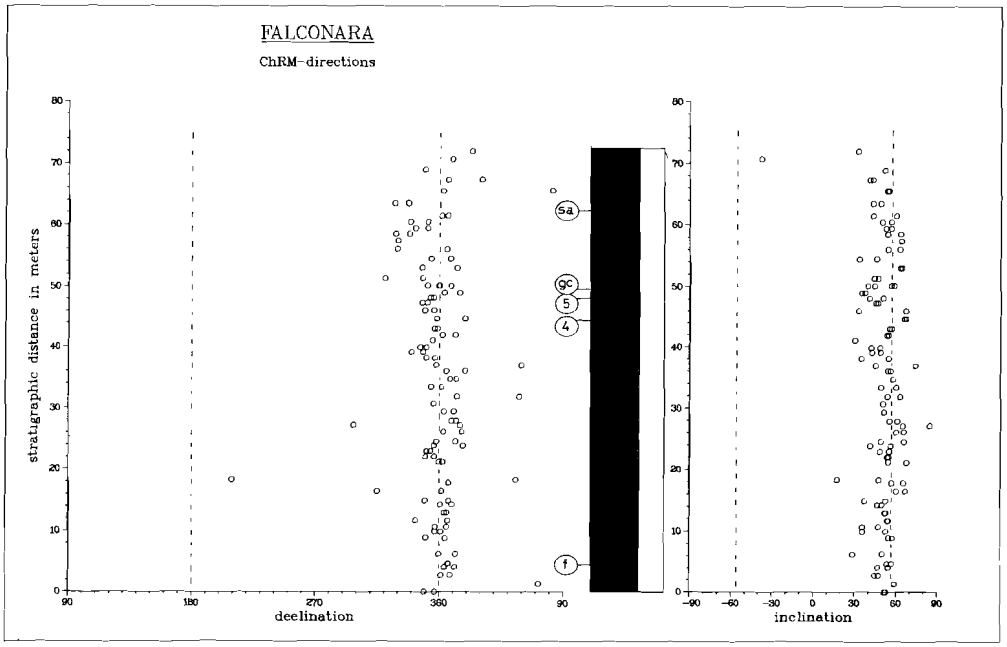

Fig. 4.16 Declination and inclination of the ChRM in section Falconara <u>without</u> bedding tilt correction. The remanence directions are scattered around the present geocentric axial dipole field direction for the present latitude of the section; sa = shift in coiling of *N. acostaensis*, f = LOD of *G. falconarae*.

For section Scicli South too, results are rather disappointing. The demagnetization results from the lower part of the section indicate that reversed polarities are present, while the top of the section shows indeterminate polarities (fig. 4.17). Part of this "indeterminate polarity zone" is probably reversed, as shown by the results of the parallel Scicli South 2 section: the top of each section consists of the same sandy layer, but in Scicli South 1 reversed polarities are only present up to 5 metres below the sandy layer (Fe), whereas in Scicli South 2 reversed polarities are clearly present up to 2 metres below this same level. Since these sections are younger than the FOD of the *G. conomiozea* group, but close to the shift in coiling of *N. acostaensis*, the reversed polarity zone represents polarity zone G- from the Cretan sections.

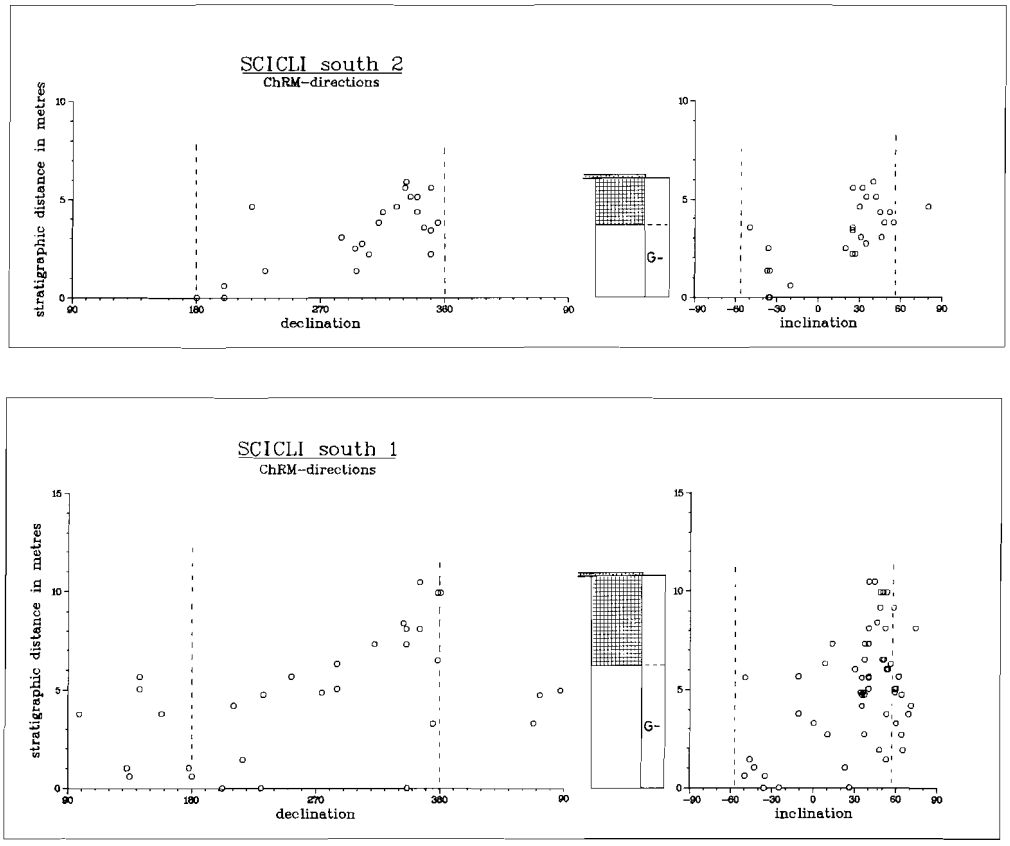

Fig. 4.17 Declination and inclination of the ChRM in section Scicli South 1 and 2. See also fig. 4.1 caption.

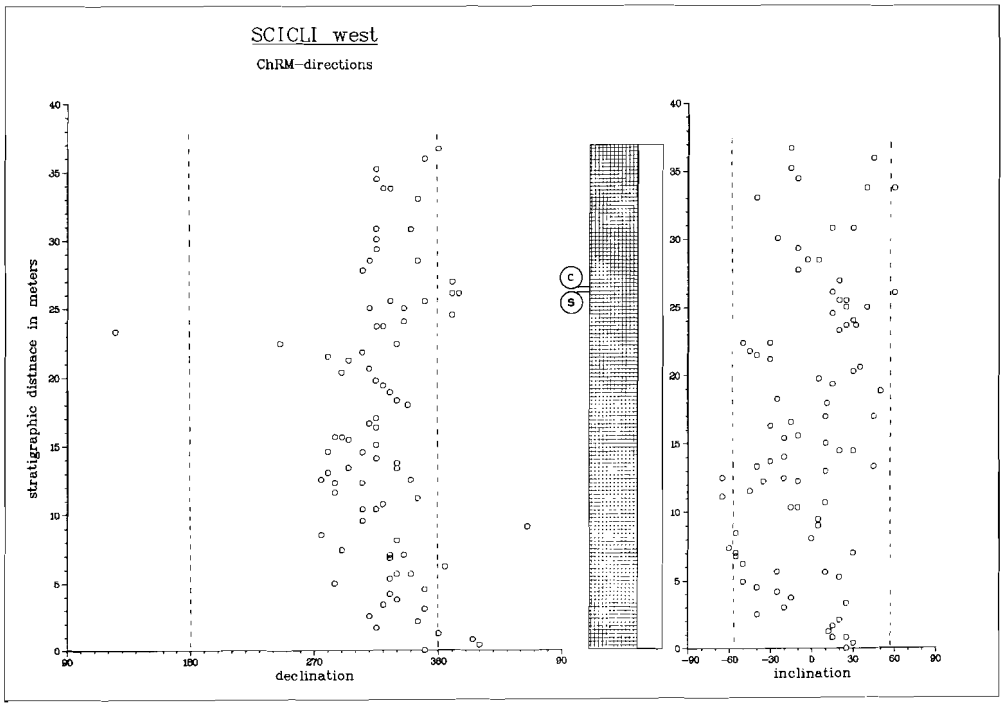

Fig. 4.18 Declination and inclination of the ChRM in section Scicli West; c = FOD of *G. continuosa*. See also fig. 4.1 caption.

In section Scicli West no polarity zonation could be determined (fig. 4.18). Furthermore, this section is by far the oldest section we sampled and there is no (biostratigraphic) overlap with any of the other sections. ChRM directions show predominantly northwesterly directions and both negative and positive inclinations, as if these had been randomly generated.

The Mussotto section in the Piedmont basin in northern Italy shows three polarity zones (fig. 4.19), none of which can be reliably correlated with any of the Cretan sections. The section is older than the LOD of *G. menardii* form 4, but how much older in terms of polarity zones is not sure.

The Castellania section in the Rio Mazzapiedi area shows clearly reversed polarities in the middle and upper part of the section. In the middle part a zone with indeterminate polarities is found, which

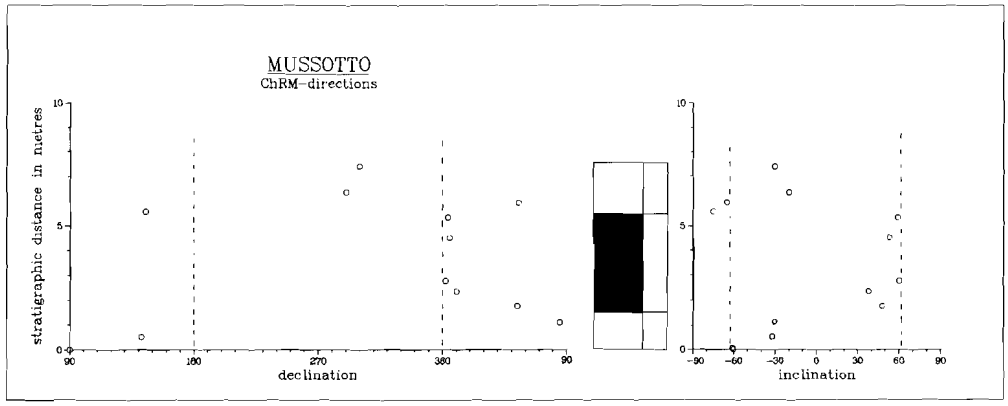

Fig. 4.19 Declination and inclination of the ChRM in section Mussotto. See also fig. 4.1 caption.

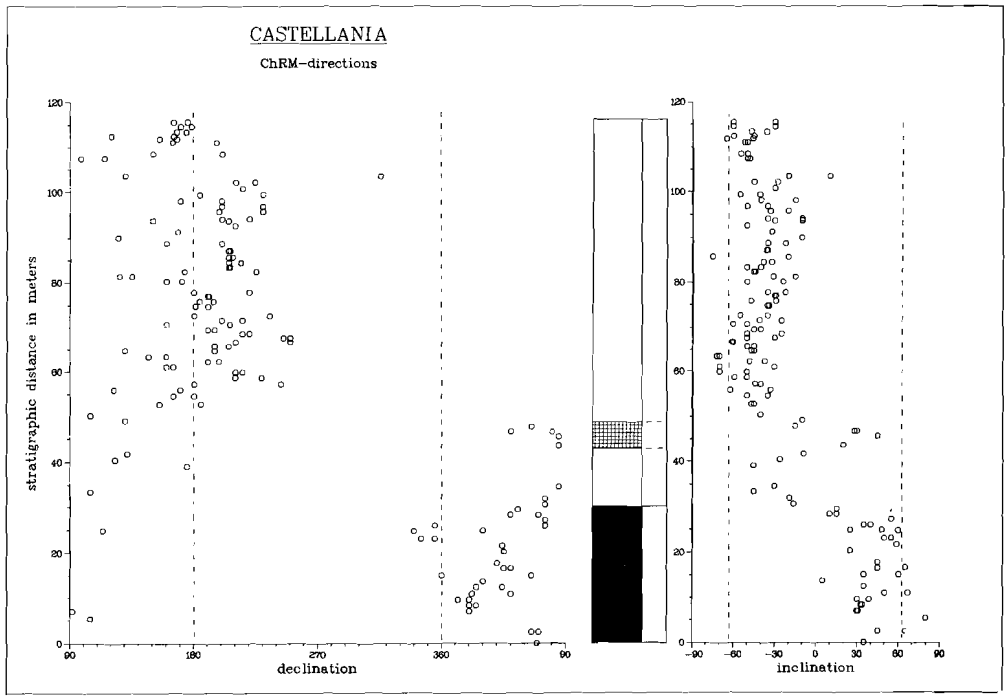

Fig. 4.20 Declination and inclination of the ChRM in section Castellania. See also fig. 4.1 caption.

may be due to a secondary overprint (fig. 4.20). Unfortunately, the section contains no firm biostratigraphic datum levels due to the meagre faunal content. Furthermore, the existing fauna may have been reworked and indicates a very rapid accumulation rate (Zachariasse, personal communication). Therefore, no correlation can be established with the Cretan sections either.

The pilot samples throughout the Luzzena section show only reversed polarities. Because of the large sampling interval it cannot be concluded that normal polarities are not present, but probable reworking of the fauna (Borsetti et al., 1975) and a very high sedimentation rate suggest that the whole section represents a single, reversed polarity zone. Since the sediments in this section are deposited during the post-evaporitic phase, which is called "Lago Mare" in italian literature and is close to the Miocene-Pliocene boundary, the reversed polarities may represent the lower reversed polarity (sub)zone of the Gilbert chronozone.

MAGNETOBIOSTRATIGRAPHY FOR THE UPPER MIOCENE OF CRETE

Figure 4.21 shows the position of the western Cretan sections arranged relative to the base of polarity zone E-. When corrected for a small fault in the upper part of section Potamida 2 (Langereis, 1979; Drooger et al., 1979b) the polarity reversal sequence of this section correlates excellently with the sequences in sections Potamida 1 and 3. Section Potamida 3 is the only section in western Crete where a part of polarity zone G- is revealed, apart from section Makronas which is probably totally reversed. The upper part of section Potamida 4 is corrected for the observed fault and a possible correction for faulting in the lower part is shown.

Fig. 4.21 Position of all western Cretan sections relative to selected polarity reversal horizons. Sections Potamida 2 and 4 have been corrected for faulting. The composite polarity stratigraphy for western Crete is given in the column furthest to the right. For the composite column the lengths of the polarity zones of section Skouloudhiana have been normalized to the average sedimentation rate of the other sections. See next page.

W.Crete
G-
F+
E-
D+
C-
B-
A-
Skoulouthiana
Makronas
covered 13 m
Vasilopoulo
Episcopi extension
Episcopi resampling
Episcopi
Kotsiana 1
Kotsiana 2
Polamida 4
Polamida 3
Polamida 2
Polamida 1
20
15
10
5
0
m

In sections Potamida 1,2 and 3 the FOD of the *G. conomiozea* group is recorded approximately in the middle of polarity zone E-. The anomalous position of the FOD of the *G. conomiozea* group at the boundary of polarity zones E- and F+ in section Potamida 4 is related to a fault. This clearly illustrates that if a biohorizon coincides with a "polarity reversal horizon", then a hiatus or fault has probably occurred.

The FOD of *G. menardii* form 5 occurs in polarity zone C- in all western Cretan sections. Since section Potamida 1 has been sampled and studied in most detail, both magnetostratigraphically as well as biostratigraphically, its relative position is probably most reliably determined in this section. Moreover, in section Potamida 1 it is absolutely certain that no faulting has occurred, since the stratigraphic continuity can be checked by means of the undisturbed layering of more and less indurated clays and of the ferruginous levels. Only in section Kotsiana 2 does the entry of *G. menardii* form 5 seem to be found somewhat earlier; this may be due to some small scale faulting and/or to a slightly higher accumulation rate.

A sudden and instantaneous re-appearance of sinistrally keeled globorotaliids above the FOD of *G. menardii* form 5 is recorded only in polarity zone D+ of sections Potamida 1 and 3. Since the stratigraphic interval in which this occurs is small (cf. Zachariasse, 1979) and since the (paleontologic) sampling distance is generally three to four times the sampling distance used in sections Potamida 1 and 3, the re-appearance has probably been missed in the sampling records of the other sections.

The LOD of *G. menardii* form 4 is recorded in section Skouloudhiana, where it falls within polarity zone A-, and in section Kotsiana 1, where it has only been recorded in the normal polarity zone below A-, probably because the restricted paleontologic sampling in this section.

On the basis of the reversal sequences of the overlapping western Cretan sections a composite polarity stratigraphy is constructed in such a way that the lengths are normalized to a uniform accumulation rate. If this is done correctly, the relative lengths of

the successive polarity zones provide us with a polarity pattern which displays the relative time durations of the individual zones and which can be used for correlation with the magnetic polarity time scale based on sea-floor anomalies. In fact, it is hardly necessary, as we shall see, to normalize the lengths of the polarity zones encountered in the western Cretan sequences.

From figure 4.21 it can be seen that sections Potamida 1, 2 and 3 have polarity zone E- in common, the thickness of which appears t be identical in all sections. The same holds for zone D+ in sections Potamida 1, 2 and 4, Kotsiana 2, Episcopi and Vasilopoulo, suggesting an almost equal sedimentation rate in these sections.

The length of polarity zone F+ can only by established in section Potamida 3. Because the lithology of the upper part of this section, which is more silty/sandy than the underlying clays, indicates a higher accumulation rate, the length of zone F+ is probably somewhat exaggerated relative to the length of the older polarity zones. Since it is not known by which factor the length of this zone must be adjusted, the lengths of the upper three polarity zones D+, E- and F+ of the composite column correspond to their actual measured lengths in the western Cretan sections.

Section Skouloudhiana is the only section in which the length of zone C- can be determined. The length, however, is notably shorter than the minimum length of this zone in sections Potamida 1 and Kotsiana 2. This probably indicates that the average accumulation rate in section Skouloudhiana has been lower than in the other sections.
Therefore, polarity zone C- of section Skouloudhiana has to be 'stretched' by at least a factor of 1.2 so that it becomes adjusted to the accumulation rate of the other sections.
On the other hand, this adjustment factor has a maximum value of 1.3, since otherwise polarity zone D+ in section Skouloudhiana would become longer than its length in the other sections. The average correction factor used here to normalize the lengths of the polarity zones in section Skouloudhiana is thus fixed at 1.25. The same accumulation rate correction has of course been applied to the other polarity zones of this section.

As shown in figure 4.22, the relative lengths of the six polarity zones A- to F+ of section Kastelli correlate excellently with the corresponding six polarity zones of the composite section of western Crete. The same holds for the position of the various biohorizons relative to the polarity sequence of the two regions. The lithology of the zone F+ in section Kastelli indicates a somewhat higher

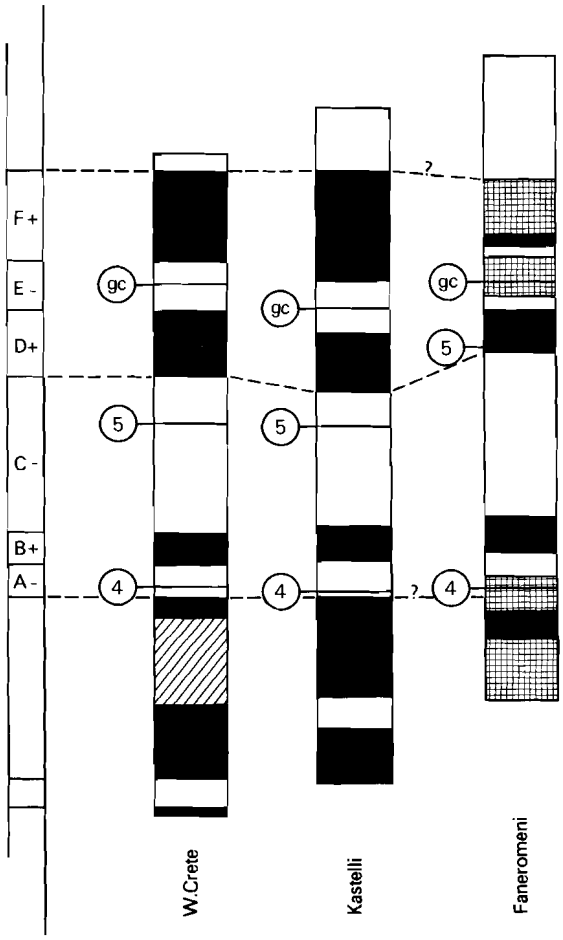

Fig. 4.22 Correlation of the composite column of western Crete, section Kastelli and section Faneromeni. The lengths of the polarity zones of the latter two sections have been normalized to the average accumulation rate of the western Cretan sequence, both by a factor of 1.95; gc = FOD of the G. *conomiozea* group, 5 = FOD of G. *menardii* form 5, 4 = LOD of G. *menardii* form 4.

accumulation rate, similar to section Potamida 3, and hence the relative length of polarity zone F+ is somewhat exaggerated in both polarity sequences. Apparently the accumulation rates in western and central Crete have varied slightly in much the same way. Meulenkamp et al. (1979) noted already that the sedimentary history and structural development of Crete during the Tortonian and Early Messinian were fundamentally the same all over the island. The present magnetostratigraphic results show that this is also true in appreciable detail. Correlation between the polarity patterns below the succession of six polarity zones is doubtful due to the non-exposed interval in western Crete on the one hand, and due to the uncertain stratigraphic continuity below polarity zone A- in section Kastelli on the other hand.

The upper six polarity zones of the composite column in western Crete have a total thickness of 56.5 metres, whereas those in section Kastelli have a thickness of 29 metres, indicating that the average sedimentation rate in the latter section has been a factor of 1.95 less. In fig. 4.22 the polarity zones of the section Kastelli are adjusted by the same factor of 1.95 in order to facilitate comparison with the composite column of western Crete.

The polarity zonation of section Faneromeni correlates well with the western and central Cretan results with respect to several characteristics (fig. 4.22). The long reversed polarity zone C- can easily be recognized as well as the shorter polarity zones B+ below it and D+ above it. The LOD of *G. menardii* form 4 may occur in a reversed polarity zone as is the case in the other polarity reversal sequences, but the lower boundary of polarity zone A- is not certain due to the indeterminate polarities in the lower part of the section.

The FOD of the *G. conomiozea* group probably occurs in a reversed polarity zone, since both below and beneath this datum reversed ChRM's could be determined. Polarity zone F+ seems to be relatively short with respect to western Crete and Kastelli, even if indeterminate polarities in the upper part are normal. The top of the Faneromeni section is reversed and correlates with polarity zone G-; the lower reversal boundary of this zone cannot be determined either, due to indeterminate polarities in that part of the section.

The polarity reversal sequence of the Faneromeni section in figure 4.22 is shown on the same scale as that of the Kastelli section. Although the total length of the upper six polarity intervals in section Faneromeni is not known, exactly the proposed correlation of figure 4.22 suggests that the sedimentation rate has been approximately the same as in the Kastelli section.

In general, the relative lengths (the pattern) of the successive polarity zones in central Crete and the relative lengths of zone B+, C- and D+ in eastern Crete compare well with those in western Crete suggesting that the sedimentation rates in those regions did not vary greatly or in the same way as all over the area of Crete. An odd coincidence is that the three biohorizons occur in the successive reversed polarity zones, with the exception of the FOD of five in section Faneromeni.

Minor variations in the position of biohorizons relative to the polarity patterns are believed to have been caused by factors such as differences in the distance between samples, by minor fluctuations in the sedimentation rate and/or by minor faults. The influence of these factors separately is difficult to ascertain. A more general approach shows that the combined influence of these factors results in a correlation coefficient between the polarity patterns of western and central Crete of 0.999, which infers a 99% significant correlation.

Since the sampling (table 2.1) in the Cretan sections was detailed, it is not very likely that one or more polarity zones have been missed. This can be illustrated by some simple calculations. The average duration of a polarity zone during the Tertiary is approximately .225 Ma; this duration is of the order of .200-.210 Ma for the last 10 Ma. The average sampling interval for most western sections is of the order of 40-60 cm and for the Kastelli section 70-80 cm. Taking an average duration of 0.2 Ma for a polarity zone during the last 10 Ma, the upper six polarity zones of both the upper six polarity zones of both western and central Crete represent a time interval of the order of 1.2 Ma. This amounts to an average sedimentation rate of 4.7 cm/1000 years for the western Cretan sections and of 2.4 cm/1000 years for central Crete (and eastern

Crete). An average sampling interval of 50 cm in western Crete then represents a time interval of ca. 10,000–11,000 years, and a sampling interval of 70–80 cm in central Crete an interval of ca. 30,000 years. Since the minimum recorded duration of Late Miocene polarity (sub)zones is approximately 0.05 Ma, this high resolution virtually rules out the possibility that polarity (sub)zones have been missed. Since a polarity reversal takes place in ca. 8,000–10,000 years, the theoretically shortest possible duration of a polarity (sub)zone is approximately 20,000 years. The maximum resolution in sea-floor anomaly studies is ca. 30,000–40,000 years, and hence the shortest possible polarity zones could be missed in anomaly profiles. "Tiny wiggles" on anomaly profiles (see also LaBrecque et al., 1977) may be due to such short duration reversals (or to excursions of the geomagnetic field) or to geomagnetic intensity fluctuations, either real or artificial (e.g. due to screening of the magnetization: cf. Hartstra, 1982c). However, the sampling (time) interval of 10,000–11,000 years in western Crete should even be able to record such short polarity zones. It certainly gives a fair chance of recording transitional directions and indeed, in many sections such directions have been recorded (see figs. 4.1–4.15).

CORRELATION WITH THE MAGNETIC POLARITY TIME SCALE

Now that a composite polarity stratigraphy for western Crete and a well correlated polarity stratigraphy for central Crete have been established, the next important step is to correlate these sequences to a recent magnetic polarity time scale (Lowrie and Alvarez, 1981). So that this can be done, it is necessary for the accumulation rates to have been essentially uniform and (more or less) constant in both reversal sequences.

The uniformity of the accumulation rate is conclusively demonstrated by the correlation of the western Cretan sections, showing a near-equality of the relative lengths of the polarity zones, and by the positive and significant correlation between the composite western Cretan sequence and section Kastelli, showing the same polarity pattern. The constancy of the accumulation rate is based on the homogeneity of the massive clays in general and on the stable floral/faunal patterns (Drooger et al., 1979a). Moreover, the uniform

grain-size distribution inferred from the rock-magnetic properties (chapter 5) yields additional evidence for a fairly constant accumulation rate. Only in the top parts of the sequences studied, i.e. in zone F+, is a slightly higher accumulation rate suggested on the basis of the lithology, as well as on the basis of the magnetic properties. All evidence together allows us to assume that the observed polarity patterns in the western Cretan and Kastelli sections closely reflect the polarity pattern of the geomagnetic field.

For a correct correlation an undisturbed magnetic signal is essential, i.e. a doubling or a lack of polarity zones may lead to erroneous conclusions. Therefore, the possibility of faults is considered carefully and whenever the existence of faults are substantiated, they are indicated and corrected for (fig. 4.21).
Furthermore, it was realized that using the ages of the biostratigraphic datum levels, as far as these are reliably known in literature, may lead to circular reasoning, i.e. the correlations tend to be made to fit previously established results instead of using an independent approach.

The method employed here to correlate the observed polarity patterns of western and central Crete with the polarity time scale is based on a statistical comparison with every possible sequence of six successive polarity zones during a certain time-interval. This is done by calculating the correlation coefficients of the time-duration patterns of the polarity time scale and of the length patterns of the Cretan sequences.

We determined the correlation coefficients for all possible correlations between 0 and 15 Ma, which allows for ample time both before and after the Late Miocene. Since the western Cretan sequence and section Kastelli represent one and the same signal we are most interested in the correlations which show the highest correlation coefficient for both sequences together. Figure 4.23 shows that in that case only three correlations appear at the 97.5% level; consequently the age of the FOD of the *G. conomiozea* group in the middle of polarity zone E- has corresponding values of 3.1, 5.6 and 11.7 Ma. The fact that over a period of 15 Ma only three probable correlations are found, implies that a most probable correlation can be established, provided that two other possible correlations can be

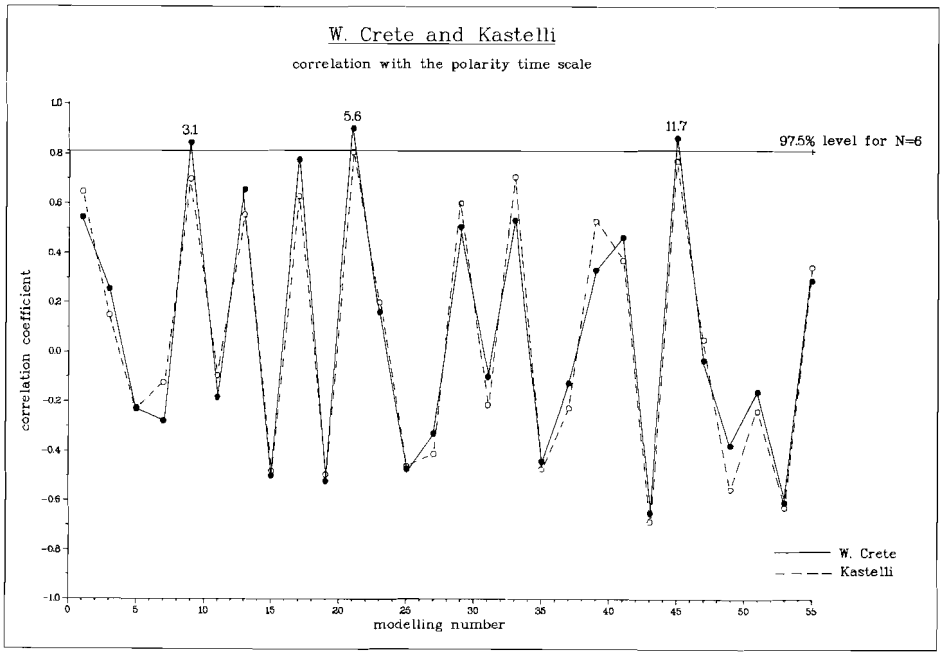

Fig. 4.23 Correlation coefficients of the pattern of lengths of polarity zones A- through F+ of the western Cretan composite section (solid line) and of the Kastelli section (dashed line) and the pattern of time-duration of each succession of six polarity zones between recent and 15.1 Ma of the magnetic polarity time scale. For the correlations that show highest coefficients for both Cretan sequences together we give the corresponding ages of the FOD of the *G. conomiozea* group.

conclusively eliminated. This implies that radiometric control on the Cretan polarity stratigraphy is needed to determine the correct correlation. Since no direct radiometric measurements are available, indirect radiometric control will have to be provided by the age-range of the FOD of *G. conomiozea*, preferably established in the Mediterranean area.

On Aegina (Greece) a Lower Pliocene planktonic foraminiferal association has been dated radiometrically at 4.4 + 0.2 Ma (Benda et al., 1979); this indicates that the FOD of the *G. conomiozea* group in the Mediterranean is definitely older.

Radiometric dating of volcanic rocks in southern Spain (Van Couve-

ring et al., 1976) and in Morocco (Arias et al., 1976) indicate a lower age limit of about 7.0 Ma for the FOD of the *G. conomiozea* group.

Therefore, the Cretan polarity patterns can be realistically correlated with the polarity time scale over a time-interval which corresponds with an age for the FOD of the *G. conomiozea* group of between approximately 4.4 and 7.0 Ma. The most probable correlation corresponds therefore with an age of 5.33 Ma for the upper reversal boundary of polarity zone F+ and with an age of approximately 5.6 Ma for the FOD of the *G. conomiozea* group, which is well within the realistic time-interval for this datum. It may be assumed that the relative lengths of polarity zones based on sea-floor anomalies are more or less correct, but there may be cumulative errors in the ages of reversal boundaries because of the large interpolation time used to obtain these ages (Harrison et al., 1979). However, since polarity reversals younger than 3.40 Ma (the Gauss-Gilbert boundary, used as a calibration point for sea-floor anomaly time scales) have been accurately dated by means of K/Ar methods (see also Mankinen and Dalrymple, 1979) the cumulative errors for polarity reversals in the Late Miocene are negligible. A more direct estimate of the errors involved can be made as follows. In general, individual K/Ar age determinations have an error of about 1%, but inter-laboratory measurements suggest an error of up to 2% for K/Ar ages (Harrison et al., 1979). The reversal boundary of the Gauss and Gilbert chronozones has been accurately established at 3.40 + 0.07 Ma and is based on multiple polarity and K/Ar age determinations (Mankinen and Dalrymple, 1979). The lower reversal boundary of anomaly 5 (chronozone 9) has been established at 10.30 + 0.30 Ma (Harrison et al., 1979) on the basis of their Icelandic data. The error in the age determinations between 5 and 7 Ma derived from the errors in the K/Ar age determinations is then approximately 0.15 Ma.

It should be stressed that the accuracy of the ages established for the polarity reversals between 3.40 and 10.30 Ma does neither depend on the accuracy of the determination of sea-floor anomaly boundaries nor on the relative constancy of sea-floor spreading. The determination of the exact ages depends ultimately on the extent and accuracy of radiometric dating and the direct calibration of these

ages to the magnetic polarity time scale based on sea-floor anomalies, which in its turn can be refined by high-precision techniques.

The exact ages are not as relevant as the fact that the most appropriate correlation of the Cretan polarity sequences is the one by which the Cretan succession of six polarity zones corresponds to polarity chronozones 5 (anomaly 3A) and 6, and by which the FOD of the *G. conomiozea* group occurs in the middle of the reversed polarity subchronozone of chronozone 5 (the reversed "event" of "epoch" 5 in older literature) (see fig. 4.25).

This correlation yields a accumulation rate of 4.2 cm/1000 years in the western Cretan section and of 2.2 cm/1000 years in section Kastelli.

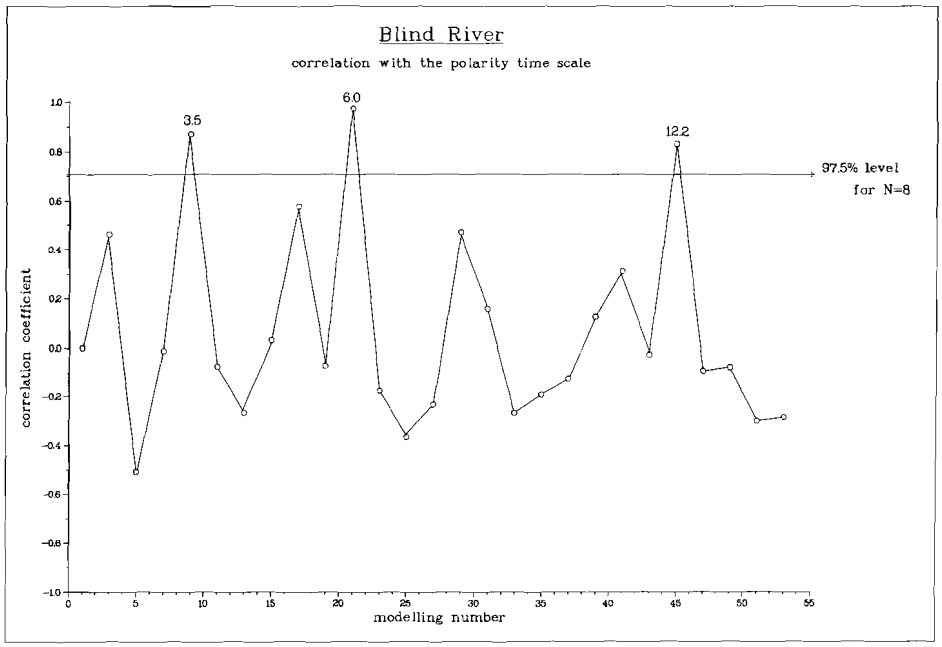

Fig. 4.24 Correlation coefficients between the pattern of lengths of eight polarity zones in the New Zealand Blind River section (Kennett and Watkins, 1974) and the pattern of time-duration of each succession of eight polarity zones between recent and 15.1 Ma of the magnetic polarity time scale. For the significant correlations we give the corresponding age of the evolutionary FOD of *G. conomiozea*.

in Italy. As the sudden spreading of the *G. conomiozea* group most probably represents a migrational event (Zachariasse, 1979a, 1979b; Wernli, 1980), an intra-Mediterranean time-lag of such an extent seems highly unlikely.

Another objection to calibrating the FOD of the *G. conomiozea* group to polarity chronozone 8 is that the non-evolutionary beginning of *G. conomiozea* morphotypes in the Mediterranean would amply antedate their evolutionary appearance in the Pacific (Loutit and Kennett, 1979). This latter argument, however, may be invalid if Scott (1980) is right asserting that the Mediterranean *G. conomiozea* group is not related to the New Zealand taxon.

Radiometric ages for the FOD of *G. conomiozea* (Van Couvering et al., 1976; Arias et al., 1976) indicate that this biohorizon is definitely younger than is suggested by calibrating this event close to the boundary of polarity chronozones 8 and 7.

All evidence together indicates that the polarity reversal sequences measured by Nagakawa et al. (1974, 1975) in Tortonian-Messinian transitional strata of northern Italy are incorrectly assigned to polarity chronozones 8 and 7. Evidently these polarity sequences represent a younger magnetic signal.

An age of 5.6 Ma for the FOD of the *G. conomiozea* group in the Mediterranean, however, does not match with the reported age-range of 6.0-7.0 Ma (Ryan et al., 1974; Van Couvering et al., 1976; Arias et al., 1976).

Radiometric ages most directly related to the FOD of the *G. conomiozea* group are provided by Arias et al. (1976). In the Izarorene section in Morocco these authors dated several tuff layers from an interval slightly below the FOD of *G. conomiozea*. Radiometric dating thus provides a maximum age for this biostratigraphic event. However, the range of radiometric ages for individual tuff layers is very large, varying between 5.6 + 0.3 (sic) and 7.1 + 0.4 Ma for the K/Ar dating and between 6.3 + 1.1 and 6.8 + 0.6 Ma for the fission track dating. Therefore a maximum age for the FOD of *G. conomiozea* in Morocco, ranging from 5.6 + 0.3 to 7.1 + 0.4 Ma, is not necessarily in conflict with an inferred age of 5.6 Ma for the FOD of the *G. conomiozea* group in Crete.

In southern Spain marine sediments with intercalated volcanic lava flows, dated at 6.9 Ma, contain planktonic foraminiferal asso-

ciations which predate the FOD of *G. conomiozea* and which are of presumably Late Tortonian Age (Van Couvering et al., 1976). These

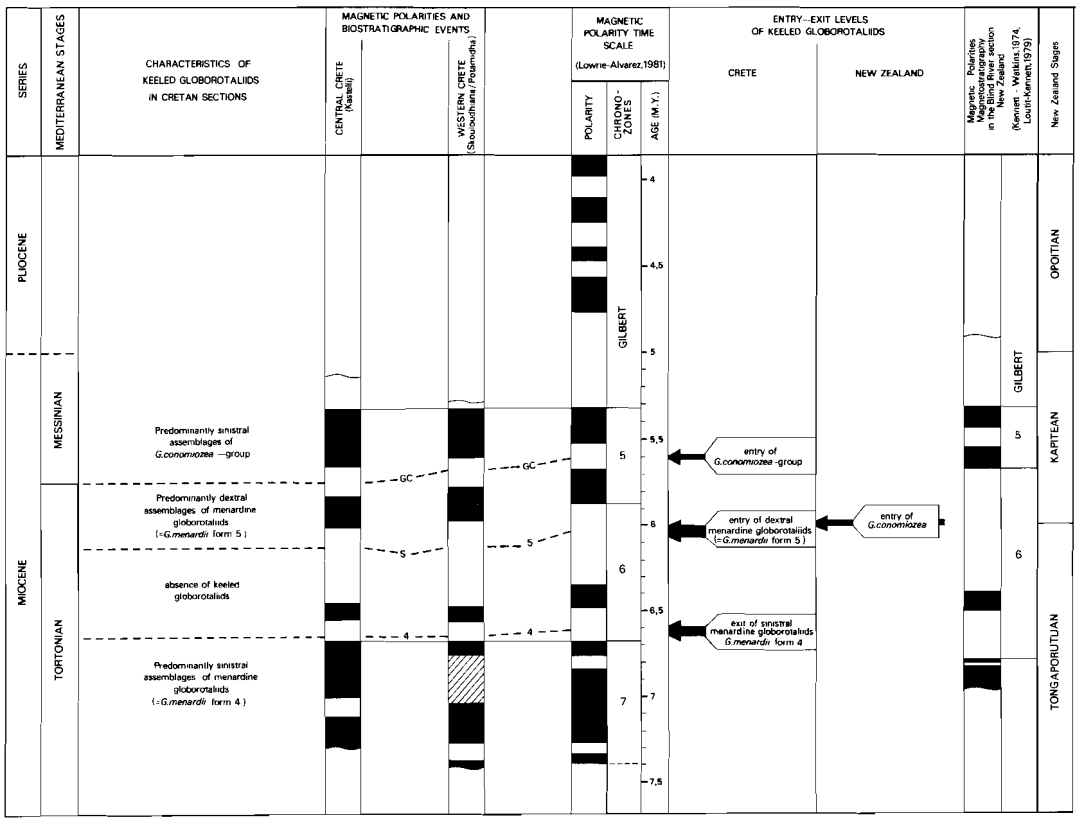

Fig. 4.25 Late Miocene biostratigraphic events, magnetic polarity zones and chronostratigraphic units in the Mediterranean and in New Zealand and their calibration to the magnetic polarity time scale.

marine sediments are overlain by continental deposits containing a mammalian fauna (Libritle fauna) correlatable with the mammalian fauna level VI at Crevillente, which in turn correlates with marine sediments containing *G. conomiozea* (de Bruijn et al., 1975). Thus the FOD of *G. conomiozea* can only indirectly be calibrated to this radiometric age of 6.9 Ma, which gives at best a maximum age determination for this event.

The age of 6.3 Ma for the FOD of *G. conomiozea* in the Mediterranean, given by Ryan et al. (1974), is based on the re-interpretation

of the paleomagnetic data from the Blind River section in New Zealand (Kennett and Watkins, 1974) and on the assumption that the New Zealand FOD of *G. conomiozea* is time-equivalent with the Mediterranean FOD of *G. conomiozea*. Although the re-interpreted magnetic correlation for the Blind River is generally accepted, Ryan et al. did not place the FOD of *G. conomiozea* in accordance with the original data of Kennett and Watkins (1974). If it were positioned correctly, the FOD of *G. conomiozea* would occur in the younger reversed interval of polarity chronozone 6 with an extrapolated age of ca. 6.1 Ma (Loutit and Kennett, 1979; this paper, fig. 4.25).

The results of the present study demonstrate that the diachrony between the New Zealand FOD of *G. conomiozea* and the FOD of the *G. conomiozea* group in the Mediterranean is 0.4 Ma. This need not be surprising, considering the widely different paleo-oceanographic histories. In fact, it would be more surprising if the evolution of fauna in separate, antitropical distribution areas had been absolutely synchronous. The diachrony between both biohorizons might be ascribed to the different nature of their corresponding events, the one in New Zealand being evolutionary and the one in the Mediterranean being migrational.

AGE OF THE TORTONIAN-MESSINIAN BOUNDARY AND THE MAIN EVAPORITIC PHASE

Unfortunately no reliable magnetobiostratigraphic data are available to determine the degree of synchrony of the FOD of the *G. conomiozea* group in the Mediterranean.

Section Falconara contains the recently proposed boundary stratotype for the Tortonian-Messinian boundary as denoted by the FOD of *G. conomiozea* (Colalongo et al., 1979b), but from this study it has become clear that the entire section shows only recent, normal polarity magnetizations that are due to a secondary CRM.

Section Castellania on the other hand contains no reliable biostratigraphic datum levels due to a meagre faunal content and possible reworking. The upper part of the Mussotto section as sampled by d'Onofrio et al. (1975) is reported to contain the FOD of the *G. conomiozea* group, but only the lower part of the section is

suited for paleomagnetic sampling. The latter part, which we sampled, is definitely older than the LOD of *G. menardii* form 4 and hence this latter datum cannot be compared with the Cretan results.

Evidence for the supposed time equivalence of the Mediterranean FOD of the *G. conomiozea* group, however, has been provided recently by a refined calcareous nannoplankton stratigraphy (Theodoridis, 1983): both in Crete and in Sicily the FOD of the *G. conomiozea* group nearly coincides with the entry level of *Reticulofenestra rotaria*. In addition, the FOD of the *G. conomiozea* group in the Falconara section (Zachariasse and Spaak, 1983) coincides with the level proposed as the physical reference point for the Tortonian-Messinian boundary (Colalongo et al., 1979b). Therefore, this boundary must have an age of 5.6 Ma.

Since the youngest sediments incorporated in our study reach into the Gilbert chronozone (fig. 4.25) and antedate the abrupt coiling change in *N. acostaensis*, the latter event must be younger than the base of the Gilbert chronozone whose age is fixed at 5.3 Ma (Lowrie and Alvarez, 1981). In the Mediterranean the abrupt coiling change in neogloboquadrinids occurs at a level slightly below the main evaporitic phase (Zachariasse, 1975; Colalongo et al., 1979), which means that the Messinian evaporitic body has a lower age limit of about 5.3 Ma.

The age of the Miocene-Pliocene boundary is commonly fixed at about 5.0 Ma and is based on the calibration of multiple biostratigraphic criteria to the magnetic polarity time scale (Berggren, 1973; Cita and Gartner, 1973; Berggren and Van Couvering, 1974), all of which are dubious as far as the Mediterranean is concerned. Commonly, the base of the Mediterranean Pliocene is recognized on the basis of the sedimentary expression of the post-Messinian flooding and must certainly be older than 4.4 + 0.2 Ma according to Benda et al. (1979) and is probably older than 4.7 Ma according to the radiometric age of the supposedly Lower Pliocene Orciatico trachyte in Tuscany (Selli, 1970). Whatever the precise age of the base of the Pliocene in the Mediterranean may be, it is evident that the new age of 5.6 Ma for the Tortonian-Messinian boundary severely reduces the time-span of the Messinian.

Adopting the age of 5.0 Ma for the Miocene-Pliocene boundary

would imply that the evaporites and post-evaporitic Lago Mare sediments were deposited over some 300,000 years. Given the thickness of more than 1000 metres for the Messinian evaporitic body in the central parts of the Mediterranean basins (e.g. Leenhardt, 1973; Selli, 1973; Mulder, 1973; Hsu et al., 1977) the evaporites must have accumulated at rates of more than 3 metres per 1000 years.

Accumulation rates of this order of magnitude are known for anhydrites and halites precipitated in the central parts of Permian concentration basins (Richter-Bernburg, 1953) as well as for gypsum growth in recent salinas (Dronkert, 1977).

CONCLUSIONS

The ages given in this chapter for the FOD of the *G. conomiozea* group and hence the Tortonian-Messinian boundary, as well as the ages for the FOD of *G. menardii* form 5, the LOD of *G. menardii* form 4 (see fig. 4.25) and the lower age limit for the Messinian evaporitic body, are the most exact determined so far in the Mediterranean area.
Further adjustments and revisions because of new K/Ar ages and magnetic anomaly boundaries may alter these ages slightly, although probably not significantly. Essentially, the value and validity of magnetostratigraphy as a tool for absolute age determinations, although depending on the accuracy and extent of K/Ar age determinations and sea-floor-anomalies, is conclusively demonstrated.

In using this tool, several things must be considered. A successful correlation depends on the number of polarity reversals as well as on the specific polarity pattern (fingerprint): more polarity reversals and more specific patterns reduce the number of possible correlations. Also one has to be able to estimate or know the (variations in) accumulation rates and to know that hiatuses are absent or can be corrected for. In this respect, it is noteworthy that a slight reduction in the length of polarity zone F+ - which is justified on the basis of the lithology - would improve the correlation (fig. 4.25). Furthermore, if the correlation is not unique, it is essential that the age-range of the sampled series can be delimited, if possible by direct (radiometric) age determination.

Indirect age control may be provided by biostratigraphic control, but it should be emphasized that such age determinations must be tied to biostratigraphic datum levels from the same area. Neglecting this last constraint might easily lead to circular reasoning. For instance, the FOD of *G. conomiozea* has been observed in chronozone 6 in New Zealand, therefore one might conclude that polarity zone E- in Crete represents chronozone 6 as well (cf. Ryan et al., 1974). This study, however, has demonstrated that diachrony of this datum is more likely than synchrony.

chapter five

SOME ROCK-MAGNETIC PARAMETERS

INTRODUCTION

Rock-magnetic parameters are an important source of information about the magnetic minerals and hence the primary or secondary origin of the natural remanent magnetization components. Among the many rock-magnetic parameters (and ratios of these parameters) three have come into common use. These involve the initial susceptibility X, the saturation isothermal remanent magnetization (SIRM) and the anhysteretic remanent magnetization (ARM). In addition, the (remanent) hysteresis loop parameters are generally taken as useful indicators.

A change in the concentration and in the nature of magnetic minerals throughout a section (or core) will be reflected in changes in X, SIRM and (remanent) hysteresis loop parameters. Hence, these parameters and several parameter ratios can be used as mineralogical and grain-size indicators. The susceptibility appears to be the least sensitive indicator, while the saturation remanence (SIRM) for (titano)magnetites shows an appreciable, gradual intensity decrease with increasing grain-size (Dankers, 1978; Hartstra, 1982b). Neither X nor SIRM is a useful grain-size indicator by itself, however, for each is dependent on the concentration of the magnetic mineral(s) in a sediment as well. Lanser (1980) argued that for not too large concentrations of magnetite the ratio X/SIRM will be independent of this concentration and termed it the "grain-size ratio". This ratio increases with increasing grain-size. It should be pointed out, however, that the term grain-size ratio only applies if the magnetic mineral consists of predominantly the same (titano)magnetite. Changes in mineralogy influence this ratio considerably: e.g. hematites show values of 0.002 - 0.006 * 10-3 m/A virtually independent

of grain-size (Dankers, 1978), whereas magnetites have values ranging 0.050 - 1.000 * 10-3 m/A depending on grain-size (Hartstra, 1982b). The ratio is not very sensitive to variations in grain-sizes smaller than 5 um; for (titano)magnetites and (titano)maghemites it appears to converge to a value of 0.020 - 0.060 * 10-3 m/A, whereas for grain-sizes from 10 to more than 150 um it rapidly increases to a value of 1.000 * 10-3 m/A (Dankers, 1978; Hartstra, 1982b).

The remanent coercive force Hcr (or Br) can be determined from the remanent hysteresis curve. A saturation IRM is given in a direct field and an anti-parallel IRM is then progressively built up to saturation. The field required to reduce the initial SIRM to zero is the remanent coercive force. In the paleomagnetic laboratory 'Fort Hoofddijk' we can reach a maximum direct field of 2 Tesla. Therefore, in the present study saturation is often not reached for hematite or goethite. The remanent coercive force is largely independent of the concentration of magnetic material and since the Hcr-values for magnetite and hematite are generally different it may serve as a magnetic mineralogy indicator. Both for magnetite and hematite Hcr decreases with increasing grain-size; for magnetite from ca. 40-60 mT for grains less than 5 um to ca. 10 mT for multi-domain grains. Values for hematite are 150-200 mT for grains less than 5 um and decrease to ca. 50 mT (Dankers, 1978; Hartstra, 1982b).

The X/SIRM ratio and Hcr together yield useful information concerning the magnetic mineralogy and the grain-size involved. Considering the low values of the X/SIRM ratio for hematite, the contribution of hematite to this ratio is negligible if magnetite, especially of multi-domain size, is present: ca. 0.050 * 10-3 m/A for single-domain magnetite up to 1.000 * 10-3 m/A for multi-domain magnetite, whereas hematite has values of 0.002 - 0.006 * 10-3 m/A. Generally, a higher X/SIRM ratio can therefore be taken as an indication of coarser magnetite. Coarsening of the magnetite results at the same time in a lower Hcr value.

However, a coarsening of the magnetite is usually accompanied by a coarsening of the sediment itself, which is then more susceptible to weathering, resulting in the production of hematite or goethite. In the case of single-domain magnetite, its (S)IRM dominates the S(IRM) of hematite to such an extent that even if hematite is

present the Hcr measured is that of magnetite. In the case of multi-domain magnetite, its (S)IRM is still higher than the (S)IRM of hematite, but the influence of hematite will become noticeable in the (higher) Hcr values, depending, of course, on the concentration of hematite. Hence, a coarsening of the magnetite generally results in a higher X/SIRM ratio and in lower Hcr values if hematite is not present, but in higher Hcr values if hematite (or goethite) is present e.g. because of weathering. The latter is generally observed in the Cretan sections, especially in the Potamida sections and section Kastelli, where a coarsening of the sediment indicates a higher accumulation rate towards the top of those sections. Usually the X/SIRM ratio in the Cretan sections has values of 0.050 - 0.100 * 10-3 m/A, indicating very fine grained magnetite, whereas the top of the sections show values of 0.200 - 0.400 * 10-3 m/A, typical for pseudo single domain to multi-domain magnetite (cf. Hartstra, 1982b).

A feature that is frequently observed is a slightly higher X/SIRM ratio at places where weathering has taken place. The X/SIRM ratio then has values of 0.10 - 0.20 * 10-3 m/A. Such places are further characterized by a (very) small ChRM component relative to the secondary normal polarity magnetization component (see also fig. 3.27 and the discussion in chapter three). Usually, the (single domain) magnetite responsible for the ChRM dominates the X and SIRM and hence their ratio. If the ChRM component is very small, the magnetic minerals carrying the secondary component (less fine grained magnetite and maghemite) will determine the X/SIRM ratio, which is then somewhat higher.

Although strictly not a rock-magnetic parameter in the usual sense, the ChRM intensities may serve as a useful indicator in combination with other parameters. Since total NRM intensities may represent the vectorial resultant of two or more magnetizations they cannot be used for correlation purposes. It is therefore more practical to compare the intensities of the characteristic remanent magnetization, or rather the intensities of the NRM after (entire or major) removal of viscous and secondary magnetizations. Due to overlapping blocking temperature or coercivity spectra, that part of the ChRM that survives the treatment necessary to remove the viscous and secondary remanence component is then also removed. The low temperature and soft part of the ChRM is necessarily removed as well.

In the case of the Cretan section the intensities of the NRM after treatment with 50 mT or 200 oC were used (cf. chapter three), for the Falconara section the total NRM intensities and the intensities after treatment with 100 oC are shown. Both X and SIRM have been determined for all sections discussed in this chapter, whereas the Hcr is determined only for the Potamida sections, the Skouloudhiana section and the Falconara section.

THE POTAMIDA AND SKOULOUDHIANA SECTIONS

The ChRM intensities of section Potamida 1 are shown in figure 5.1a. In general, intensity fluctuations are matched by similar corresponding fluctuations both in X and SIRM (fig. 5.1b), suggesting that small variations in the concentration or nature of the magnetic minerals are responsible. A decrease in ChRM intensities can be seen at polarity reversal horizons and frequently close to ferruginous levels . The polarity transition from D+ to E- shows a decrease in intensity, whereas the magnetic properties do not change; this suggests that the lower intensity of the ChRM is due to a lower geomagnetic field at the time of deposition (see also Valet and Laj, 1981). Close to the polarity transitions from polarity zone C- to D+ and from E- to F+, however, ferruginous levels are present (Fe 2 and Fe 4, respectively). Therefore it is not certain whether the decrease in the intensities should be ascribed to the polarity transition, to the presence of a ferruginous level or to a combination of both.

Although both X and SIRM show relatively large fluctuations, their ratio is rather constant for a major part of the section and lies in the range 0.05 - 0.08 * 10-3 m/A, indicating very fine grained magnetite as the magnetic mineral (Hartstra, 1982b). This strongly supports the the view that the magnetic mineral responsible for the ChRM can be determined on the basis of the thermal demagnetizations, IRM acquisition curves and the low temperature treatment, i.e. very fine grained, single domain magnetite. Similarly, the remanent coercive forces are rather constant throughout most of the sections, indicating very fine grained magnetite as well, except close to ferruginous levels and in the top of the section. The constant X/SIRM ratio and the constant remanent coercive forces furthermore indicate a constant and uniform grain-size distribution, most probably due to an almost constant accumulation rate.

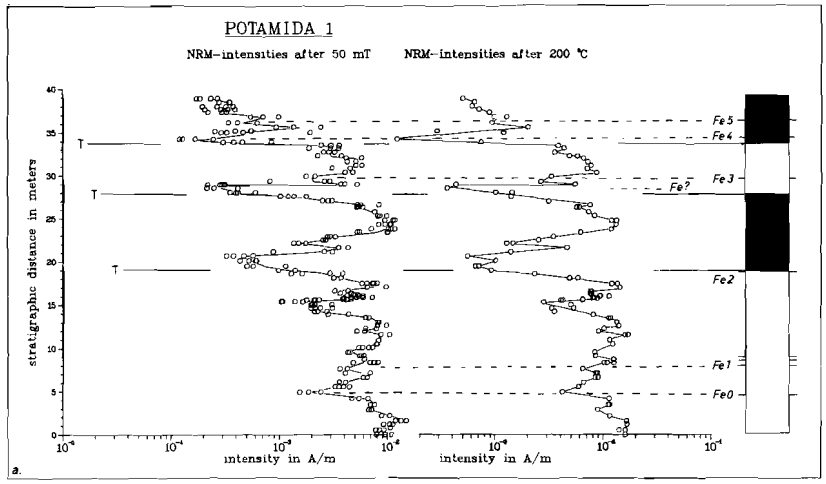

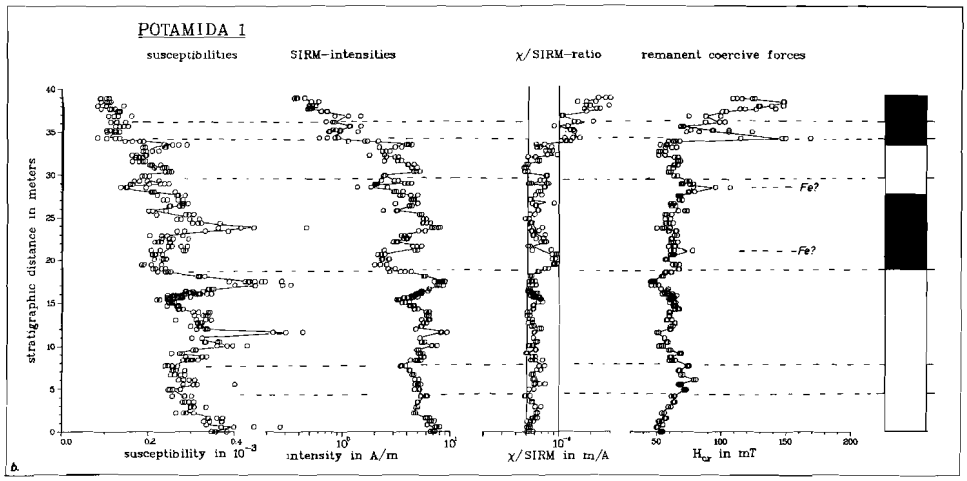

Fig. 5.1 a) NRM intensities after treatment with an alternating field of 50 mT and with a temperature of 200 °C in section Potamida 1. Solid lines connect average intensities per level; dashed lines indicate lowered intensity related to ferruginous levels (Fe) or a layer of finely bedded clay (L); polarity reversal horizons (T) often show corresponding lower intensities. These intensities closely represent the intensities of the ChRM (see text). The polarity zonation and lithostratigraphic information are shown for (chronostratigraphic) comparison. b) Susceptibility X, saturation IRM (SIRM), X/SIRM ratio and remanent coercive force H_{cr} versus stratigraphic distance in section Potamida 1.

It should be noted that the ChRM intensities, X and SIRM decrease towards the top of the section, approximately from Fe 4 upwards, whereas the X/SIRM ratio and Hcr increase. This X/SIRM ratio indicates a coarsening of the magnetite grains and at the same time the higher Hcr values indicate more intensive oxidation due to weathering because the sediment becomes less homogenous and more silty.

The ChRM intensities in section Potamida 2 (fig. 5.2a) are somewhat difficult to compare with those of section Potamida 1 because of the fault in the upper part of the section. Nevertheless, the same features can be recognized as in section Potamida 1. At the polarity transition from polarity zone D+ to E- the rock-magnetic properties remain rather constant (fig. 5.2b), but an appreciable decrease in intensity is found. Although ferruginous levels Fe 2 and Fe 5 have not been observed in section Potamida 2, the presence of these levels is indicated, especially by the remanent coercivities (fig. 5.2b). Two more such (possibly discontinuous) Fe-levels can be inferred, one above Fe 3 and one above the assumed Fe 2, on the basis of higher Hcr values. The latter can be recognized in section Potamida 1 as well (fig. 5.1b) by the higher Hcr values.
The X/SIRM ratio is somewhat higher than in the previous section, but generally well within the range 0.06 - 0.10 * 10-3 m/A, except close to some Fe levels and in the upper part of the section above Fe 4, which agrees with the results of the Potamida 1 section.

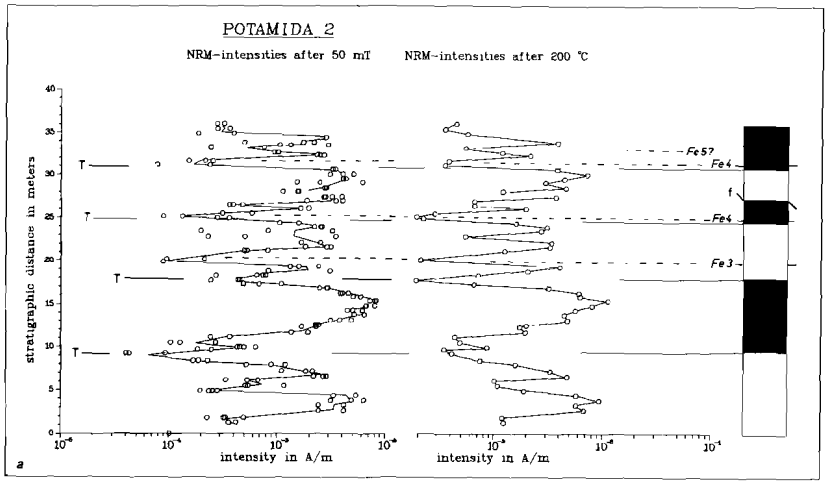

For caption see next page

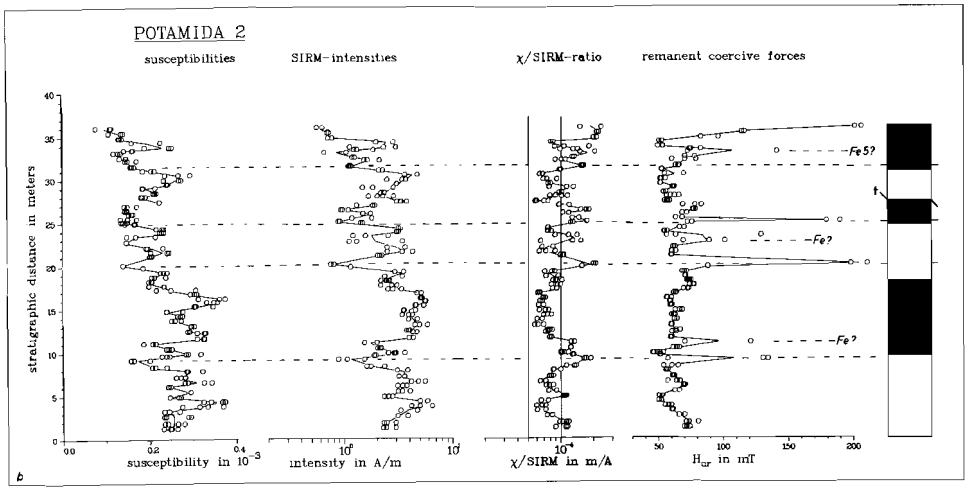

Fig. 5.2 a) on previous page: NRM intensities after 50 mT and after 200 °C in section Potamida 2. b) Susceptibility, saturation IRM, X/SIRM ratio and remanent coercive force in section Potamida 2. See also fig. 5.1 caption.

A change in the rock-magnetic parameters due to a lithologic change and possibly the resulting increased weathering can be most clearly observed in Potamida 3. The ChRM intensities show a considerable decrease in the upper part of the section, starting in the lower part of polarity zone F+ (fig. 5.3a) and corresponding with a similar decrease at the identical stratigraphic positions in the Potamida 1 and 2 sections. This change is reflected in the rock-magnetic parameters: both the X/SIRM ratio and the Hcr show a considerable increase (fig. 5.3b) and indicate a coarsening of the magnetite and the presence of hematite due to weathering. This is also in agreement with the IRM acquisition curves shown in fig. 3.38b.

The same feature can be recognized in the Potamida 4 section and again at the same stratigraphic position (fig. 5.4a,b): the upper part of the section, correlating with the upper parts of the former sections, again shows lower ChRM intensities and corresponding rock-magnetic properties. The major part of the section above the larger non-exposed interval, however, shows constant magnetic properties similar to those found in the former sections, and points to a constant grain-size distribution and hence a constant accumulation rate.

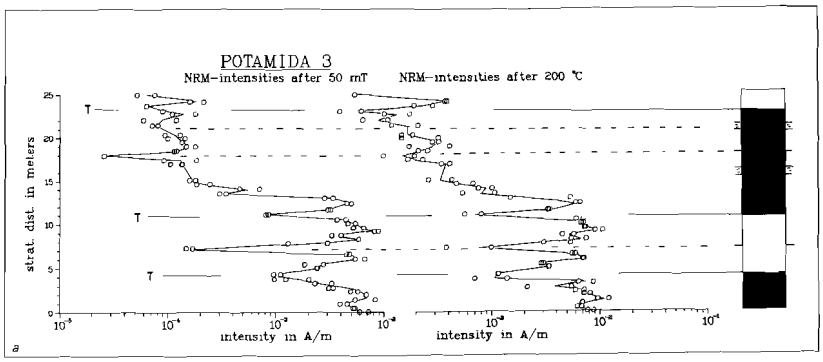

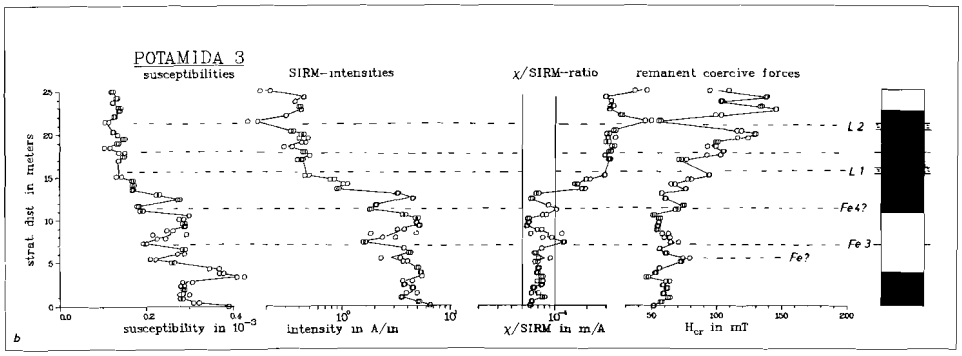

Fig. 5.3 a) NRM intensities after 50 mT and after 200 °C in section Potamida 3. b) Susceptibility, saturation IRM, X/SIRM ratio and remanent coercive force in section Potamida 3. See also fig. 5.1 caption.

In the lowermost part some very high Hcr values are found, indicating increased weathering and oxidation, but reversed polarities can still be established. In the lower part of polarity zone C- in the Potamida 4 section, between the two non exposed intervals (fig. 5.4), the ChRM intensities are lower than in the upper part of polarity zone C- and in polarity zones D+ and E-.

Similar changes occur in the Skouloudhiana section: in the lower part of polarity zone C- lower ChRM intensities can be seen as well as a level with appreciably higher intensities (fig. 5.5a,b) This level may correspond to the same feature in Potamida 4. The ferruginous and somewhat thicker, sandy level in section Skouloudhiana, approximately one metre above the levels showing increased intensi-

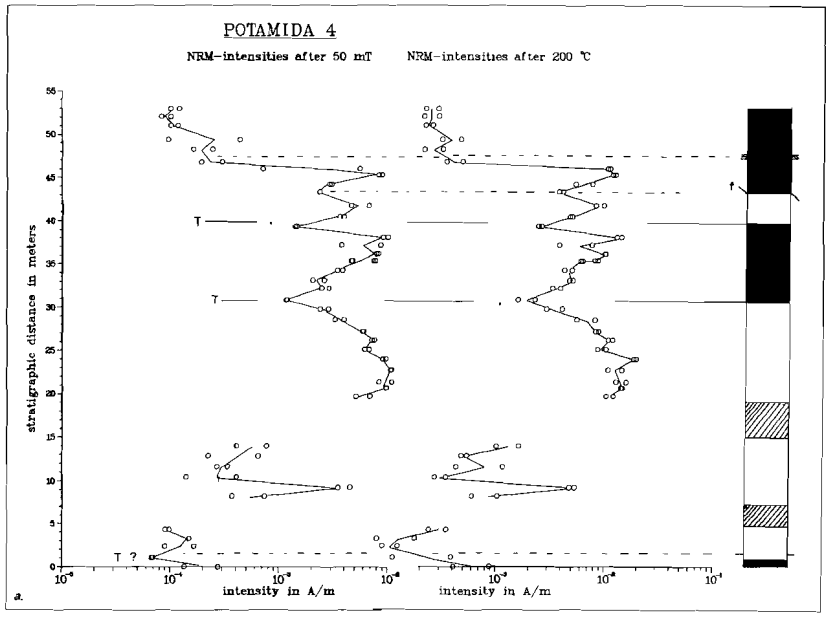

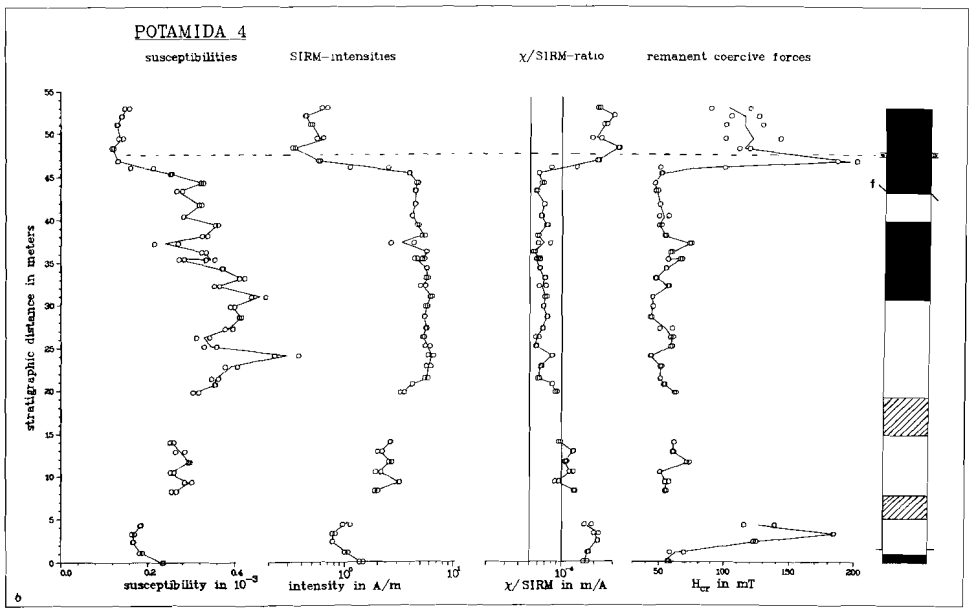

Fig. 5.4 a) NRM intensities after 50 mT and after 200 °C in section Potamida 4. b) Susceptibility, saturation IRM, X/SIRM ratio and remanent coercive force in section Potamida 4. See also fig. 5.1 caption.

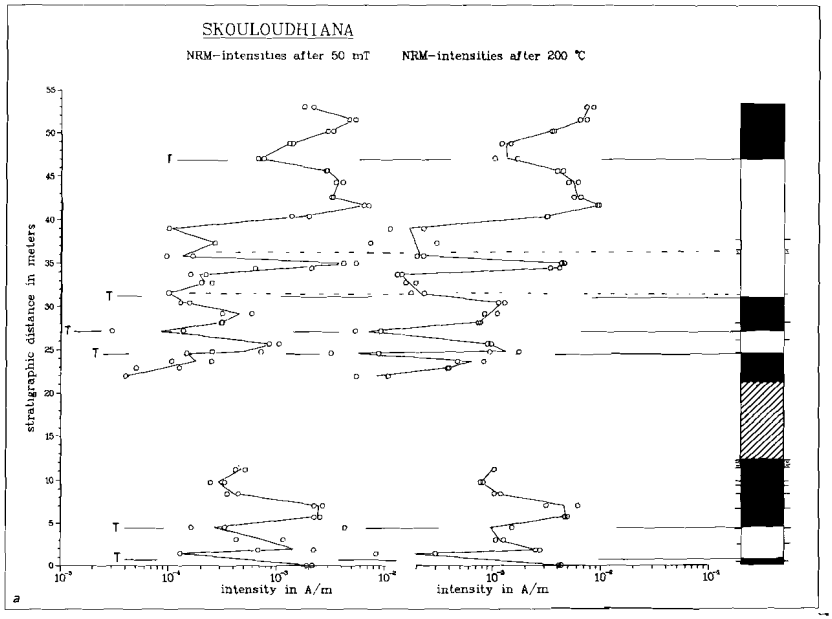

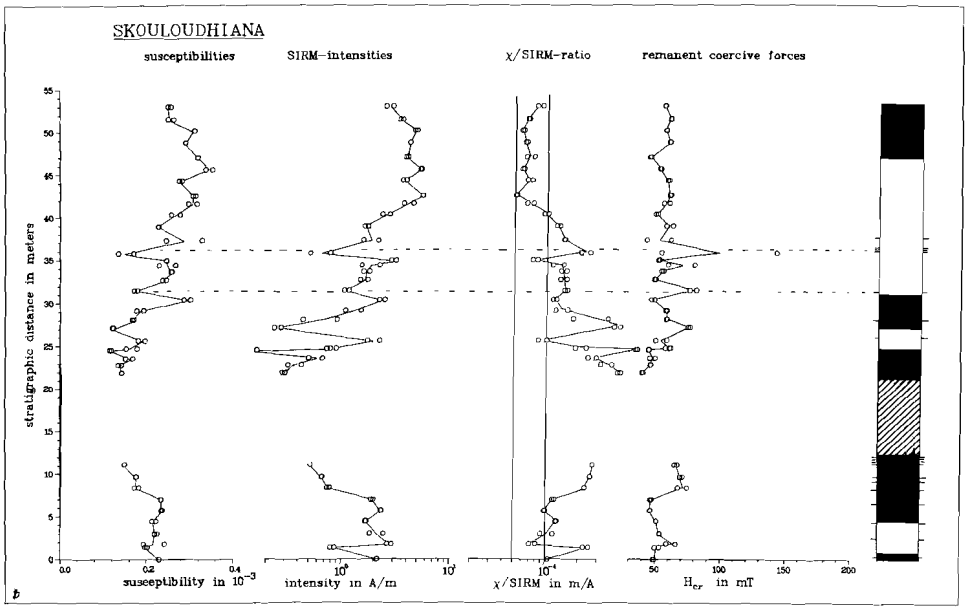

Fig. 5.5 a) NRM intensities after 50 mT and after 200 °C in section Skouloudhiana. b) Susceptibility, saturation IRM, X/SIRM ratio and remanent coercive force in section Skouloudhiana. See also fig. 5.1 caption.

ties, has not been observed in section Potamida 4, so there is no hard evidence that the higher intensities are from one and the same stratigraphic level.
The higher values of the X/SIRM ratio in the Skouloudhiana section combined with the lower values of Hcr below polarity zone A- indicate a coarser grain-size of magnetite and possibly a somewhat higher accumulation rate. Apparently the somewhat coarser grain-size is not accompanied by increased weathering and the formation of hematite (i.e. higher Hcr values). This fits in with the observation that the clay in this part of the section is homogenous and permits no weathering, whereas the lithologic change in the top of the Potamida sections is distinctly visible.

It has become clear that the ChRM intensities and rock-magnetic properties of the Potamida sections and the Skouloudhiana section can be correlated rather well with respect to chronostratigraphically corresponding levels, as can be deduced from the polarity zonation. The general constancy of remanent coercive forces and X/SIRM ratios reflects the rather homogeneous composition of the magnetic mineralogy. This in turn corresponds with the homogeneity of the open-marine clays and also indicates that a more or less constant accumulation rate can be assumed, except in the upper part of the sections (polarity zones F+ and G-, e.g. in sections Potamida 3 and 4), where the lithology as well as the rock-magnetic properties indicate a somewhat higher accumulation rate. Similarly, the magnetic properties below polarity zone A- suggest a somewhat coarser grain-size and probably a slightly higher accumulation rate. It is important to notice that the constant accumulation rate over the upper six polarity zones, A- through to F+, proposed in chapter 4, is corroborated by the results in this chapter. It is clear that if the accumulation rate in the upper part of polarity zone F+ were to be somewhat reduced, the correlation with the polarity time scale would show an even better fit than it does already (see chapter 4).

The largest interruptions in the relative constancy of the magnetic properties are found close to the ferruginous levels (see figs. 5.1-5.5). These interruptions are due to oxidation of the magnetic minerals close to these levels, since these levels are more

permeable than the dense clay and facilitate weathering. It should be noted that close to some levels there is a drastic change in magnetic properties (e.g. in section Potamida 2, fig. 5.2) whereas close to others there are no such changes. This is due to the varying distance of the samples from these levels and depends on whether or not the samples were taken within their "sphere of influence". Moreover, because of the sometimes discontinuous and very thin nature (seams) of the ferruginous levels (Drooger et al., 1979b) presumably not all of them have been observed in the field. For instance, Fe 5 has not been observed in section Potamida 2 and 3, but at the corresponding stratigraphic level an appropriate change in the magnetic properties can be observed, especially in section Potamida 2 (cf. figs. 5.1, 5.3). Similarly, an unnoticed ferruginous level may exist, for example, some two metres above Fe 2 in sections Potamida 1 and 2, as indicated by the somewhat higher Hcr values at this level (figs. 5.1, 5.2).

THE KOTSIANA SECTIONS

The ChRM intensities of section Kotsiana 1 are more than an order of magnitude less than those in the other western Cretan sections (fig. 5.6a). The same applies to both the initial susceptibility and the intensity of the saturation remanence (fig. 5.6b). Both follow closely changes in the intensity of the ChRM, indicating that a slightly and relatively higher concentration of magnetic minerals is responsible for the higher intensity values. The X/SIRM ratio is appreciably higher than in the other sections and indicates a coarser grained magnetic mineralogy (cf. Hartstra, 1982b). Below the thick sand layer in the lower part of the section, the X/SIRM ratio is ca. 1.0 * 10-3 m/A, corresponding with large-grained, multi-domain magnetite. This is in agreement with the viscous magnetizations found in this part of the section, where no reliable polarities could be determined.

The higher X/SIRM ratio is most probably related to a higher accumulation rate. The relatively greater length of polarity zone A- in section Kotsiana 1 with respect to the same zone in section Skouloudhiana (see fig. 4.22) also points to a higher accumulation rate.

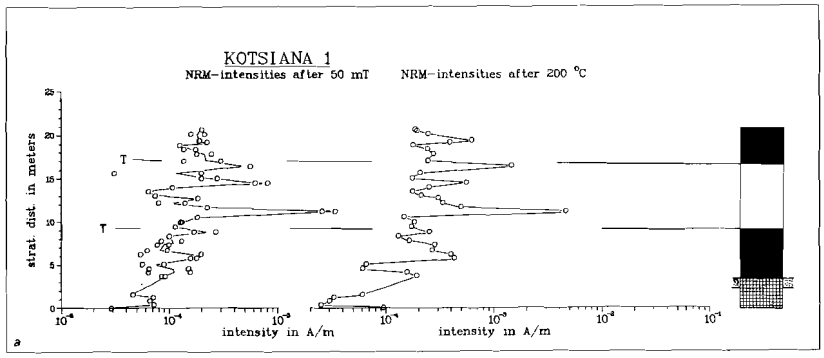

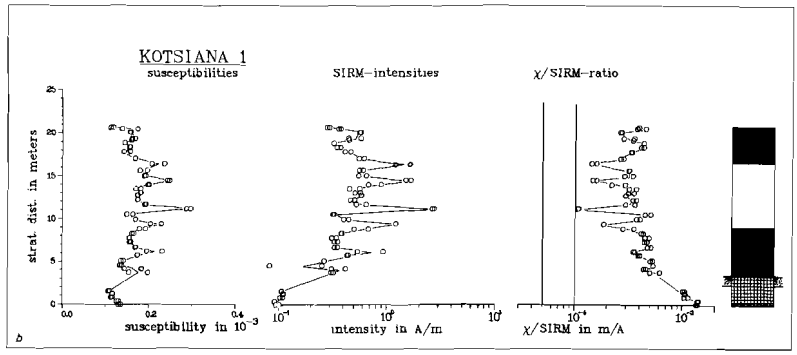

Fig. 5.6 a) NRM intensities after 50 mT and after 200 °C in section Kotsiana 1. b) Susceptibility, saturation IRM and X/SIRM ratio in section Kotsiana 1. See also fig. 5.1 caption.

The characteristics of section Kotsiana 2 are similar to those of the Potamida and Skouloudhiana sections. The ChRM intensities are of the same order of magnitude (fig. 5.7a) and the changes therein correspond with changes in X and SIRM (fig. 5.7b). The X/SIRM ratio is remarkably constant except at a level which may correspond to level Fe 3, just below the FOD of the *G. conomiozea* group, and at a level a few metres below this "Fe 3". At the base of the section the X/SIRM ratio is somewhat higher due to slightly increased weathering. Jointing has been observed in this part of the section. A slightly higher X/SIRM ratio is observed in the topmost levels, concurring with a relatively large secondary component (cf. fig. 3.32).

In general, the constant X/SIRM ratio is of the same order as in the Potamida sections and reflects a constant magnetic mineralogy resulting from a more or less continuous and uniform accumulation rate.

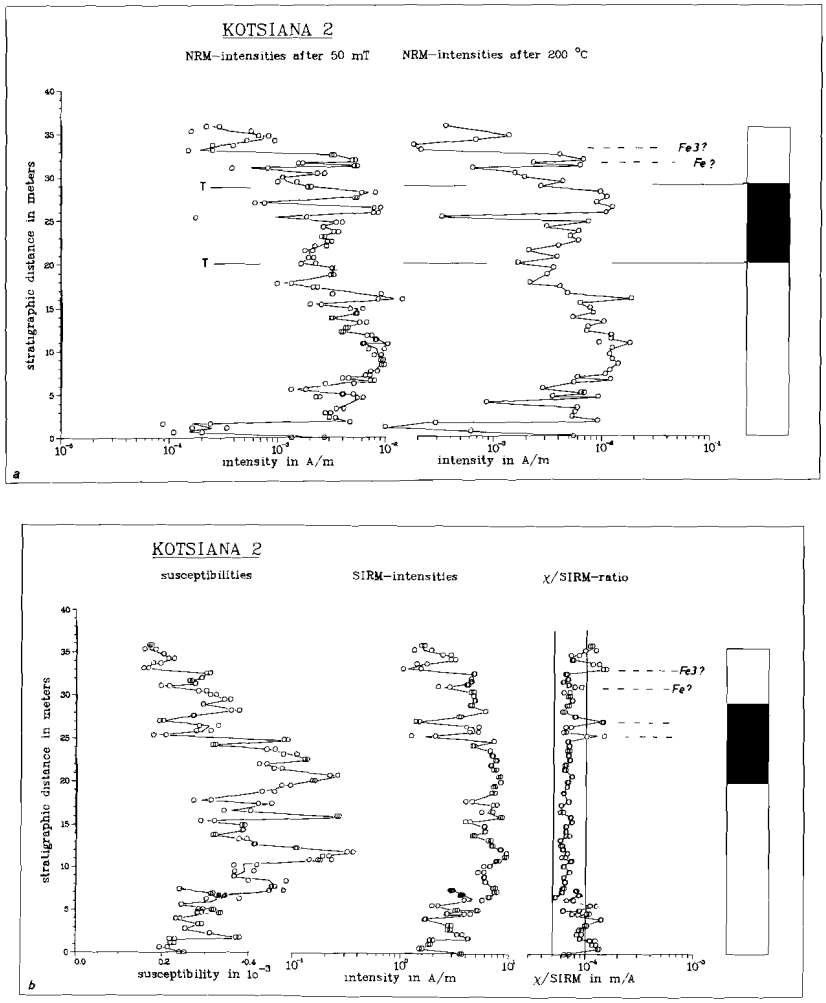

Fig. 5.7 a) NRM intensities after 50 mT and after 200 °C in section Kotsiana 2. b) Susceptibility, saturation IRM and X/SIRM ratio in section Kotsiana 2. See also fig. 5.1 caption.

THE EPISCOPI AND VASILOPOULO SECTIONS

The Episcopi section (fig. 5.8) shows in general the same characteristics as observed in the Potamida section, Skouloudhiana and Kotsiana 2 sections: changes in ChRM intensities correspond with changes in X and SIRM, and the X/SIRM ratio is again of the same order as in those sections, showing an almost constant value. Only in the upper part of section Episcopi is the zone of indeterminate

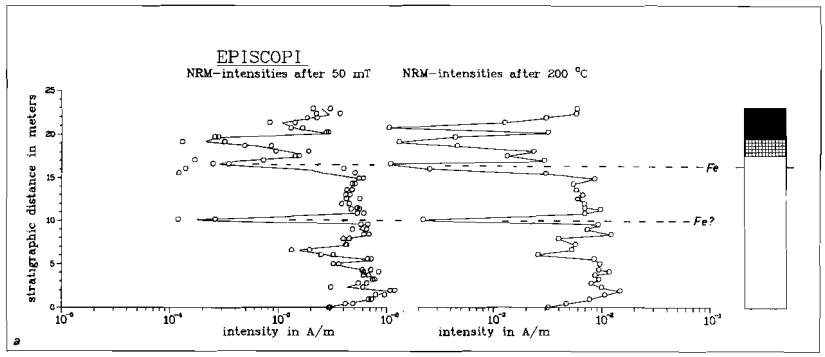

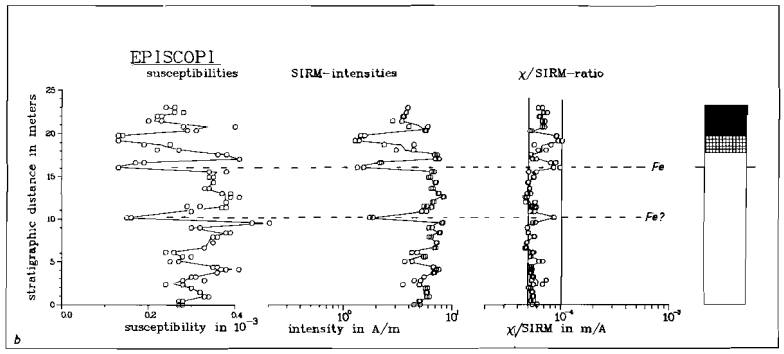

Fig. 5.8 a) NRM intensities after 50 mT and after 200 °C in section Episcopi. b) Susceptibility, saturation IRM and X/SIRM ratio in section Episcopi. See also fig. 5.1 caption.

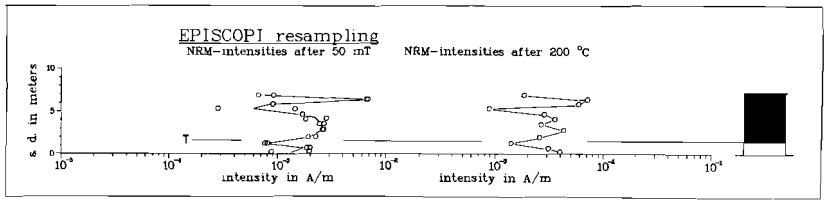

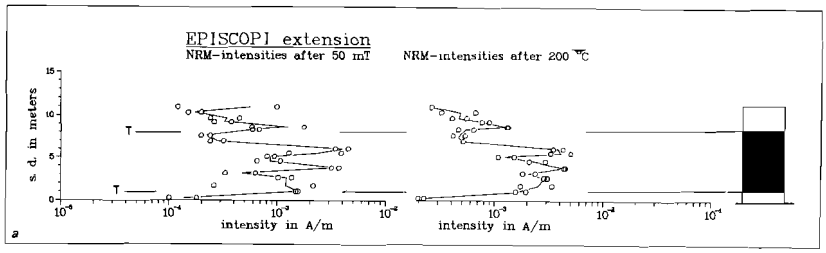

For caption see next page

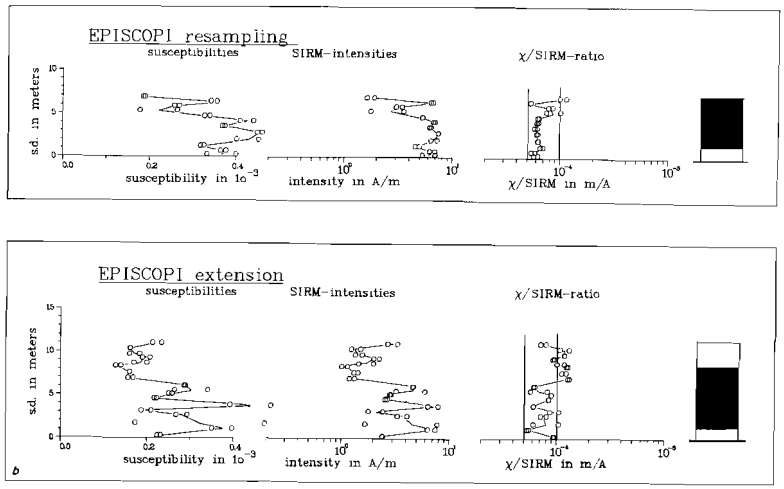

Fig. 5.9 a) NRM intensities after 50 mT and after 200 °C in sections Episcopi Resampling and Extension. b) Susceptibility, saturation IRM and X/SIRM ratio in sections Episcopi Resampling and Extension. See also fig. 5.1 caption.

polarities reflected in the (lower) ChRM intensities (fig. 5.8a) and in the magnetic properties (fig. 5.8b): both X and SIRM show lower values, and their ratio is higher than normal. This zone is characterized by joints close to a small fault with a throw of 85 cm. Therefore the upper part of section Episcopi was resampled from the ferruginous level upwards. This resampled part (Episcopi Resampling, fig. 5.9) shows no indeterminate polarities and the X/SIRM ratio in particular indicates a constant magnetic mineralogy, except in the topmost levels which are taken close to the topographic top of the section.

The outcrop of section Episcopi Extension is somewhat weathered due to a number of joints and this shows up in the ChRM intensities and the magnetic properties (fig. 5.9). The X/SIRM ratio is less constant than in section Episcopi and Episcopi Resampling; the upper part of the section shows clearly the effects of increased weathering as observed in the field from the numerous joints and often tan-coloured clay. Furthermore, the demagnetization diagrams from the upper part of the section show a relatively very large secondary magnetization component (see fig. 3.34), which is probably due to oxidation of the fine-grained magnetite carrying the ChRM.

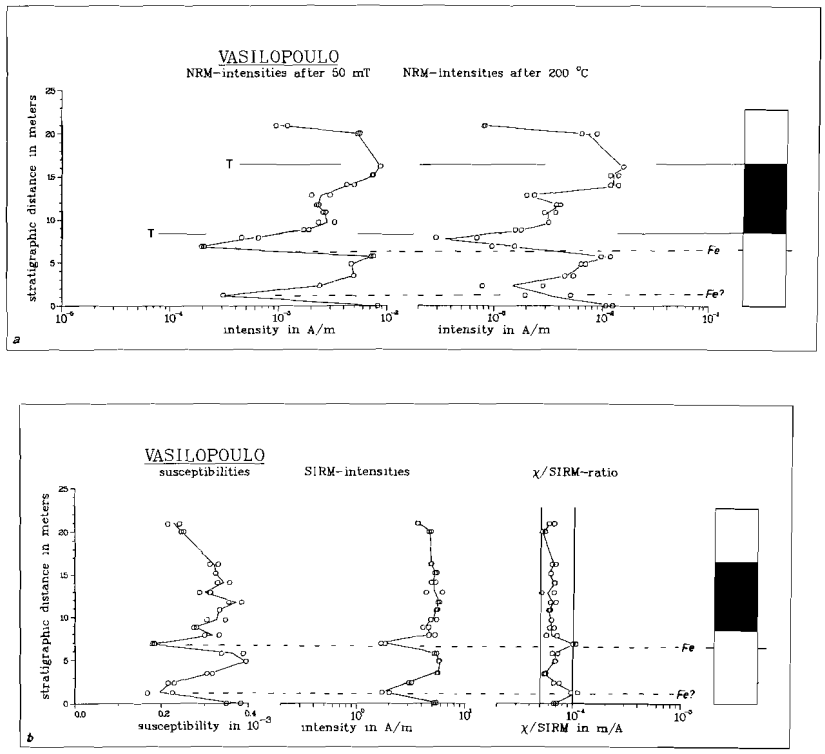

Fig. 5.10 a) NRM intensities after 50 mT and after 200 °C in section Vasilopoulo. b) Susceptibility, saturation IRM and X/SIRM ratio in section Vasilopoulo. See also fig. 5.1 caption.

The Vasilopoulo section shows magnetic characteristics very similar to those of the Episcopi section. Samples close to the ferruginous level show a decrease in intensity (fig. 5.10a) corresponding with a decrease both in X and in SIRM (fig. 5.10b). Below the FOD of *G. menardii* form 5 ChRM intensities and magnetic properties reveal the presence of another Fe-level (fig. 5.10) at the same stratigraphic position as in section Episcopi (fig. 5.8), which indicates that this is one and the same Fe level.

THE KASTELLI SECTION

The Kastelli section in central Crete shows ChRM intensities of ca. 10-3 A/m in the lower part of the section, and of ca. 10-2 A/m

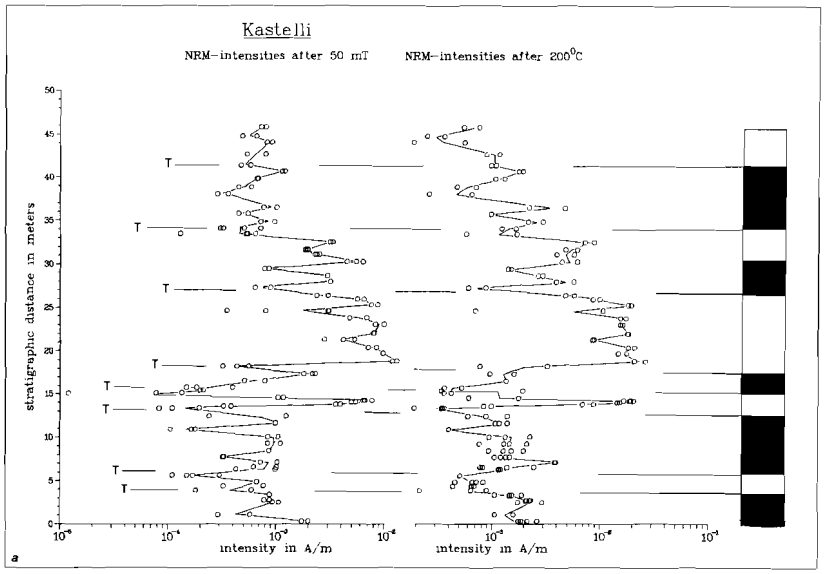

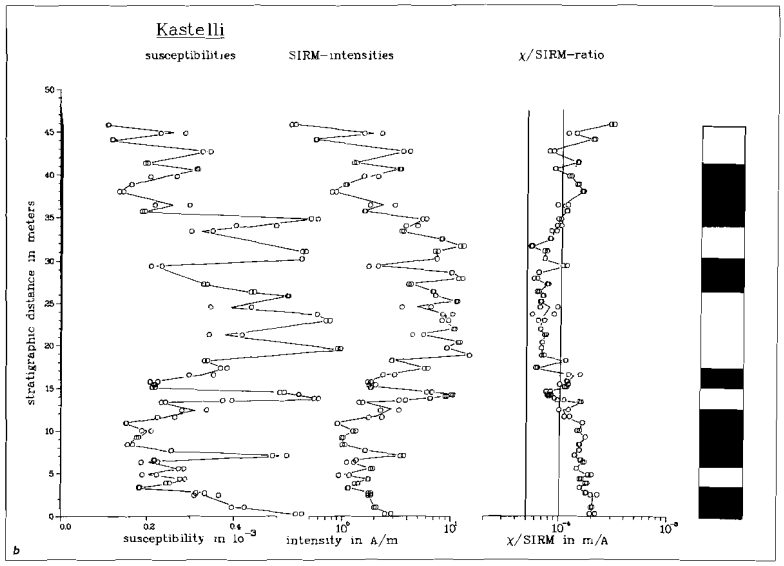

Fig. 5.11 a) NRM intensities after 50 mT and after 200 °C in section Kastelli. b) Susceptibility, saturation IRM and X/SIRM ratio in section Kastelli. See also fig. 5.1 caption.

in the middle part , which decreases to less than 10-3 A/m towards the top of the section (fig. 5.11a). These values are of the same order as in the western Cretan sections. The SIRM values are in the

range of 6–12 A/m (in polarity zones C–, D+ and E–) whereas those e.g. in section Potamida 1 are in the range of 2–7 A/m in the corresponding polarity zones. This could be connected with the fact that the accumulation rate in the Kastelli section is lower by almost a factor of two, e.g. due to a relatively lower carbonate production while the terrigenous input of detrital magnetite remains the same. This would produce a increased concentration of magnetite and hence higher ChRM and SIRM intensities.
The X/SIRM ratio in the middle part of the section (fig. 5.11b) has similar values as in the western Cretan sections, in the range of 0.050 – 0.100 * 10–3 m/A. This ratio increases towards the top of the section from polarity zone F+ upwards, which can be correlated with a similar change in western Crete (sections Potamida 3 and 4, figs. 5.3 and 5.4). This again reflects the increased accumulation rate as found in the western Cretan sections, corresponding with coarser grained magnetite as the carrier of the remanence. In the lower part the X/SIRM ratio increases as well, from polarity zones B+ and A– downwards; this increase is also observed in section Skouloudhiana and at similar chronostratigraphic levels, i.e. with respect to the same polarity zones.

THE FALCONARA SECTION

In figure 5.12a the intensities of the total NRM and of the NRM after heating to 100 oC of section Falconara (Sicily) are shown. Generally some 20–40% of the total NRM survives heating to 100 oC except in the middle part of the section and except at some irregular levels. The fact that only 20–40% of the total NRM remains supports the existence of a goethite component, as already indicated by the demagnetization results and the IRM acquisition curves (figs. 3.50, 3.51). The marls of the diatomite–marl sequence in the top of the section show intensities that are one order of magnitude lower than in the clays and marls in the part below and throughout this sequence only 20% of the total NRM remains after heating to 100 oC. The low and constant coercive forces (40 mT) of these marls suggest, in combination with the IRM acquisition curves (see e.g. SF 50 1A in fig. 3.51; see also fig. 3.50f) that large-grained, multi-domain magnetite is the carrier of the predominantly viscous magnetization.

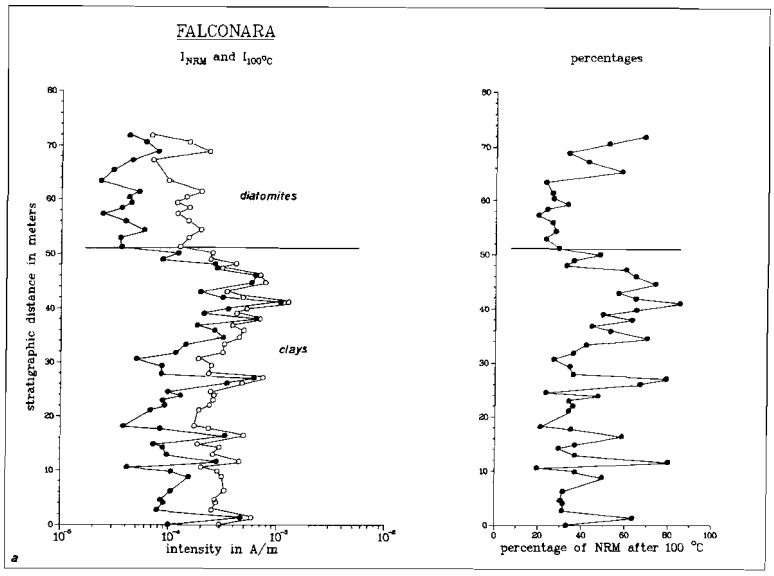

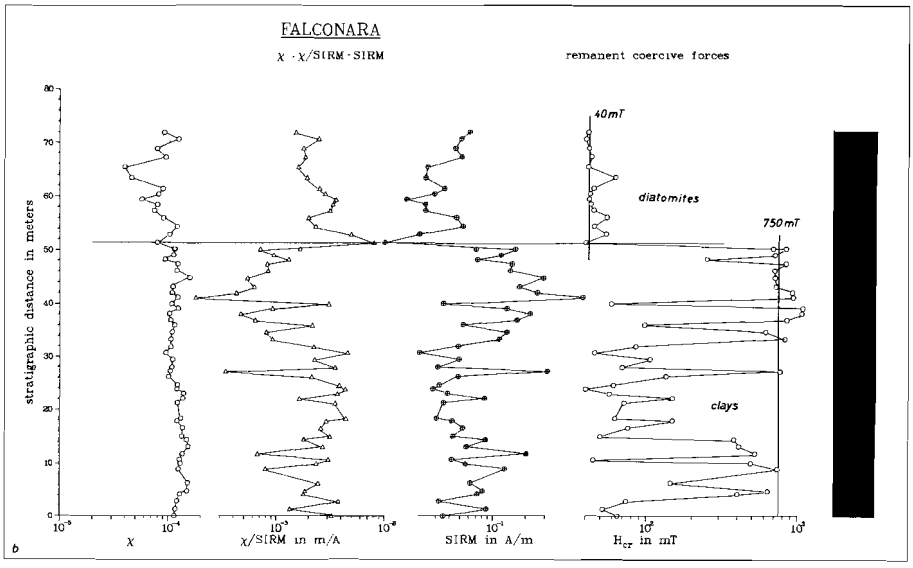

Fig. 5.12 a) Total NRM intensities and NRM intensities after treatment with 100 °C in section Falconara. The plot on the right gives the intensities of the NRM after 100 C as a percentage of the total NRM. b) Susceptibility, maximum IRM (=IRM in a direct field of 2 Tesla), X/SIRM' and remanent coercive force in section Falconara. The change in lithology is apparent both in the intensities and in the rock magnetic parameters (and especially in the H_{cr} values).

The susceptibility appears to have a rather constant and low value throughout the section. The maximum IRM - saturation is not reached in most cases - varies more strongly and is much lower than in the Cretan sections (fig. 5.12b). Since susceptibility values are rather constant, the values of the X/SIRM ratio are proportional to the reciprocal of the maximum SIRM values. This X/SIRM ratio is generally higher than 0.5 * 10-3 m/A and goes as high as 5.0 * 10-3 m/A (fig. 5.12b). Magnetites generally show values less than 1.0 * 10-3 m/A (Hartstra, 1982b) and hematites show values of 2-6 * 10-6 m/A and are largely independent of grain-size (Dankers, 1978). Typical values for goethite are not known. However, values for the X/SIRM ratio in the Falconara section may not reflect changes in magnetic mineralogy reliably since saturation is not often reached. Especially in the case of goethite, the IRM acquired in a field of 2 T is probably only a part of its SIRM; hence the ratio X/IRM(2T) is in fact determined, and this ratio is greater than the actual X/SIRM ratio.

Remanent coercive forces have rather constant values (fig. 5.12b) of ca. 40 mT in the diatomite-marl top of the section (as discussed above), but the clays show strongly varying Hcr values: predominantly high values of ca. 750 mT even with levels showing values higher than 1000 mT in the middle part of the section. Values alternating between 50-150 mT on the one hand and between 400-700 mT on the other hand are found in the lower part of the section. Generally, the Hcr values indicate a highly variable magnetic mineralogy; this is also indicated by the results inferred from the IRM acquisition curves (fig. 3.45). This variable magnetic mineralogy corresponds only partly with the lithology of the section.

In the upper part the magnetic properties are rather constant for all sample levels and for all samples from the same level which reflect the uniform appearance of the light-brown marls alternating with diatomites. The magnetic properties of the middle and especially the lower part of the section correspond less with the lithology but are more likely to be governed by the extent of oxidation (weathering) of individual specimens and depend on the distance from a joint; magnetic properties of specimens even from the same core may differ widely.

It is clear that intensive fracturing and jointing in the Falconara section has caused intensive weathering, resulting in a complex magnetic

mineralogy which carries various types of secondary remanences, all of which have a normal and recent polarity.

CONCLUSIONS

There are many rock-magnetic parameters that can be determined in order to gain insight in the magnetic properties of the studied marine clays from Crete and Sicily.
The X/SIRM ratio appears to be very useful, since it depends on the grain-size of the magnetic minerals and hence is a direct estimate of the grain-size variations and thus most probably of the variations of the accumulation rate. It is important to know any such variations if one wants to correlate polarity reversal sequences with the polarity time scale solely on the basis of the polarity patterns, and not on existing (biostratigraphic) correlations. The latter method inevitably leads to circular reasoning.
A considerable advantage of the X/SIRM ratio is that it is easily and quickly determined; the latter applies to a lesser extent to the remanent coercive force Hcr. However, it may be necessary to determine also the Hcr to give additional information on the magnetic mineral content, since the X/SIRM ratio may not be conclusive.

In the Cretan sections it has been established that in general the studied rock-magnetic parameters are very constant; consequently the accumulation rates have been very constant and thus the correlations with the polarity time scale based on sea-floor anomalies are valid.

chapter six

NRM DIRECTIONS AND ANISOTROPY

INTRODUCTION

In the present study the emphasis has been on the magnetostratigraphy of part of the Upper Miocene in the Mediterranean. The detailed analysis of the total natural remanent magnetization (chapter 3) has shown that the the characteristic remanent magnetization directions are of primary origin, particularly those of the western Cretan sections and of section Kastelli in central Crete. The polarities of the ChRM in those sections thus represent the polarity of the geomagnetic field at the time of deposition and have made it possible to determine accurately polarity zones which can be used for a magnetostratigraphic correlation (chapter 4). The fact that the polarity reversal sequences studied display identical, correlatable patterns in the different sections emphasizes the primary origin of the ChRM.

The detailed analysis of the total NRM has yielded not only the polarity but also the direction of the ChRM. Since the sections have been sampled in appreciable detail it is therefore possible to calculate an accurate and reliable mean direction per polarity zone. The established magnetostratigraphic correlation makes it possible to determine whether and to what extent changes in these mean directions occur, both geographically as well as chronostratigraphically.

With thermal demagnetization one can clearly separate the secondary and primary magnetization component whereas with alternating field (AF) demagnetization this is not always possible (cf. chapter 3). Since, moreover, thermal demagnetization produces more consistent results than AF demagnetization, only ChRM directions derived from thermal demagnetization have been used for the directional studies. Furthermore, directions derived from demagnetization dia-

grams which showed appreciable scatter or viscous remanences at higher temperatures - mostly close to a polarity reversal horizon or in the top of a section - or which did not show a linear decrease to the origin have not been used. The determination of ChRM directions is based on fitting a line through more than three and up to eight points on the demagnetization diagram, including the origin.

In addition to the ChRM directions, we have also determined the (low field) anisotropy of magnetic susceptibility throughout a number of sections.
The orientation of the magnetic grains determines the magnetic fabric of a sediment which is reflected in the anisotropy of the magnetic susceptibility. The anisotropy of magnetic susceptibility may therefore yield information concerning the magnetic fabric of a sediment and hence about processes which have played a role during or after deposition. Furthermore, tectonic stress may affect the original sedimentary fabric and cause an overprint of tectonic fabric (e.g. van den Ende, 1977).

DRM AND ANISOTROPY

A number of factors influence the process by which magnetic grains are arranged in a sediment, both during and after deposition of those grains, resulting in a depositional remanent magnetization (DRM) and an anisotropy of susceptibility. Three types of forces are of importance in setting and aligning the magnetic grains: the geomagnetic field acting on the remanent or induced magnetization of the grains, hydrodynamic forces such as depositional or bottom currents rotating the grains and gravitational forces producing the deposition of the grains.
There are several forces which randomize the alignment of magnetic minerals (see King and Rees, 1966); Brownian movement is the most important of these.

The relative importance of gravitational, hydrodynamic and magnetic forces with respect to the grain-size of the magnetic minerals imposes restrictions on the effect of these forces. For a more detailed analysis of the subject, the reader is referred to articles

by King and Rees (1966) and Rees and Woodall (1975). In summary, it appears that Brownian movement tends to randomize (magnetic) grains of less than 1 um and its influence increases with decreasing grain-size: for grains smaller than 0.1 um its randomizing effect may be greater than the effects of the orienting forces. Magnetic forces (the ambient geomagnetic field) are of paramount importance in orienting grains less than ca. 10 um. For larger grains, gravitational forces may (partly) overcome magnetic forces and will produce a tendency to foliation. Therefore, gravitational forces acting on the grains during setting may give rise to an 'inclination error' and/or a 'bedding error' (King, 1955; King and Rees, 1966). Hydrodynamic forces increase relative to magnetic forces with increasing grain-size and are of the same order of magnitude for grains larger than 100 um. For grains smaller than 10 um hydrodynamic forces are less than magnetic forces by more than one order of magnitude (cf. Rees and Woodall, 1975).

It should be noted that magnetic grains giving rise to susceptibility anisotropy are not necessarily the same as those responsible for the DRM (represented by the ChRM as determined in this study). The work of e.g. Rees (1961) suggests that the two may be treated independently. Hence, the DRM may have recorded reliably the geomagnetic field at the time of deposition, while at the same time the anisotropy of magnetic susceptibility may be a useful indicator of paleocurrent directions.

Generally it is assumed that the DRM resides in small (magnetite) grains, whereas the larger grains are responsible for the susceptibility anisotropy. This is in keeping with the observations made on laboratory-deposited sediments (Rees, 1961) that hydrodynamic forces generally deflect remanence directions by less than approximately 15 degrees from the magnetic field direction, whereas directions of the axis of maximum susceptibility may be deflected as much as 60 degrees and more. The experiments of Bressler and Elston (1980) on silts and fine sands also show deflections of the remanence directions of less than 10 degrees due to hydrodynamic forces.

Although it is usually assumed that DRM and susceptibility anisotropy reside in grains of different size, it should be noted that anisotropy may also arise from the distinct distribution of small

grains. A possible mechanism involved is post-depositional gravitational compaction which produces a magnetic foliation parallel to, or a minimum susceptibility perpendicular to the bedding plane. Gravitational compaction is in fact a form of deformation with the compression axis vertical and it is known that strong tectonic deformation produces a minimum susceptibility direction parallel to the shortening direction (Graham, 1966), while the remanence directions remain undisturbed (van den Ende, 1977).

The nature of the Cretan sediments (clays) indicates that compaction has most certainly taken place. The carriers of the ChRM in the Cretan sections consist of very fine grained (single domain) magnetite (cf. chapter 3, 5). Furthermore, the results given in chapter 5 show that the X/SIRM ratio that was determined results mainly from (possibly less) fine grained magnetite (Hartstra, 1982b). Therefore it seems likely that the susceptibility anisotropy in the Cretan sections is due to the distribution of these smaller grains rather than due to larger (multi-domain) grains.

ChRM DIRECTIONS

The ChRM directions of six sections - Potamida 1, 3, 4, Skouloudhiana, Kotsiana 2 and Kastelli - were established. The ChRM directions of other sections were not used for several reasons. One reason is that the directions did not satisfy the reliability criteria, e.g. the demagnetization results of section Kotsiana 1 showed considerable scatter (fig. 4.5). Another reason is that the directions showed unwanted bias towards specific sample levels (or parts of the section) which yield good results, whereas other levels or parts of the same section did not meet the directional criteria (e.g. section Episcopi). Therefor the ChRM directions will not reliably represent possible changes in the direction of the geomagnetic field (or directional changes due to the sedimentary-tectonic history) throughout a polarity zone or a section.

When the mean direction per polarity zone is being determined the specimens are given unit weight. The mean declinations (D) and inclinations (I) are listed in table 6.1 together with the precision parameter (k), the angle of confidence (a95) and the sum of the

unit vectors per specimen (R) according to Fisher (1953). In figure 6.1 the ChRM directions per section are shown together with the mean declination per polarity zone. All directions have been corrected for bedding tilt.

Table 6.1 Mean directions of the individual polarity zones in the six sections studied in this chapter. The number of specimens is given (N), as well as the mean declination (D), the mean inclination (I), the precision parameter (k), the cone of confidence at the 95% level (a_{95}) and the sum of the unit vectors (R). Furthermore, it is indicated whether or not an direction of a polarity zone has a common true mean direction (ctmd) with polarity zone D+.

section		N	D	I	k	a_{95}	R	ctmd
Potamida 1	C-	28	188.3	-45.0	109	2.6	27.75	no
	D+	12	354.8	49.3	106	4.2	11.90	
	E-	10	189.5	-43.3	149	4.0	9.94	no
	F+	6	6.0	49.1	111	6.4	5.95	yes
Potamida 3	D+	8	349.1	37.0	118	5.1	7.94	
	E-	13	180.5	-39.6	157	3.3	12.92	no
	F+	7	2.6	41.0	76	7.0	6.92	no
Potamida 4	C-	22	168.3	-45.8	93	3.2	21.77	no
	D+	15	329.4	41.4	62	4.9	14.77	
	E-	4	167.0	-48.1	253	5.8	3.99	no
	F+	7	341.0	32.6	89	6.4	6.93	no
Skouloudhiana	A-	3	159.4	-43.6	287	7.3	2.99	no
	B+	5	346.3	44.8	121	7.0	4.97	no
	C-	14	163.7	-46.2	55	5.4	13.76	no
	D+	9	327.4	37.9	120	4.7	8.93	
Kotsiana 2	C-	25	166.0	-36.1	117	2.7	24.80	no
	D+	10	339.5	43.0	120	4.4	9.93	
	E-	4	164.4	-42.1	242	5.9	3.99	yes
Kastelli	A-	8	126.0	-37.8	271	3.4	7.97	yes
	B+	2	313.9	33.1				
	C-	22	126.7	-38.7	209	2.2	21.90	yes
	D+	6	310.0	43.2	90	7.1	5.94	
	E-	6	124.3	-36.1	209	4.6	5.98	no
	F+	8	318.8	43.3	92	5.8	7.92	yes

One notices immediately that the mean declinations of the reversed polarity zones (A-, C-, E-) in the western Cretan sections are antiparallel with respect to the mean declination(s) of polarity zone(s) B+ and/or F+ within the limits determined by the cone of confidence of the mean directions (cf.table 6.1). The same applies for the mean inclinations of the normal and reversed polarity zones, with the exception of zone F+ in section Potamida 4.

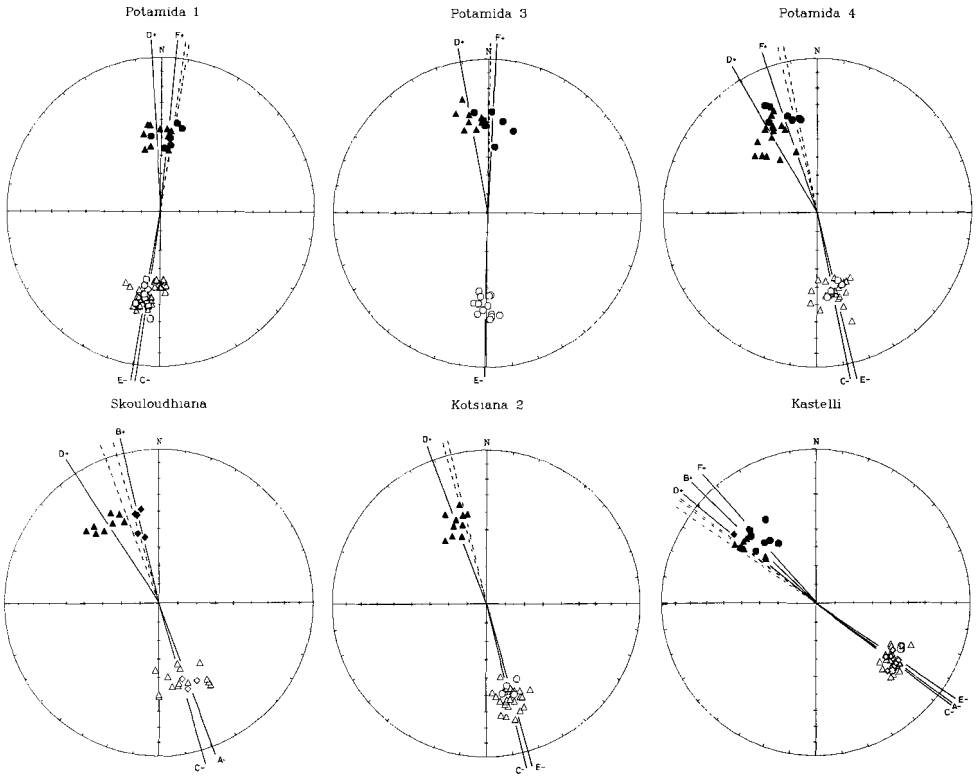

Fig. 6.1 Equal area projection of ChRM directions of sections Potamida 1, 3, 4, Skouloudhiana, Kotsiana 2 and Kastelli. Open (solid) diamonds denote ChRM directions from polarity zone A- (B+), open (solid) triangles those from C- (D+) and open (solid) circles those from E- (F+). The mean declination per polarity zone is indicated by solid lines.

This is illustrated even more clearly in figure 6.2 in which the mean directions of the reversed polarity zones have been inverted in order to facilitate comparison, and in which the cones of confidence of the polarity zones are shown. Furthermore, it appears that in all sections the mean declination of polarity zone D+ has a distinct westerly offset with respect to the mean declination of polarity zones B+ and F+ (fig. 6.1) and in the western Cretan sections also with respect to the (inverted) mean declinations of the reversed polarity zones.

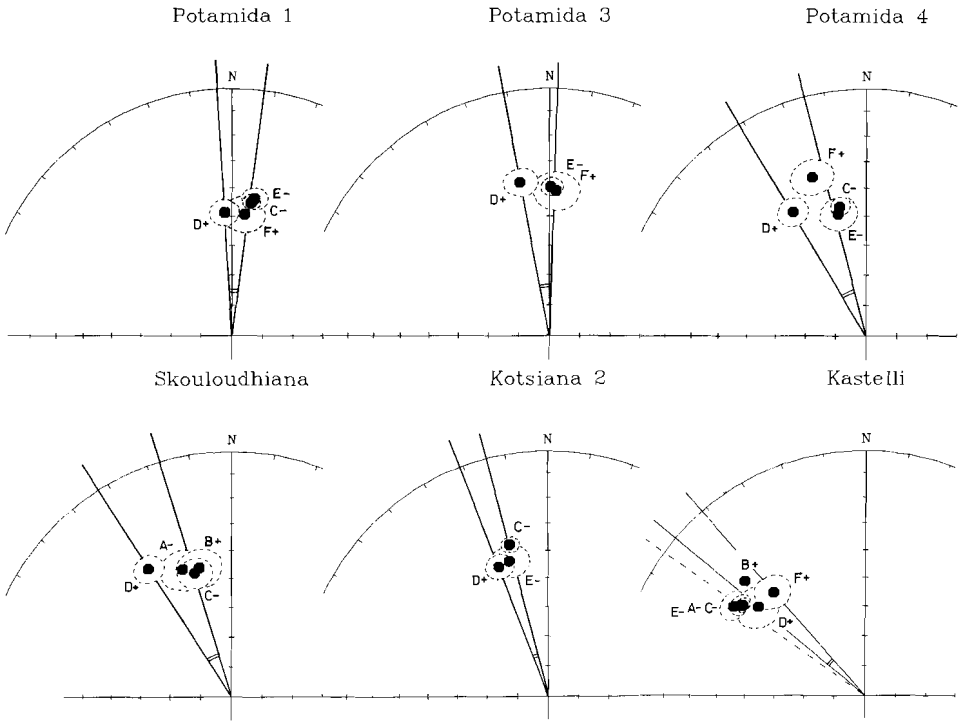

Fig. 6.2 Equal area projection of the mean ChRM directions per polarity zone, together with their circle of confidence (a_{95}). Solid lines represent the mean declination of polarity zone D+ and the mean declination of all other polarity zones together, respectively. Only in section Kastelli do solid lines represent the mean declination of polarity zone D+ and the mean declination of polarity zones B+ and F+ together; the dashed line denotes the mean declination of A-, C- and E- together.

A more exact discrimination of mean directions drawn from Fisher (1953) distributions via several conditional or approximate tests is given by McFadden and Lowes (1981). Testing the hypothesis that two populations (with a common precision parameter) share a common true mean direction (ctmd) for the results of the Cretan sections gives some more information about the significance of the mean directions of the polarity zones. If two populations do not share a common precision parameter, an approximate test may be used (McFadden and Lowes, 1981), but this appeared to be hardly necessary for the

Table 6.2 Mean directions of all specimens outside polarity zone D+. Reversed directions have been inverted, specimens are given unit weight. Only for section Kastelli have the mean directions of all reversed (inverted) and all normal specimens (minus those of D+) been listed separately. See also table 6.1 caption.

section		N	D	I	k	a_{95}	R	ctmd
Potamida 1	C-	44	8.3	45.2	114	2.0	43.62	no
	D+	12	354.8	49.3	106	4.2	11.90	
Potamida 3	all	20	1.2	40.1	119	3.0	19.84	no
	D+	8	349.1	37.0	118	5.1	7.94	
Potamida 4	all	33	346.3	43.4	66	3.1	32.51	no
	D+	15	329.4	41.4	62	4.9	14.77	
Skouloudhiana	all	22	343.7	45.5	73	3.6	21.71	no
	D+	9	327.4	37.9	120	4.7	8.93	
Kotsiana 2	all	29	345.8	36.9	118	2.5	28.76	no
	D+	10	339.5	43.0	120	4.4	9.93	
Kastelli	nor	10	317.7	41.3	82	5.4	9.98	yes
	rev	36	306.1	38.1	222	1.6	35.84	no
	all	46	308.5	38.8	120	1.9	45.63	yes
	D+	6	310.0	43.2	90	7.1	5.94	

Cretan populations. It appears that all polarity zones in in each of the sections (except for zone D+) share a ctmd (with the exception of F+ in Potamida 4; see also fig. 6.2). In other words, normal and reversed directions are anti-parallel within statistical limits. This emphasizes the fact that secondary (normal) magnetizations have been totally removed and that the ChRM directions have been determined correctly.

The mean direction (md) of D+ has been tested for a ctmd with the md's of the other polarity zones in the same section. To this end the md of the reversed polarity zones have been inverted. Only in section Potamida 1 does the md of D+ share a ctmd with the md of F+ and in section Kotsiana 2 with the md of E- (table 6.1; see also fig. 6.1), merely because of the limited number of specimens and the resulting larger a95. In all other cases in the western Cretan sections there is no ctmd of D+ with the md's of other polarity zones, either of normal or reversed polarity. On the other hand, the md's of the polarity zones other than D+ show a ctmd in each western Cretan section (with the exception of F+ in section Potamida 4 due to its low inclination). One is therefore justified in comparing per section the md of D+ with the md of the individual specimens from

all other polarity zones together. It then appears that in the western Cretan sections the md of D+ does not share a ctmd with these md's; this implies that the observation that polarity zone D+ shows a significant westerly offset is substantiated by the statistical tests.

Section Kastelli shows a somewhat different picture (figs. 6.1, 6.2). Reversed directions are not anti-parallel to the normal directions; this result differs from the western Cretan results.

The mean declination of polarity zone D+ shows a westerly offset with respect to the mean declination of polarity zones B+ and F+ together, but not with respect to the (inverted) mean declination of the reversed polarity zones (dashed line in fig. 6.2). The md of D+ shares a ctmd with the polarity zones A-, C- and F+, but not with zone E- (the md of B+ is based only on two directions and no test has been done on a ctmd of this polarity zone with D+ (see table 6.1). If we follow the same procedure as in the western Cretan sections and compare the md of D+ with the md of the individual specimens of all polarity zones together, we find that the md of D+ does share a ctmd with the md of all other specimens (table 6.2).

In addition to the generally observed declination offset of the mean of D+ some other interesting features can be seen in the Cretan sections (figs. 6.1, 6.2). The mean declination is different for every section. The declinations of section Potamida 1 imply a slight clockwise rotation of 8.3 + 2.0 degrees, whereas the results of section Potamida 3 do not deviate significantly from N-S: 1.2 + 3.0 degrees. The declinations of sections of Potamida 4, Skouloudhiana and Kotsiana 2 all show a clearly recognizable anti-clockwise rotation of approximately 15 degrees. Section Kastelli shows the largest rotation found in Crete: more than 40 degrees. A general picture of the Cretan ChRM directions is given in figure 6.3 in which the mean directions of all polarity zones are shown.

The mean inclination is consistently lower than the inclination of the geocentric axial dipole field (55 degrees) for the present latitude of Crete, ranging from 35 to approximately 50 degrees and corresponds with an average 'inclination error' of ca. 15 degrees. There is no consistent pattern with respect to polarity; for in-

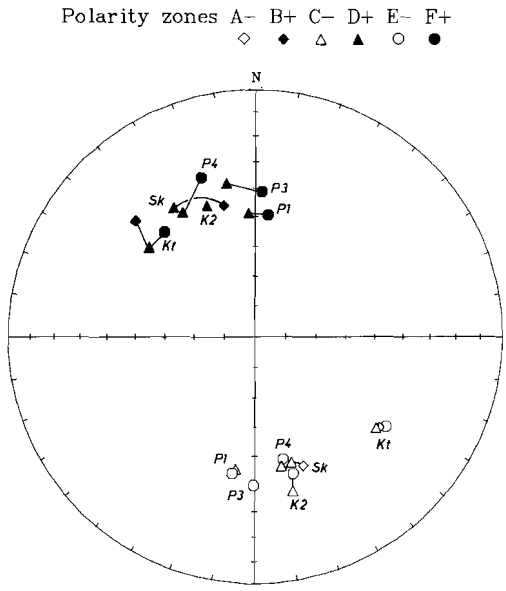

Fig. 6.3 Equal area projection of the mean ChRM directions per polarity zone of all sections. P1,3,4 = Potamida 1,3,4; Sk = Skouloudhiana; K2 = Kotsiana 2; Kt = Kastelli. See also fig. 6.1 caption.

stance in section Potamida 1 the inclinations of the reversed polarity zones seem to be somewhat shallower, but the difference is not significant: polarity zones E- , C- and F+ share a ctmd. A ctmd is found for all polarity zones except D+ in all sections with the exception of zone F+ in section Potamida 4. This zone shows an inclination as low as 33 degrees and it has no ctmd with the other polarity zones in this section.

Only in section Potamida 4 is there a significant difference between the inclination of polarity zone F+ and those of the other polarity zones in the section. The mean inclination of F+ is as low as 33 degrees, much lower than is usually observed (cf. table 6.1). It should be remembered that a fault was observed in the upper part of section Potamida 4, resulting in a 'shortening' of polarity zone E-; this may have been caused by rotation on an inclined (cylindrical) normal fault. In other words, gravity sliding may have produced a rotation about a near-horizontal axis, which is difficult to notice in the dense and homogenous clay.

Such a mechanism would explain the lower inclinations, but the declination would exhibit no or little change, depending on the strike of the fault surface and a (slight) dip of the rotation axis.

The declinations

The various sections show consistent differences in the direction of their mean declinations. These differences show up in the mean declinations of the individual polarity zones (fig. 6.1, table 6.1) as well as in the mean declinations of all specimens per section together (fig. 6.2, table 6.2).

It has been argued, because the directions are antiparallel, that these deviations are not due to insufficient removal of the secondary magnetization component. Hence they must have been caused by some geological phenomenon instead of being artefacts of the demagnetization analysis.

The effects of hydrodynamic and gravitational forces and of the geomagnetic field on the orientation of magnetic minerals have been outlined above. Depositional currents may cause a deflection of the declination towards the current, the amount of deflection increasing with current velocity and inclination of the ambient field (e.g. Rees, 1961; Bressler and Elston, 1980). On the other hand, Rees (1961) pointed out that it was mainly the ambient magnetic field which orients the very fine magnetic grains (less than ca. 1-10 um). This would prohibit a deflection due to hydrodynamic forces. Rees and Woodall (1975) calculated approximate values for gravitational, hydrodynamic and magnetic couples likely to act on magnetic grains of several grain-sizes. They found that for grains smaller than 1 um - which is the grain-size involved in most of the Cretan sections - the magnetic couple due to the remanence of the grains is the main force in aligning these grains. Although in principle a slight influence cannot be ruled out - in fact little is known about the effects of hydrodynamic forces in clays: laboratory experiments are usually performed with silts and fine sands - it seems unlikely that depositional currents will result in offsets of more than a few degrees.

Another possibility is that the observed deviations in the

declination in the Cretan sections are due to local tectonic rotations of the sections rather than to depositional mechanisms. The different degrees of the deviations may indicate that the tectonic rotations have been very local. The Kasteli section shows a rotation of more than 40 degrees (fig. 6.2), which is appreciably more than in the western Cretan sections, which show rotations varying between 8 degrees clockwise rotation in section Potamida 1 and some 15 degrees counterclockwise rotation in sections Potamida 4, Skouloudhiana and Kotsiana 2. The larger rotation of section Kasteli may be related to the tectonic history of the basins in central Crete. An analysis of fault-tectonic phases by Angelier (1975) shows that these basins are intensely faulted and that since the Late Miocene initially three main tectonic phases took place, followed by two minor phases of compression and extension, respectively.

Although the same tectonic phases have played a role in the rest of Crete, faulting has been most intense in central Crete. The larger rotation of section Kasteli seems therefore related to the intensity of tectonics. The observed rotations may be either apparent rotations due to the successive phases or may be local rotations due, for instance, to the Pleistocene period of compression. The latter phase resulted in subvertical transversal faults (decrochements) with dextral (NNW-SSE) as well as sinistral (NNE-SSW) displacements (Angelier, 1975). From the results of Angelier (1975), Mercier et al. (1979) it can be seen that in Crete the directions of tension change from NE-SW in the Late Miocene and NNW-SSE in the Pliocene to NW-SE in the Middle Pleistocene to Recent. They wonder whether such changes are due to slight counter-clockwise rotation of the direction of tension, the material (in this case Crete) being stable, or to clockwise rotation of the material (the direction of tension being stable). Although it should be stressed that the rotations observed in Crete may be of local importance only, the predominance of counter-clockwise rotations of material suggests a completely different mechanism. A possible solution may be that a counter-clockwise rotation of Crete (if it occurred at all) was accompanied by an even greater counter-clockwise rotation of the extensional regimes.

The Inclinations

In general the inclinations are approximately in the range of 40–45 degrees, hence they show values which are 10–15 degrees lower than the inclination values of ca. 55 degrees of the geocentric axial dipole field at the present latitude of the sections.

There are some differences in inclination, both between the mean inclinations of the polarity zones in a section as well as between the mean inclinations per section. However, statistical tests (McFadden and Lowes, 1980) show that the inclinations of polarity zones per section do not differ significantly. Following the same line of reasoning as for the deviations of the declination, it can be argued that the generally low values of the inclinations – low with respect to the inclination of the geomagnetic field at the present latitude of Crete – are not a consequence of the insufficient removal of the secondary magnetization component. The low inclination may be due to an 'inclination error', as proposed by King (1955). A somewhat different explanation for this inclination error was given by Griffith et al. (1960), but both proposed models are based on the same process, i.e. gravitational couples interfere with the magnetic couples at the moment of deposition. Calculated, approximate values of the gravitational couples likely to act on magnetic particles show that this couple is stronger than the magnetic couples arising from the earth's magnetic field, for grain-sizes larger than 1 um (Rees and Woodall, 1975). Since the grain-size involved in Cretan sections is smaller than 1 um, one would expect the ambient magnetic field to predominantly align the magnetic grains and hence no inclination error. In accordance with this, no inclination errors have been found, for example, in deep-sea sediments (e.g. Keen, 1963)

The lower inclination may be a consequence of an off-centred dipole geomagnetic field. Wilson (1971) and later McElhinney (1973), the latter using twice as much data, found that Late Tertiary paleomagnetic poles lie on the 'far side' of the pole with respect to the site longitude, whereas more recent paleomagnetic poles coincide with the geographical pole, i.e. the pole according to a (time-average) geocentric axial dipole field.
Wilson (1971) suggested that an important change in the configu-

ration of the geomagnetic field has taken place over the last few million years, i.e. a late Tertiary off-centred axial dipole versus a more recent geocentric axial dipole. This would agree with the observation that in the Cretan results the inclination of the younger secondary component is steeper than the inclination of the primary component. However, Laj et al. (1982) argue that their results for similar marine sediments in the Aegean region, of Miocene as well as Pliocene Age, do not indicate any correlation between the presence of the inclination error and the age or geographical position of the formation.

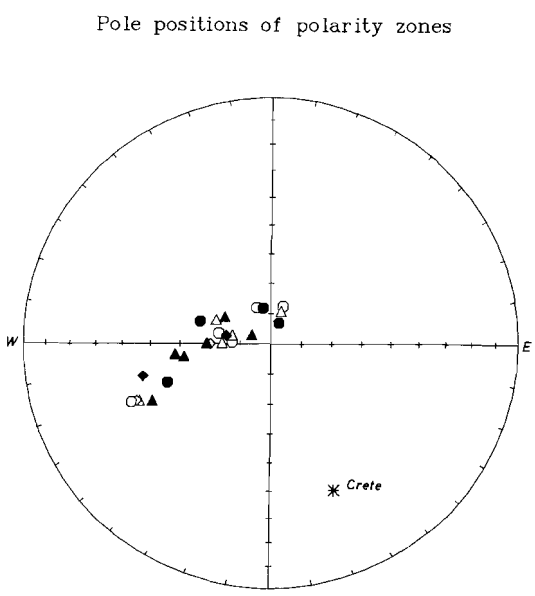

Fig. 6.4 Equal area projection of pole positions determined from the directions of fig. 6.3; all pole positions are grouped on the far side of the geographic pole (=centre of the plot) with respect to the site longitude. Asterix denotes the present position of Crete.

A plot of the pole positions per polarity zone shows that they are grouped on the far side of the geographical pole with respect to the site longitude (fig. 6.4) due, of course, to the low inclinations. Moreover, the population of the poles has an elongated shape

with a long axis at right angles to the direction of the site. The same phenomenon has been noticed by van den Ende (1977) in Permian redbeds in the Dome de Barrot. He found, using a chi-square test, that the population of the poles was not according to a Fisher (1953) distribution. After a correction for the inclination error, using the empirical formula which relates the inclination in the sediment to the inclination of the ambient field (King, 1955), the distribution of the poles became Fisherian. However, the method used by van den Ende (1977) has only effect for very low inclination values such as those found in the Permian rocks: any inclination error correction for inclinations in the range of 25-60 degrees produces absolute but not relative changes in inclination and hence the shape of the distribution of the derived paleomagnetic poles will remain essentially the same.

The observed low inclination values could also indicate deposition at lower latitudes and hence a northward displacement of Crete since the Late Miocene. Such a displacement, however, would not be in keeping with the reconstruction of the pattern of motion over the Eastern Mediterranean for the last 13 Ma by Le Pichon and Angelier (1978), in which the Aegean Region has been spreading gravitationally to the SW, in front of advancing Turkey.

An alternative explanation for the inclination error is provided by Laj et al. (1982); they attribute the low values to the compaction of the sediments. According to these authors, the inclination error seems to be related to the carbonate content in the sediment, the error being smaller when the amount of carbonate is high. Although they do not elaborate on the process involved, a possible mechanism may be related to the shape as well as to the properties of the clay minerals, but is independent of the shape of the magnetic grains. Lowrie and Alvarez (1975) attempted to remove the magnetic fractions from clay residues, but noticed that the ferromagnetic grains were strongly attached to the clay minerals. This may be due to electrostatic forces between both types of grains. Because of the platy shape of the clay minerals they will tend to align (horizontally) upon gravitational compaction, or rather, the alignment will increase with respect to the sediment before compaction. The magnetic grains, attached to the clay minerals, will therefore follow the increased alignment and hence display a shallower (more horizontal) inclination or an inclination error.

The deviating declination of polarity zone D+

The westerly deviation of polarity zone D+ in western Crete with respect to the mean declination of the other polarity zones has an average value of approximately 13 degrees (fig. 6.5). An explanation for this phenomenon is not straightforward.

The deviation is found throughout polarity zone D+ and is not due to an offset of specific parts or sampling levels (biasing) or to the occurrence of transitional directions close to a polarity reversal horizon, since the latter have not been included.

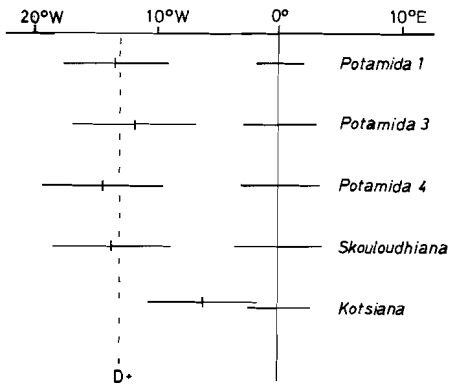

Fig. 6.5 Westerly deviation of polarity zone D+ with respect to the mean declination of the other polarity zones. Bars indicate circle of confidence (a_{95}; cf. table 6.2). Dashed line represents the average offset of the declination of D+ (13^{o}).

Furthermore, it seems unlikely that the deviation is due to different environmental or depositional factors: the magnetic properties (chapter 5) are very constant throughout polarity zones C-, D+ and E- and indicate a consistent and very fine-grained magnetic mineralogy. It was already shown earlier that an influence of depositional currents (hydrodynamic forces) is not probable considering the grain-size involved.

It is known that there are long-term variations of the geomagnetic field of the order of 100,000 years, and that these are probably related to the 100,000 years eccentricity cycle of the

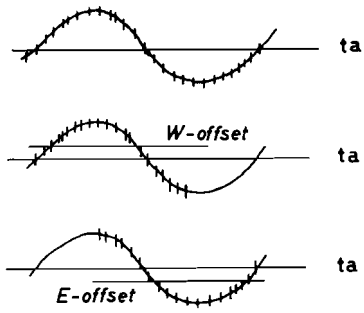

Fig. 6.6 a) Long term variation of the geomagnetic field: regular sampling of a complete cycle yields a true average (ta) direction. b) and c) Effect of the observed average direction if only a part of the period is sampled.

Earth's orbit. If a complete cycle is sampled in a sedimentary succession, the mean direction represents the 'true' average geomagnetic field, provided no biasing is introduced, e.g. due to too small a number of samples (see fig. 6.6a). If only a part of the cycle is sampled, a deviation may be found, depending on which part of the cycle has been sampled (fig. 6.6b,c). Variations of more than 20 degrees have been recorded in the Cretan sections. In fig. 6.7 the average declinations and inclinations per sampling level are plotted together with the a95 for polarity zone C- in section Potamida 1. Especially from the declinations it can be seen that there are significant variations, varying between 180 and 200 degrees. Coincidental sampling of half a cycle may yield an average deviation of more than 10 degrees from the 'true' average. However, since it is known that zone D+ has a duration of ca. 0.2 Ma (chapter four) it should represent two complete cycles of the long-term variation and the detailed sampling at more or less uniform intervals should always result in a 'true' average.

Furthermore, with an average accumulation rate of 4.2 cm/1000 years in the western Cretan sections, one cycle of the long-term variation of 100,000 years takes place in 420 cm of sediment. An average and uniform sampling distance of 40-55 cm (such as was used in a number of sections) means that 8-10 samples per cycle are

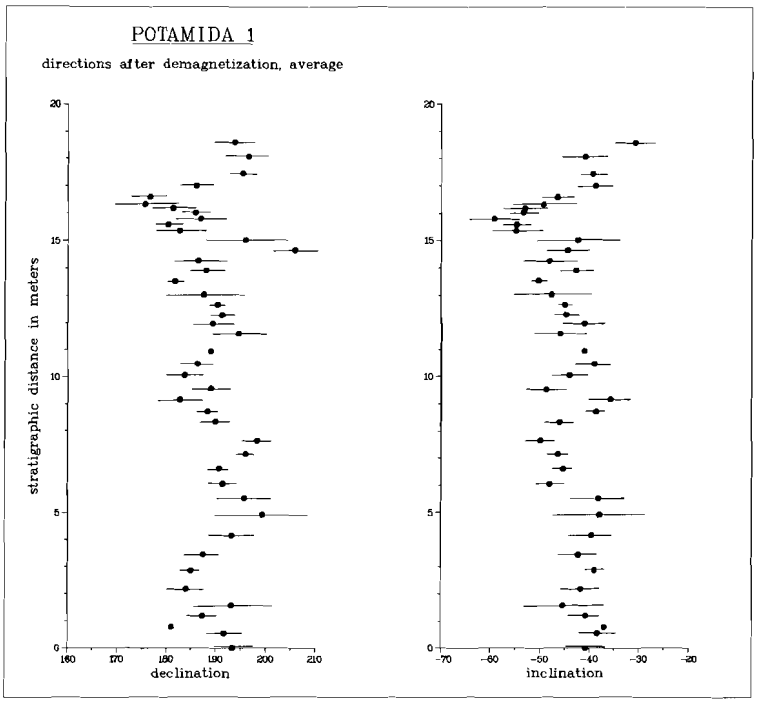

Fig. 6.7 Mean ChRM directions per sampling level of polarity zone E- in section Potamida 1; bars represent a_{95}. In view of the quality of the ChRM directions derived from AF demagnetizationss in this zone and in this section, these directions have been included in the computations. Long-term variations of the geomagnetic field can be seen clearly and are in the order of 20^{o}.

taken. A higher resolution would be preferable to determine more accurately the amplitude and wavelength of such variations, but is more than adequate to determine the unbiased mean directions per polarity zone.

The most probable explanation for the observed offset is that during polarity zone D+ the regional direction of the geomagnetic field has shown a westerly deviation. To our knowledge, no such deviations during a particular polarity zone have been recorded in literature, although it should be noted that no sedimentary sequences have been sampled in such detail. Consequently the recorded deviation of polarity zone D+ must have had a duration of ca. 200,000 years.

ANISOTROPY OF SUSCEPTIBILITY

The anisotropy of the magnetic susceptibility of rocks, described by the axes of maximum (Kmax), intermediate (Kint) and minimum (Kmin) susceptibility, is determined by the magnetic fabric of the rock, which in its turn depends on the orientation of the magnetic grains present. Magnetic susceptibility anisotropies of individual grains are related to the grain shape, directly by shape anisotropy (magnetite, maghemite) or indirectly by magnetocrystalline anisotropy (hematite, goethite and pyrrhotite). The anisotropy of the magnetic susceptibility of sediments is usually due to the shape of magnetic grains and reflects the orientation of these grains. A primary depositional/sedimentary fabric is caused by the (statistical) alignment of these grains by mechanical forces during deposition.

On the other hand, the magnetic grains responsible for the anisotropy of the magnetic susceptibility need not be responsible for the remanence. Hence, the NRM may have recorded reliably the geomagnetic field at the time of deposition and at the same time the anisotropy of magnetic susceptibility may be a useful indicator of paleocurrent directions.

Gravity is the most important force acting on grains larger than 10 um; it results in deflection of (non-spherical) magnetic grains towards the horizontal, and causes a (primary) depositional fabric with Kmin axes normal to bedding and Kint axes randomly dispersed within the bedding plane. In the case of fine grains of less than approximately 10 um, a depositional magnetic fabric is most probably due to post-depositional gravitational compaction, rather than to gravitational settling (which is the case for larger grains.

Hydrodynamic forces tend to align (non-spherical) grains in the direction of the current, causing a grouping of Kmax axes. This can be used as a paleocurrent indicator (Rees, 1961).

Another important factor is that the ambient (geomagnetic) field acts on ferromagnetic grains. Magnetic orientating couples due to the ambient field acting on the induced moment in anisotropic grains dominate hydrodynamic couples for grain-sizes of less than ca. 10 um (Rees, 1961; Rees and Woodall, 1975). Magnetic orientating couples

due to the ambient field acting on the remanence of magnetic grains dominate hydrodynamic couples for grains less than 100 um (in the case of strong remanence such as is carried by magnetite).

The anisotropy of the magnetic susceptibility of one specimen per sampling level has been measured in the sections Potamida 1, 2, 3, Skouloudhiana, Kotsiana 1, 2 and Kastelli. A limited number of specimens were also measured throughout sections Potamida 4, Episcopi and Vasilopoulo.

Table 6.3 Susceptibility and susceptibility anisotropy parameters for ten Cretan sections. Usually one specimen per sampling level has been measured, except in sections Potamida 4, Episcopi and Vasilopoulo, where specimens from regularly spaced sampling levels throughout the section were taken. The number of samples measured are listed (N), as well as the mean bulk susceptibility (X), the lineation (L), the foliation (F), the anisotropy degrees (P and P') and the T-parameter.

section	N	X	L	F	P	P'	T
Potamida 1	94	306	1.0068	1.0372	1.0443	1.0477	0.6894
Potamida 2	61	259	1.0065	1.0438	1.0507	1.0552	0.7376
Potamida 3	45	225	1.0082	1.0359	1.0443	1.0472	0.6254
Potamida 4	14	300	1.0109	1.0459	1.0573	1.0609	0.6124
Skouloudh.	39	228	1.0070	1.0484	1.0558	1.0608	0.7430
Kotsiana 1	36	177	1.0029	1.0342	1.0372	1.0414	0.8394
Kotsiana 2	41	349	1.0068	1.0483	1.0553	1.0605	0.7488
Episcopi	15	334	1.0049	1.0302	1.0352	1.0382	0.7180
Vasilopoulo	9	317	1.0028	1.0387	1.0416	1.0466	0.8650
Kastelli	50	436	1.0069	1.0390	1.0461	1.0498	0.6967

A number of anisotropy parameters can be calculated; Hrouda (1981) lists some 25 examples used in literature. At the paleomagnetic laboratory 'Fort Hoofddijk' several parameters are computed as a standard procedure, among them the lineation L = Kmax/Kint and the foliation F = Kint/Kmin. The degree of anisotropy P' and the T parameter, characterizing the shape of the susceptibility ellipsoid, are calculated according to Jelinek (1981; see also Hrouda, 1981). The anisotropy of magnetic susceptibility tensor is calculated according to a method developed by Jelinek (1977) and Jelinek (1978) statistics are used to determine the mean susceptibility tensor from a number of specimens. An AC bridge (KLY-1) was used for the anisotropy measurements. Hrouda (1982) reports that the principal direc-

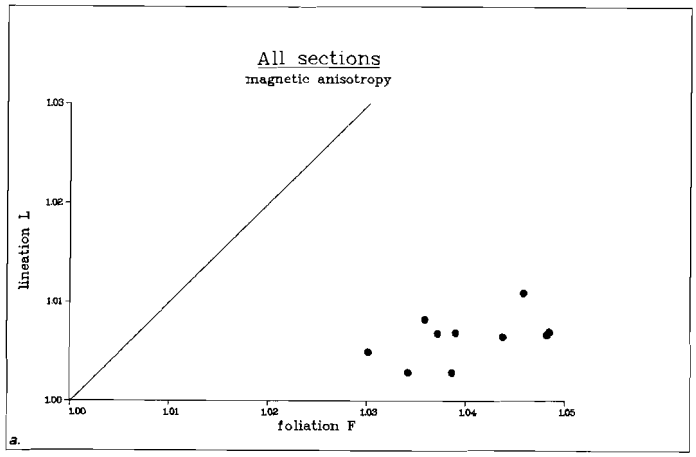

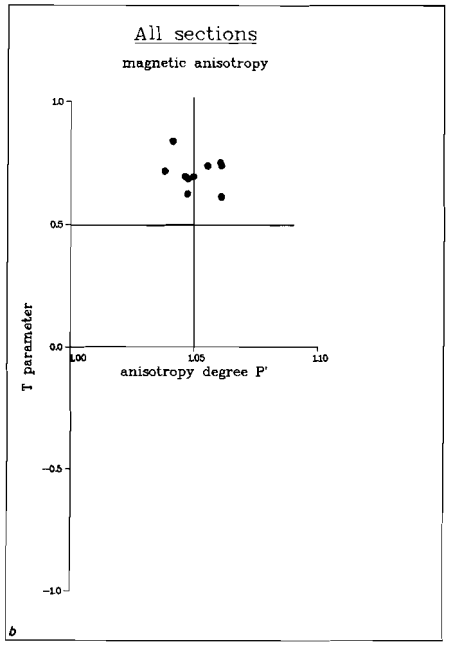

Fig. 6.8 a) Foliation versus lineation of ten Cretan sections, averaged per section. b) Anisotropy degree versus the T parameter, averaged per section.

tions measured on various types of instruments generally agree very well, but the anisotropy magnitudes differ significantly, the KLY-1 AC bridge showing lowest magnitudes. The magnitude difference was

confirmed by measurements on the same set of samples from section Potamida 1, measured both on a Digico spinner (Gif sur Yvette) and on a KLY-1 AC bridge (Utrecht).

Table 6.3 gives the mean susceptibilities and anisotropy parameters of the Cretan sections. The lineation L is plotted versus the foliation F in figure 6.8a and the shape parameter T versus the degree of anisotropy P' in figure 6.8b for all sections. The values of the latter figure correspond with those compiled by Hrouda (1982) for both laboratory deposited and natural sediments.

It can be seen that a clear foliation is present of the order of 3.5 - 5.0 per cent, whereas only a slight lineation is present, generally less than 1.0 per cent. The foliation in each section coincides (virtually) with the bedding plane, i.e. the Kmin axes are entirely or almost perpendicular to the bedding plane, indicating a dominating depositional fabric (fig. 6.9). Although the lineations are very small, there is a distinct and clear grouping of the Kmax axes in most sections. Moreover, the average lineations per sections have the same directions (WNW-ESE) for all sections within their ellipse of confidence (according to Jelinek, 1978; not shown) with the exception of the section Potamida 1, which shows an average lineation perpendicular to those of the other sections.

In figure 6.9 the Kmin and Kmax directions are shown on the lower hemisphere of an equal-area projection before and after correction for bedding tilt (tc). It should be noted that, except in sections Kastelli and Episcopi, tilt correction results in the Kmin axes being deflected from the vertical. Often this is hardly (or not) significant (e.g. sections Potamida 2, Skouloudhiana), but a distinct deflection results especially in the Kotsiana sections.

DISCUSSION

Before we discuss the directions of the principal axes of susceptibility, it should be noted that for fine grains of less than approximately 10 um, magnetic orientating couples (due to susceptibility anisotropy in individual grains) dominate hydrodynamic couples during deposition (Rees and Woodall, 1975). This is similar to the process which occurs with magnetic couples due to particle

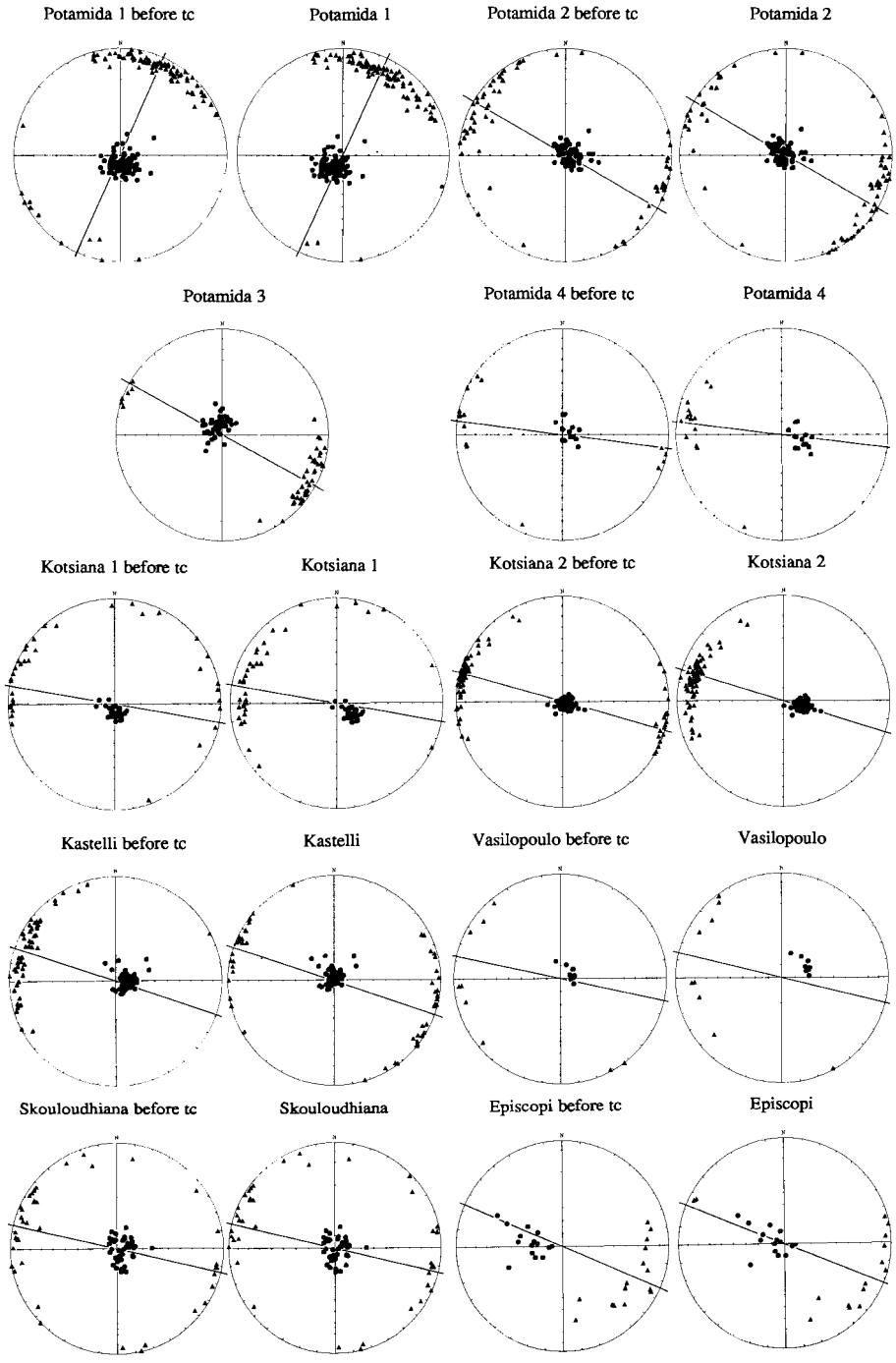

Fig. 6.9 Equal area projection of the directions of the maximum (triangles) and minimum (circles) susceptibility axes of ten Cretan sections, before and after bed ding tilt correction (tc). A predominantly depositional magnetic fabric is observed in all sections. Solid lines denote the average lineation direction; except in section Potamida 1 these directions are all WNW-ESE, corresponding to a recent extensional tectonic regime direction.

remanence, except that such couples are more than an order of magnitude stronger than those due to anisotropy.

As was pointed out above, considering the grain-sizes involved, hydrodynamic couples were not dominant in aligning the grains responsible for the NRM. However, since the magnetic grains giving rise to anisotropy of magnetic susceptibility need not be responsible for the remanence, it may be that gravitational and hydrodynamic forces did play a role in aligning (a part of) the magnetic minerals. On the other hand, the results from chapter 5 indicate that the observed susceptibility is dominated by fine-grained magnetite in major parts of the Cretan sections. If we assume for the time being that the lineations are due to hydrodynamic forces, it follows that, according to the model developed by Granar (1958) and the results obtained by Rees (1961), a (depositional) current should have been present during deposition in a roughly E-W direction in all sections except Potamida 1. This is in conflict with sediment transport directions for most of the sections derived from detailed stratigraphic studies (Meulenkamp, 1979), which indicate paleocurrents mainly towards the north. In the Kastelli section a paleocurrent direction towards the south has been found (Meulenkamp, personal communication).

A more likely explanation for the observed lineations is that these are due to tectonic deformation. The magnetic fabric appears to be a very sensitive indicator of deformation (Crimes and Oldershaw, 1967) and the ellipsoid of the anisotropy of magnetic susceptibility changes shape during progressive deformation of a sediment with an originally depositional fabric (Graham, 1966). Simulation experiments by van den Ende (1977) show that the first stage of deformation quickly results in the Kmax axes being oriented perpendicular to the compression (or parallel to the extension). Initially, the Kmin axis remains perpendicular to the bedding but in later stages becomes reoriented parallel to compression. The initial stages of deformation described above can be recognized in the Cretan sections: there is a small, but persistent lineation (WNW-ESE) in all sections except Potamida 1. The direction of this lineation is virtually parallel to the extensional tectonics in Crete for the Middle Pleistocene to Recent period as deduced by Mercier (1977) and Angelier (1977), on the basis of an analysis of

the tectonic deformation of the Aegean Arc. The direction of the extension agrees with the results of fault plane analysis determined from seismic focal mechanisms (Ritsema, 1973, 1974).

In almost all sections the Kmin axes are deflected from the bedding pole; only the Kmin axes in sections Kastelli and Episcopi are absolutely perpendicular to the bedding plane (fig. 6.9). In most studies deflections of less than 15 degrees are considered as normal for a sedimentary fabric (see Hrouda, 1981 and references therein), but considering the detailed and consistent results (e.g. section Kotsiana 2 in figure 6.9) it is believed that these deflections are not coincidental. Tectonic deformation of the original depositional magnetic fabric could explain in principle the observed slight deviations of the Kmin axes from the pole of the bedding. Tectonic deformation has probably reached the phase when the Kmin axes start to be affected (cf. van den Ende, 1977).

One exception can be seen in figure 6.9: the lineations observed in section Potamida 1 are perpendicular to the lineations observed in the other sections (fig. 6.9). Close to the Potamida 1 section (within 100 metres) a large and approximately NNE-SSW running fault is observed. Apparently this fault dominates the magnetic fabric of the rock in its vicinity.

It is emphasized that before the most recent tectonic (extensional) phase reoriented the Kmin axes, these axes need not have been perpendicular to the (original and depositional) bedding plane, but might have been affected by earlier tectonic phases. The magnetic fabric of rocks can reveal only the most recent tectonic phase that is acting or has acted on these rocks, but it is rarely able to reveal the history of the subsequent tectonic phases which may have altered the magnetic fabric repeatedly.

It can be concluded, however, that the observed anisotropy of magnetic susceptibility reflects primarily a depositional fabric. The observed slight but persistent lineations are a result of - probably recent and extensional - tectonic deformation, and are not due to depositional currents.

REFERENCES

Alvarez W., Arthur M.A., Fisher A.G., Lowrie W., Napoleone G., Premoli Silva I. and Roggenthen W.M. (1977). Upper Cretaceous-Paleocene magnetic stratigraphy at Gubbio, Italy - V. Type section for the Late Cretaceous-Paleocene geomagnetic reversal time scale. Geologic Society of America Bulletin, 88:383-389.

Angelier J. (1975). Sur l'analyse des phases superposées de la tectonique cassante: la néotectonique et les failles du massif de l'Ida (Créte, Grèce). Ann. Soc. Geol. Nord, XCV(3):183-200.

Angelier J. (1977). Sur l'évolution tectonique depuis le Miocéene Supérieur d'un arc Insulaire Méditerranéen: l'arc Egéen. Revue de Géographie Physique et de Géologie Dynamique, (2), XIX, fasc. 3, 271-294.

Arias C., Bigazzi G., Bonadonna F.P., Morlotti E., Radicati di Brozolo F., Rio D., Torelli L., Brigatti M.F., Giuliani O. and Tirelli G., (1976). Chronostratigraphy of the Izarorene section in the Melilla Basin (northeastern Morocco). Boll. Soc. Geol. It., 95:1681-1694.

As J.A. (1960). Instruments and measuring methods in paleomagnetic research. Mededelingen en Verhandelingen van het KNMI, 78:1-56.

As J.A. and Zijderveld J.D.A. (1958). Magnetic cleaning of rocks in paleomagnetic research. Geophys. Journal RAS, 1:308-319.

Benda L., Jonkers H.A., Meulenkamp J.E. and Steffens P., (1979). Biostratigraphic correlations in the Eastern Mediterranean Neogene. 4. Marine microfossils, sporomorphs and radiometric data from the Lower Pliocene of Ag. Thomas, Aegina, Greece. Newsl. Strat., 8(1):61-69.

Berggren W.A., (1972). Cenozoic biostratigraphy and paleobiogeography of the North Atlantic. Initial reports of the Deep Sea Drilling Project, Washington (U.S. Government Printing Office), 12:965-1001.

Berggren W.A., (1973). The Pliocene time-scale: calibration of planktonic foraminiferal and calcareous nannoplankton zones. Nature, 243:391-397.

Berggren W.A. and Van Couvering J.A., (1974). The Late Neogene: biostratigraphy, geochronology and paleoclimatology of the last 15 million years in marine and continental sequences. Paleogeogr., Paleoclimatol., Paleoecol., 16(1-2), 216 pp.

de Bruijn H., Mein P., Montenat C. and van der Weerd A., (1975). Correlations entres les gisements des rongeurs et les formations marines du Miocene terminal d'Espagne méridionale (Prov. d'Alicante et de Murcia). Proc. Kon. Nederl. Akad. Wet., ser. B, 78(4):282-313.

Chang S.R. and Kirschvink J.L. (in the press). Possible biogenic magnetite fossils from the Miocene Potamida clays of Crete. In: Kirschvink, Jones and MacFadden (editors), Magnetic biomineralization and magnetoreception in organisms.

Cita M.B., Premoli Silva and Rossi R., (1965). Foraminiferi planctonici del Tortoniano-tipo. Riv. Ital. Paleont., 71(1):217-308.

Borsetti A.M., Carloni G.C., Cati F., Ceretti E., Cremonini G., Elmi C. and Ricci Lucchi F. (1975). Paleogeografia del Messiniano nei bacini peradriatici dell'Italia settentrionale e centrale. Giornale

di Geologia, XL(1):21-72.
Bressler S.L. and Elston D.P. (1980). Declination and inclination errors in experimentally deposited specularite-bearing sands. Earth Planet. Sci. Letters, 48:227-232.
Brunhes B. (1906). Récherces sur la direction d'aimantation des roches volcaniques. J. Phys., 5:705-724.
Cita M.B. and Gartner S., (1973). The stratotype Zanclean foraminiferal and nannofossil biostratigraphy. Riv. Ital. Paleont., 79(4):503-558.
Cita M.B. and Ryan W.B.F. (1973). Timescale and general synthesis. In: Initial Reports of the Deep Sea Drilling Project, Washington (U.S. Government Printing Office), 13:1405-1415.
Cita M.B. and Ryan W.B.F. (1979). Late Neogene environmental evolution. Initial Reports of the Deep Sea Drilling Project, Washington (U.S. Government Printing Office), 47:447-459.
Colalongo M.L., di Grande A., d'Onofrio S., Gianelli L., Iaccarino S., Mazzei R., Romeo M. and Salvatorini G. (1979a). Stratigraphy of Late Miocene Italian sections straddling the Tortonian-Messinian boundary. Boll. Soc. Paleont. Ital., 18(2):258-302.
Colalongo M.L., di Grande A., d'Onofrio S., Gianelli L., Iaccarino S., Mazzei R., Poppi Brigatti M.F., Romeo M., Rossi A. and Salvatorini G. (1979b). A proposal for the Tortonian-Messinian boundary. Ann. Géol. Pays Hellén., Tome hors série, 1979, fasc. I, 285-294. VIIth International Congress on Mediterranean Neogene, Athens (1979).
Cox A., Doell R.R. and Dalrymple G.B. (1963a). Geomagnetic polarity epochs and Pleistocene geochronometry. Nature, 198:1049-1051.
Cox A., Doell R.R. and Dalrymple G.B. (1963b). Geomagnetic polarity epochs: Sierra Nevada. Science, 142:382-385.
Cox A. (1969). Geomagnetic reversals. Science, 163:237-245.
Crimes T.P. and Oldershaw M.A. (1967). Palaeocurrent determinations by magnetic fabric measurements on the Cambrian rocks of St. Tudwal's Peninsula, North Wales. Geol. J., 5:217-232.
Dankers P.H.M. (1978). Magnetic properties of dispersed natural iron-oxides of known grain size. PhD Thesis, State University of Utrecht, pp. 142.
Dronkert H., (1977). A preliminary note on a recent sabkha deposit in S. Spain. Inst. Invest. Geol. Diput. Prov. Univ. Barcelona, 32:153-166.
Drooger C.W., Meulenkamp J.E., Langereis C.G., Wonders A.A.H., van der Zwaan G.J., Drooger M.M., Raju D.S.N., Doeven P.H., Zachariasse W.J., Schmidt R.R. and Zijderveld J.D.A., (1979a). Problems of detailed biostratigraphic and magnetostratigraphic correlation in the Potamidha and Apostoli sections in the Cretan Neogene. Utrecht Micropal. Bull.,21.
Drooger C.W., Langereis C.G., Meulenkamp J.E. and Zijderveld J.D.A., (1979b). The correlation of both Potamidha sections: retrospect and final conclusions. Utrecht Micropal. Bull.,21:215-222.
Dunlop D.J. (1972). Magnetic mineralogy of unheated and heated red sediments by coercivity spectrum analysis. Geophys. Journal RAS, 27:37-55.
Dunlop D.J. (1979). On the use of Zijderveld vector diagrams in multicomponent paleomagnetic studies. Physics of the Earth and Planetary Interiors, 20:12-24.
van den Ende C. (1977). Paleomagnetism of Permian red beds of the Dôme de Barrot (S. France). PhD Thesis, State University of Utrecht.
Ensley R.A. and Verosub K.L. (1982). A magnetostratigraphic study of the sediments of the Ridge Basin, southern California and its tectonic and sedimentologic implications. Earth Planet. Sci. Letters,

59:192-207.
Fisher R. (1953). Dispersion on a sphere. Proceedings of the Royal Society, A217:295-305.
Fortuin A.R. (1977). Stratigraphy and sedimentary history of the Neogene deposits in the Ierapetra region, eastern Crete. GUA Papers of Geology, series 1, No 8.
Foster J.H. and Opdyke N.D. (1970). Upper Miocene to Recent magnetic stratigraphy in deep-sea sediments. Journal of Geophys. Research, 75,4465-4473.
Freudenthal Th., (1969). Stratigraphy of Neogene deposits in the Khania Province, Crete, with special reference to foraminifera of the family Planorbulinellidae and the genus *Heterostigina*. Utrecht Micropal. Bull., 1.
Gianotti A. (1953). Microfaune della serie tortoniana del Rio Mazzapiedi-Castellania (Tortona-Alessandria). Riv. Ital. Paleont., Mem. 6:167-308.
Goree W.S. and Fuller M.D. (1976). Magnetometers using RF-drive
van Gorsel J.T. and Troelstra S.R. (1981). Late Neogene planktonic foraminiferal biostratigraphy and chronostratigraphy of the Solo River section (Java, Indonesia). Marine Micropaleontology, 6:183-209. squids and their applications in rock magnetism and paleomagnetism. Review of Geophysics and Space physics, 14:591-608.
Gradstein F.M. (1973). The Neogene and Quaternary deposits in the Sitia district of eastern Crete. Ann. Géol. Pays Hellén., 24:527-572.
Graham J.W. (1949). The stability and significance of magnetism in sedimentary rocks. Journal of Geophys. Research, 54:131-167.
Graham J.W. (1966). Significance of magnetic anisotropy in Appalachian sedimentary rocks. In: Steinhart and Smith (editors). The earth beneath the continents, Geophysical Monogr., 10:627-648.
Granar L. (1958). Magnetic measurements on Swedish varved sediments. Arkiv Geofys., 3:1-40.
di Grande A. (1975). Geologia dei dintorni di Scicli (Ragusa, Sicilia). Rivista Mineraria Siciliana, a. 26, 151-153:15-29.
di Grande A. and Romeo M. (1975). Stratigrafia delle marne supramioceniche di Scicli (Ragusa, Sicilia). Riv. Ital. Paleont., 31(4):491-526.
Griffiths D.H., King R.F., Rees A.I. and Wright A.E. (1960). The remanent magnetization of some recent varved sediments. Proceedings of the Royal Society, A256:359-383.
Hardenbol J. and Berggren W.A. (1978). A new Paleogene numerical time scale. In: Contributions to the Geologic Time Scale, Stud. in Geol., 6:213-234, edited by Cohee et al., American Association of Petroleum Geologists, Tulsa, Oklahoma.
Harrison C.G.A., McDougall I. and Watkins N.D. (1979). A geomagnetic field reversal time scale back to 13.0 million years before present. Earth Planet. Sci. Letters, 42:143-152.
Hartstra R.L. (1982a). High temperature characteristics of a natural titano-magnetite. Geophys. Journal RAS, 71:455-476.
Hartstra R.L. (1982b). Grain-size dependence of initial susceptibility and saturation magnetization-related parameters of four natural magnetites in the PSD-MD range. Geophys. Journal RAS, 71:477-495.
Hartstra R.L. (1982c). A comparative study of the ARM and Isr os some natural magnetites of MD and PSD grain size. Geophys. Journal RAS, 71:497-518.
Hartstra R.L. (1983). TRM, ARM and Isr of two natural magnetites of MD and PSd grain size. Geophys. Journal RAS, 73:719-737.
Heirtzler J.R., Dickson G.O., Herron E.M., Pitman III W.C. and LePichon X. (1968). Marine magnetic anomalies, geomagnetic field reversals and motions of the ocean floor and continents. Journal of Geophys.

Research, 73:2119-2136.
Henshaw Jr. P.C. and Merrill R.T. (1980). Magnetic and chemical changes in marine sediments. Review of Geophysics and Space physics, 18(2):483-504.
Hess H.H. (1960). Evolution of ocean basins. In: Engel, James and Leonard (editors). Petrologic studies: a volume to Honor A.F. Buddington. Geologic Society of America, 599-620.
Hoffman K.A. (1982). The testing of geomagnetic reversal models: recent developments. Phil. Trans. R. Soc. Lond., A306:147-159.
Hrouda F. (1981). Magnetic ansisotropy of rocks and its application in geology and geophysics. Geophysical Surveys, 5:37-82.
Hsü K.J., Montadert L., Bernoulli D., Cita M.B., Erickson A., Garrison R.E., Kidd R.B, Melieres F., Muller C. and Wright R., (1977). History of the Mediterranean salinity crisis. Nature, 267:399-403.
Irving E. (1957). The origin of the palaeomagnetism of the Torridonian Sandstone Series of Northwest Scotland. Phil. Trans. Roy. Soc. London, A250:100-110.
Jelinek V. (1973). Precision AC bridge set for measuring magnetic susceptibility of rocks. Studia geophys. geod., 17:36
Jelinek V. (1977). The statistical theory of measuring anisotropy of magnetic susceptibility of some igneous and metamorphic rocks. Geofyzika Brno.
Jelinek V. (1978). Statistical processing of anisotropy of magnetic susceptibility on groups of specimens. Studia geophys. geod., 22:50-62.
Jelinek V. (1981). Characterization of magnetic fabric of rocks. Tectonophysics, 79:562-567.
Johnson H.P. and Merrill R.T. (1972). Magnetic and mineralogical changes associated with low-temperature oxidation of magnetite. Journal of Geophys. Research, 77:334
Johnson H.P. and Merrill R.T. (1973). Low-temperature oxidation of a titano-magnetite and the implications for paleomagnetics. Journal of Geophys. Research, 78(23):4938
Keen M.J. (1963). The magnetization of sediment cores from the eastern basin of the North Atlantic Ocean, Deep Sea Res., 10:607-622.
Kennett J.P. and Watkins N.D., (1974). Late Miocene- Early Pliocene paleomagnetic stratigraphy, paleoclimatology, and biostratigraphy in New Zealand. Geol. Soc. America Bull., 85:1385-1398.
King R.F., (1955). Remanent magnetism of artificially deposited sediments. Mon. Notic. Roy. Astron. Soc., Geophys. Suppl., 7:115-134.
King R.F. and Rees A.I. (1966). Detrital magnetism in sediments: an examination of some theoretical models. Journal of Geophys. Research, 71:561-571.
Kirschvink J.L. (1982). Paleomagnetic evidence for fossil biogenic magnetite in Western Crete. Earth Planet. Sci. Letters, 59:388-392
LaBrecque J.L., Kent D.V. and Cande S.C. (1977). Revised magnetic polarity time scale for Late Cretaceous and Cenozoic time. Geology, 5:330-335.
Laj C., Jamet M., Sorel D. and Valente J.P. (1982). First paleomagnetic results from Mio-Pliocene series of the Hellenic sedimentary arc. Tectonophysics, 86:45-67.
Langereis C.G., (1979). An attempt to correlate two adjacent Tortonian marine clay sections in western Crete using magnetostratigraphic methods. Utrecht Micropal. Bull., 21:193-214.
Langereis C.G. and Meulenkamp J.E., (1979). Comparison of two methods used to measure lithostratigraphical intervals in sections Potamidha 1 and 2. Utrecht Micropal. Bull., 21:22-26.

Langereis C.G. and Zijderveld J.D.A., (1979). Magnetostratigraphy of two Tortonian marine clay sections in western Crete. Ann. Géol. Pays. Hellén., Tome hors série, 1979, fasc. II, 711-716. VIIth International Congress on Mediterranean Neogene, Athens, (1979).
Langereis C.G., Zachariasse W.J. and Zijderveld J.D.A. (1984). Late Miocene magnetobiostratigraphy of Crete. Marine Micropaleontology, 8:261-281.
Lanser J.P. (1980). Paleomagnetism of some Late Quaternary sediments. PhD Thesis, University of Amsterdam, pp. 145
Leenhardt O., (1973). Distribution and thickness of the Messinian evaporites in the western Mediterranean. In: Drooger C.W. (Editor), Messinian events in the Mediterranean. North-Holland Publ. Co., 39-43.
LePichon X. and Angelier J. (1978). The Hellenic arc and trench system: a key to the neotectonic evolution of the eastern Mediterranean Area. Tectonophysics, 60:1-42.
Loutit T.S. and Kennett J.P., (1979). Application of carbon isotope stratigraphy to Late Miocene shallow marine sediments, New Zealand. Science, 204:392-397.
Lowrie W. and Alvarez W. (1975). Paleomagnetic evidence for rotation of the Italian peninsula. Journal of Geophys. Research, 80:1579-1592.
Lowrie W. and Alvarez W., (1981). One hundred million years of geomagnetic polarity history. Geology, 9:392-397.
Lowrie W. and Heller F. (1982). Magnetic properties of marine limestones. Review of Geophysics and Space physics, 20(2):171-192.
Mankinen E.A. and Dalrymple G.B. (1979). Revised geomagnetic polarity time scale for the interval 0-5 m.y. B.P. Journal of Geophys. Research, 84:615-626.
Matuyama M. (1929). On the direction of magnetization of basalt in Japan, Tyosen and Manchuria. Porc. Imp. Acad. Japan, 5:203-205.
McDougall I., Saemundson K., Johanneson H., Watkins N.D. and Kristjansson L. (1977). Extension of the geomagnetic polarity time scale to 6.5. m.y.: K-Ar dating, geological and paleomagnetic study of a 3,500-m lava succession in western Iceland. Geologic Society of America Bulletin, 88:1-15.
McElhinney M.W. (1973). Palaeomagnetism and plate tectonics. Cambridge Earth Science series, Cambridge University Press, pp. 358.
McFadden P.L. and Lowes F.J. (1981). The discrimination of mean directions drawn from Fisher distributions. Geophys. Journal RAS, 67:19-33.
Mercier J.-L. (1977). L'arc égéen, une bordure déformée de la plaque euraslatique; réflexions sur un exemple d'étude néotectonique. Bull. Soc. gol. France, (7), XIX(3):663-672.
Mercier J.-L., Delibassis N., Gauthier A., Jarrige J.-J., Lemeille F., Philip H., Sébrier M. and Sorel D. (1979). La néotectonique de l'Arc Egéen. Revue de Geologie Dynamique et de Geographie Physique, 21(1), 67-92.
Meulenkamp J.E., (1969). Stratigraphy of Neogene deposits in the Rethymnon province, Crete, with special reference to the phylogeny of uniserial *Uvigerina* from the Mediterranean region. Utrecht Micropal. Bull., 2.
Meulenkamp J.E., (1979a). Lithostratigraphy and relative chronostratigraphic position of the sections Apostoli and Potamidha 1 and 2. Utrecht Micropal. Bull., 21:9-21.
Meulenkamp J.E., (1979b). Field guide to the Neogene of Crete. Publ. of the Dept. of Geol. and Pal., Univ. Athens, series A, 32.
Meulenkamp J.E., Jonkers B.A., Balder H., Grootjans P., Laagland H., Sikkema W., Stam B., Verhallen P., Voogt E. and Wildenborg T. (1981). Middle Miocene-Pleistocene sedimentary-tectonic history of

Sicily. Rapp. Comm. Int. Mer Médit., 27(8):149-150
Meulenkamp J.E., Jonkers H.A. and Spaak P., (1979). Late Miocene - - Early Pliocene development of Crete. Proceed. 6th Coll. Geol. Aegean Region, 1:137-149.
Mulder C.J., (1973). Tectonic framework and distribution of Miocene evaporites in the Mediterranean. In: Drooger C.W. (Editor), Messinian events in the Mediterranean. North-Holland Publ. Co., 44-59.
Neél L. (1955). Some theoretical aspects of rock magnetism. Phil. Mag. Suppl. Adv. Phys., 4:113-190.
Nagakawa H., Niitsuma N., Kitamura N., Matoba Y., Takayama T. and Asano K., (1974). Preliminary results on magnetostratigraphy of Neogene stage stratotype sections in Italy. Riv. Ital. Paleont., 80(4):615-630.
Nagakawa N., Niitsuma N., Kimura K. and Sakai T., (1975). Magnetic stratigraphy of Late Cenozoic stages in Italy and their correlatives in Japan, In: T. Saito and L.H. Burckle (editors), Late Neogene Epoch Boundaries. Micropaleontol., Spec. Publ., 1:64-74 (Micropaleontology Press, New York).
Ness G., Levi S. and Couch R. (1980). Marine magnetic anomaly timescales for the Cenozoic and Late Cretaceous: a précis, critique and synthesis. Review of Geophysics and Space physics, 18(4):753-770.
d'Onofrio S., Gianelli L., Iaccarino S., Morlotti E., Romeo E., Salvatorini G., Sampo M. and Sprovieri R., (1975). Planktonic foraminifera of the Upper Miocene from some Italian sections and the problem of the lower boundary of the Messinian. Boll. Soc. Paleont. Ital., 14(2):177-196.
Opdyke N.D. (1969). The Jaramillo Event as detected in oceanic cores. In: Runcorn S.K. (editor), The application of modern physics to the Earth and planetary interiors. Wiley, Interscience, 549-552.
Opdyke N.D. (1972). Paleomagnetism of deep-sea cores. Review of Geophysics and Space physics, 10:213
Rees A.I. (1961). The effect of water currents on the magnetic remanence and anisotropy of susceptibility of some sediments. Geophys. Journal RAS, 5:235-251.
Rees A.I. (1965). The use of anisotropy of magnetic susceptibility in the estimation of sedimentary fabric. Sedimentology, 4:257-271.
Rees A.I. and Woodall W.A. (1975). The magnetic fabric of some laboratory-deposited sediments. Earth Planet. Sci. Letters, 25:121-130.
Richter-Bernburg G., (1953). Uber salinare Sedimentation. Z. deutsch. Geol. Ges., 105:593-645.
Ritsema A.R. (1974). The earthquake mechanisms of the Balkan region. Royal Netherlands Meteorological Institute, Scientific Report nr. 74-4.
Ryan W.B.F. (1973). Paleomagnetic stratigraphy. Initial Reports of the Deep Sea Drilling Project, Washington (U.S. Government Printing Office), 13:1380-1387.
Ryan W.B.F. and Flood J.D. (1973). Preliminary paleomagnetic measurements on sediments from the Ionian (Site 125) and Tyrrhenian (Site 132) Basins of the Mediterranean Sea. Initial Reports of the Deep Sea Drilling Project, Washington (U.S. Government Printing Office), 13:599-603.
Ryan W.B.F., Cita M.B., Dreyfus Rawson M., Burckle L.H. and Saito T. (1974). A paleomagnetic assignment of Neogene stage boundaries and the development of isochronous datum planes between the Mediterranean, the Pacific and Indian oceans in order to investigate the response of the world ocean to the Mediterranean salinity crisis. Riv. Ital. Paleont., 80(4):631-688.

Schmidt R.R., (1973). A calcareous nannoplankton zonation for the Upper Miocene-Pliocene deposits from the southern Aegean area with a comparison to Mediterranean stratotype localities. Proc. Kon. Nederl. Akad. Wet., ser. B, 76:287-310.
Scott G.H., (1980). Upper Miocene biostratigraphy: does *Globorotalia conomiozea* occur in the Messinian ? Rev. Esp. Micropal., 12(3):489-506.
Selli R., (1970). Report on the absolute age. CMNS Proc. IV Session, Bologna 1967. G. Geol., 25(1):51-59.
Selli R., (1973). An outline of the Italian Messinian. In: Drooger C.W. (Editor), Messinian events in the Mediterranean. North-Holland Publ. Co.,150-171.
Sissingh W., (1972). Late Cenozoic ostracoda of the South Aegean island arc. Utrecht Micropal. Bull., 6.
Sturani C. and Sampo M. (1973). Il Messiniano inferiore in facies diatomitica nel bacino terziario piemontese. Mem. Soc. Geol. Ital., 12(3):335-358.
Theodorides S.A. (1984). Miocene calcareous nannoplankton zonation and revision of the genera *Discoaster* and *Helicosphaera*. Utrecht Micropal. Bull., 32.
Tjalsma R.C., (1971). Stratigraphy and foraminifera of the Neogene of the eastern Guadalquivir Basin (southern Spain), Utrecht Micropal. Bull., 4.
Valente J.-P., Laj C., Sorel D., Roy S. and Valet J.-P., (1982). Paleomagnetic results from Mio-Pliocene marine sedimentary series in Crete. Earth Planet. Sci. Letters, 57:159-172.
Valet J.-P. and Laj C. (1981). Paleomagnetic record of two sucessive Miocene geomagnetic polarity reversals in western Crete. Earth Planet. Sci. Letters, 54:53-63.
Valet J.-P., Laj C. and Langereis C.G. (1983). Two different R-N geomagnetic reversals with identical VGP paths recorded at the same site. Nature, 5924:330-332.
Van Couvering J.A., Berggren W.A., Drake R.E., Aguirre E. and Curtis G.H., (1976). The terminal Miocene event, Marine Micropaleont., 1:263-286.
Vine F.J. and Matthews D.H. (1963). Magnetic anomalies over oceanic ridges. Nature, 199:947-949.
Watkins N.D. (1972). Review of the developments of the geomagnetic polarity time scale and discussion of prospects for its finer definition. Geol. Soc. Amer. Bull., 83:551-574.
Watkins N.D., Kester D.R. and Kennett J.P. (1974). Paleomagnetism of the Pliocene-Pleistocene boundary section at Santa Maria de Catanzaro, Italy, and the problem of post-depositional precipitation of magnetic minerals. Earth Planet. Sci. Letters, 24:113-119.
Wernli R., (1980). Le Messinien a *Globorotalia conomiozea* (foraminifère planctonique) de la cote méditerranéenne marocaine. Eclogae Geol. Helv., 73(1):71-93.
Wilson R.L., (1971). Dipole offset - The time average paleomagnetic field over the past 25 million years. Geophys. J. of the RAS, 22:491-504.
Zachariasse W.J., (1975). Planktonic foraminiferal biostratigraphy of the Late Neogene of Crete (Greece). Utrecht Micropal. Bull., 11.
Zachariasse W.J., (1979a). Planktonic foraminifera from Potamidha 1: taxonomic and phyletic aspects of keeled Globorotaliids and some environmental estimates. Utrecht Micropal. Bull., 21:129-166.
Zachariasse W.J., (1979b). The origin of *Globorotalia conomiozea* in the Mediterranean and the value of its entry level in biostratigraphic correlations. Ann. Géol. Pays Hellén., Tome hors série, 1979, fasc. III, 1281-1292. VIIth International Congress on Mediterranean

Neogene, Athens (1979).
Zacharlasse W.J. and Spaak P. (1983). Middle Miocene to Pliocene paleoenvironmental reconstruction of the Mediterranean and adjacent Atlantic Ocean: planktonic foraminiferal record of southern Italy. Utrecht Micropal. Bull., 30.
van der Zwaan G.J. (1979). The pre-evaporite Late Miocene environment of the Mediterranean; stable isotopes of planktonic foraminifera from section Falconara, Sicily. Proceed. Kon. Ned. Akad., series B, 82(4):487-502.
van der Zwaan G.J., (1982). Paleoecology of Late Miocene Mediterranean foraminifera. Utrecht Micropal. Bull., 25.
Zijderveld J.D.A. (1967). A.C. demagnetization of rocks: analysis of results. In: Collinson et al. (editors). Methods in paleomagnetism. Elsevier, Amsterdam, 254-286.
Zijderveld J.D.A. (1975). Paleomagnetism of the Esterel rocks. PhD Thesis, Krips Repro BV, Meppel.

CURRICULUM VITAE

Toegevoegd op verzoek van het College van Decanen van de Rijks Universiteit te Utrecht.

De auteur van dit proefschrift behaalde in 1971 het diploma Gymnasium B aan Het Nieuwe Lyceum te Bilthoven. In datzelfde jaar werd met de geofysica studie begonnen aan de Rijksuniversiteit te Utrecht. Het kandidaatsexamen (G4) werd in november 1975 afgelegd, het doctoraalexamen met hoofdvak Fysica van de Vaste Aarde en met bijvakken Structurele en Toegepaste Geologie en Informatica werd in januari 1979 afgelegd. Van 1975 tot 1979 werden assistentschappen vervuld bij het paleomagnetisch laboratorium 'Fort Hoofddijk'. Vanaf februari 1979 tot oktober 1983 was de auteur werkzaam als wetenschappelijk medewerker, verbonden aan het paleomagnetisch laboratorium. Vanaf oktober 1983 is de auteur in dienst van Rijkswaterstaat als medewerker van de Dienst Informatieverwerking.